A Pore-Scale Experiment to Evaluate Enhanced Vapor Diffusion in Porous Media

By

Thomas S. Silverman

Submitted in Partial Fulfillment of the Requirements for the Degree of Master of Science in Hydrology

New Mexico Institute of Mining and Technology
Socorro, New Mexico

January, 1999

Abstract

A pore-scale experiment was performed to determine whether the rate of water vapor diffusion through a pore-throat is enhanced by the presence of liquid trapped in the pore-throat. The experiment demonstrated that enhanced vapor diffusion (EVD), first presented by Philip and de Vries (1957), exists on a pore scale and does not require a thermal gradient. A diffusion cell with two vapor reservoirs bridged by a single "pore-throat" was used to test EVD. Using a brine-concentration-induced vapor pressure gradient, we demonstrate that the rate of water vapor transport through a liquid-filled pore-throat is enhanced relative to the flux through a gas-filled pore-throat. The enhancement is shown to be a quadratic function of liquid-island length. An ancillary experiment with two parallel pore-throats showed that water vapor is transported simultaneously through both gas and liquid-filled pore-throats if both are available. The vapor flux through each pore in the dual-pore-throat diffusion cell is inversely proportional to the resistance of the gas or liquid-filled pore-throat. Lastly, an isotopic tracer test was performed to compare the rates of deuterium transfer through gas or liquid-filled pore-throats. The rate of deuterium transfer to the downgradient reservoir is faster in the presence of a liquid-filled pore-throat despite the slower self-diffusion coefficient of deuterium through liquid than through gas.

Acknowledgements

I would like to thank Sandia National Laboratories for funding this research. My personal thanks go to Dr. John Wilson for all his help over the past two years. I would also like to thank Drs. Steve Webb, Cliff Ho, and Fred Phillips for their continued help along the way. In addition, I would like to thank Andy Campbell for helping with the isotope experiments, Rob Bowman for answering random physical chemistry problems, and Bill Demarco for teaching me how to take a good photograph. Also, thanks to Bob Glass for experimental design suggestions, Mitch Plummer for his perpetual interest in the subject, and Graydon Aulich and Bill Winn for the lunchtime brainstorms. Thanks to Jason Wise for his help automating the experiments, Eli Ludwig for long days in the isotope lab and Dennis McMahon for his help organizing the insightful "Science Sunday" lecture series. Without him, I would never have thought about how best to thaw a turkey.

Table of Contents

List of Tables

List of Figures

Introduction

Vapor diffusion plays an important role in the transport of fluids and contaminants in the vadose zone. The diffusive flux of a gas through a porous medium is generally smaller than through free space due to the presence of the solid matrix, which leads to a more tortuous path. In this paper, both air and gas are used to mean air, while vapor means water vapor. A modified form of Fick's law, where F equals diffusive flux of water vapor (g m^{-2} s^{-1}), describes vapor diffusion in a porous medium.

$$F = - a \alpha v D \nabla \rho \tag{1}$$

In Equation (1) ρ is the vapor density (g m^{-3}), α is a unitless tortuosity factor found by dividing the straight-line distance by actual diffusion path length through the gas-phase, a is the volumetric air content in the porous media ($m^3$of air/m^3), and D is the water vapor diffusion coefficient (m^2 s^{-1}) in free space at a given temperature and pressure. v is the "mass flow factor" (unitless) which is a ratio of total pressure divided by the difference between total pressure and vapor pressure. This value is one at normal soil temperatures and is often omitted from the vapor diffusion equation. Equation (1) is referred to as the simple theory of vapor transfer in a porous medium (Philip and de Vries, 1957).

The diffusion coefficient for water vapor in air is described by (de Vries and Kruger, 1966)

$$D = 0.217\left(\frac{p_o}{p_{atm}}\right)\left(\frac{T}{T_o}\right)^{1.88} \tag{2}$$

where p_{atm} is atmospheric pressure (p_o = 1 atm = 1.013 x 10^5 Pa) and T is absolute temperature (°K; T_0 = 273 °K). Equation (2) describes the sensitivity of the diffusion coefficient to changes in pressure and temperature.

Since tortuosity (α) and volumetric air content (a) both have values less than one, the rate of water vapor diffusion in a porous medium should be less than the rate in free space. It follows that the vapor diffusion rate would be further limited in a partially saturated porous medium where isolated liquid wedges, or "islands" exist between pore-throats since both α and a values decrease further. Some researchers, however, have observed evidence to the contrary. Gurr et al (1952) and Taylor and Cavazza (1954) found that transport of water vapor in a partially saturated porous medium exceeds the expected rate of vapor diffusion as predicted by Equation (1). Philip and de Vries (1957) summarized their experimental data on water vapor transfer in porous medium under temperature gradients and found that the actual transfer rate exceeded the expected rate (as calculated by Equation (1)) by up to 18 times.

In 1957, Philip and de Vries proposed two mechanisms to explain the enhanced rate of vapor flux through porous medium. The first mechanism postulated that differences in thermal conductivities in soil create higher local temperature gradients within the gas-filled pores than the overall thermal gradient of the soil. Philip and de Vries (1957) introduced a correction factor to account for the lower thermal conductivity of the water vapor compared to both the liquid and solid phase. The correction factor, ζ, which replaces the tortuosity factor, α,

is simply the microscopic temperature gradient across the gas-filled pore relative to the macroscopic temperature gradient across the entire soil.

$$\zeta = \frac{(\nabla T)_a}{\nabla T} \tag{3}$$

The second mechanism of enhancement postulated that the liquid-islands within the pore-throats actually transmit water vapor. Figure 1 shows a liquid-island in static steady state, where liquid fills the pore-throat between two pore bodies. With no temperature gradient, the radii of curvature at points A and B are equal, as shown by the solid lines, and Philip and de Vries predict zero enhancement. A thermal gradient imposed in the direction of the arrow will drive vapor flow from left to right. Water vapor condenses on the upgradient side of the island and evaporates from the downgradient side, subsequently increasing and decreasing the radii of curvature at points A and B respectively (shown by the dashed lines). The difference in curvature at points A and B drives capillary flow downgradient. The curvatures at points A and B continue to change until the capillary flow equals the rate of condensation and evaporation at points A and B respectively. At steady state, the condensation of a water vapor molecule on the up-gradient side of the island is instantaneously balanced by the vaporization of a different water molecule on the down-gradient side of the island, thus appearing to eliminate travel time of the vapor molecule through the liquid-island. Instead of forming a barrier to vapor transport, the presence of liquid-islands appears to enhance the apparent vapor diffusion rate by neglecting the diffusion path length through the liquid-island. It follows that a longer liquid-island should result in a

faster vapor flux. Webb and Ho (1997) present pore-scale modeling results of this behavior.

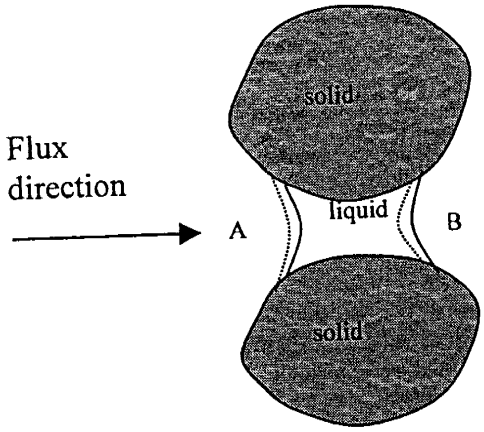

Figure 1. A schematic diagram of a liquid-island within a solid matrix

In addition to reducing flow distance, the presence of the liquid-islands results in an effective increase in cross sectional area for vapor diffusion. Philip and de Vries proposed replacing the porosity term, a, with $a + f(a)\theta$. This equation includes the product of the volumetric water content θ (m^3 m^{-3}) and a function of a, defined by

$$f(a) = \begin{cases} 1 & if\ a \geq a_k \\ \dfrac{a}{a_d} & if\ a < a_k \end{cases} \tag{4}$$

where a_k is the gas-filled porosity when liquid continuity begins. Any additional increase in the water content above the initial point of liquid continuity serves to reduce the vapor phase transport and increase the liquid phase transport through the porous media. Equation (1) can be rewritten to include both mechanisms of enhancement,

$$F = - [a + f(a)\theta]\ \zeta v\ D \nabla \rho \tag{5}$$

Philip and de Vries (1957) introduce η as the mechanistic enhancement factor in a porous media, which is defined as the ratio of (5) to (1) or,

$$\eta = \frac{[a + f(a)\theta]\zeta}{a\alpha} \tag{6}$$

and enhanced vapor diffusion (EVD) can be defined as

$$F = -\eta a \alpha v D \nabla \rho \tag{7}$$

Jury and Letey (1979) determined that the enhancement factor proposed by Philip and de Vries generally underestimated experimentally determined values and proposed a modification using an equation by Cary (1963) to describe water vapor transport under a temperature gradient as

$$F = \frac{-\beta(D\, pH_v)}{R^2 T^3} M_w^2 \nabla T \tag{8}$$

where p is the saturated vapor pressure of water vapor (Pa), H_v equals the latent heat of vaporization (J g^{-1}), R is the ideal gas constant (8.3143 J mol^{-1} K^{-1}), M_w is the molecular weight of water (g mol^{-1}) and β is the empirical constant representing the phenomenological enhancement factor (-) (Jury and Letey, 1979). Using the ideal gas law,

$$p = \rho RT/M_w \tag{9}$$

and the Clausius-Clapyron equation,

$$\frac{dp}{dT} = \frac{\rho H_v M_w}{RT^2} \tag{10}$$

the complete equation of enhanced vapor diffusion (EVD) in a porous media can thus be defined as

$$F = -\beta D \nabla \rho \tag{11}$$

Although β was derived using a temperature gradient from Equation (6), we can generalize to the case of a vapor density gradient.

A number of investigators have inferred the existence of EVD in porous media by various means. Cary (1979) proposed a theoretical model for β based on experimental measurements of water flow and indirect measurements of heat flow, which matched his calculated β values. Cass et al. (1984) proposed a model of β, the phenomenological enhancement factor, which corresponded well with experimental results for lysimeter sand and a silt loam, but did not conform closely to the models of Cary (1979) and Jury and Letey (1979). Jackson (1964) proposed a non-equilibrium thermodynamic model of β. In all these approaches, the enhancement of vapor diffusion has been inferred; it has never been directly measured. Additionally, several experiments have been performed to assess the dependence of β on temperature (Letey; 1968; Jury and Letey, 1979; and Cass et al, 1984), porosity, and water content (Jury and Letey, 1979). Although the method of calculating β continues to be debated, the conceptual model of enhanced vapor transport proposed by Philip and de Vries has been generally accepted since its publication in 1957.

Although EVD has been examined on a macroscopic scale, to the best of our knowledge, no experiments have yet examined it at the pore scale. In this paper we present a pore scale experiment to test the second mechanism of enhancement, which states that the rate of vapor transport is enhanced by the presence of liquid trapped in a pore-throat. In this experiment we examine enhancement in a single pore-throat, not a porous media. We refer to

enhancement, E, as the ratio of vapor flux through a liquid-filled pore-throat to the vapor flux through a gas-filled pore-throat, or

$$E = \frac{F_l}{F_g} \tag{12}$$

where F_l and F_g refer to vapor flux through liquid and gas, respectively. This experiment examines vapor diffusion through a glass pore-throat under gas and liquid-filled conditions. For these experiments, diffusion was not driven by a temperature gradient as Philip and de Vries suggested was necessary, but by brine concentration differences in two liquid reservoirs on either side of the pore-throat. A brine concentration difference and a temperature difference, however, both manifest themselves as a vapor pressure difference, which ultimately drives diffusive transport. Therefore, EVD should exist under a brine concentration gradient.

Objectives

The objective of our experiment was to test at the pore scale the hypothesis that under a brine concentration gradient, the presence of a liquid-filled pore-throat enhances vapor diffusion relative to a gas-filled pore-throat. A secondary objective was to determine the relation between liquid-island length and vapor flux enhancement. Two ancillary experiments were conducted. In the first, parallel pore-throats, one liquid-filled and the other gas-filled, were employed in order to assess the effect of an alternative vapor pathway on EVD. In the second, a deuterium tracer was used to determine whether the flux of an

isotopic tracer is also enhanced for a liquid-filled pore-throat relative to a gas-filled pore-throat.

Methods

A vapor pressure gradient can be imposed by gradients of temperature, gas pressure, capillarity, or liquid phase composition. Typically, vapor pressure differences in larger experiments have been driven by temperature gradients. However, due to the small size of this experiment, a consistent temperature gradient would be difficult to maintain. Capillary pressure gradients could be used to impose vapor pressure gradients but very small pore diameters would be required to produce adequate differences in vapor pressure. Such small pores would yield fluxes too small to be accurately measured. We therefore chose to impose a vapor pressure gradient using brine-filled reservoirs. The vapor pressure above an aqueous solution depends on the activity of the solution. The activity decreases as the solute concentration increases. The vapor pressure gradient in this experiment was imposed by placing a pure water reservoir at one end of the apparatus and a saturated brine solution in the reservoir at the other end. An intermediate brine concentration was used in the liquid-island.

Figure 2 shows a schematic of the single-pore-throat diffusion cell. The glass apparatus was designed to mimic a porous media where a gas or liquid-filled pore-throat exists between gas-filled pore bodies. The column on the left contained nearly pure water (actually 1 μM LiCl solution, relative humidity =

100%) while the column on the right contained a saturated LiCl solution (relative humidity at saturation = 11%) with solid LiCl crystals at the bottom to ensure brine saturation—and hence a constant vapor pressure gradient—through the duration of the experiment. When the system was at steady state, the rate of water vapor evaporation from the pure water reservoir equaled the rate of vapor condensation on the LiCl solution. Experiments were terminated before the solid LiCl completely dissolved from the downgradient reservoir. Appendix A details the procedure used during each experiment.

The drawn glass between vertical columns represented the pore-throat. It was tapered towards the center, reaching a minimum diameter of approximately 1 mm near the midpoint. The small diameter of the pore-throat provided most of the resistance to gas-phase vapor transport. According to the vapor-flux enhancement hypothesis, the travel distance through this high resistance area should be effectively negated. This should produce a noticeable difference between vapor fluxes through a liquid-filled pore-throat compared to a gas-filled pore-throat. The pore-throat was intended to have symmetrical dimensions so that changes in radii of curvature could be compared from one side to the other. However, the manufacturing process of the glass diffusion cells required melting the glass at the juncture between horizontal and vertical columns. Thus, a symmetrical taper was difficult to achieve. Appendix B shows the design specifications of the diffusion cell. For reference, photographs of both the single and dual-pore-throat apparatus are included in Appendix B.

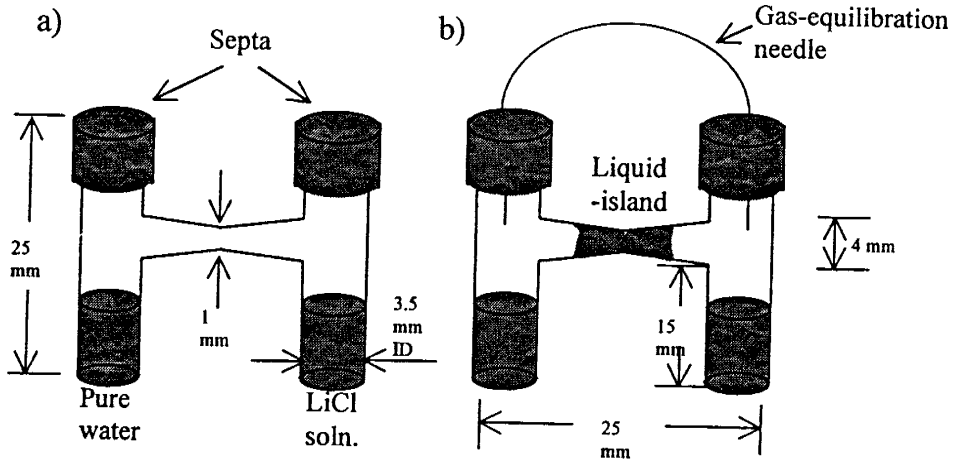

Figure 2. Single-pore-throat cell with a) gas-filled pore-throat, and b) liquid-filled pore-throat.

Solution levels in the vertical columns and the length of the liquid-island were monitored via still camera and interval timer. The equipment used in this experiment is listed in Appendix B. Photographic slides were taken every 2 to 4 hours. In order to analyze the data, the developed slide images were projected onto a screen where changes in water level and island length were measured. For accuracy, the projected images were enlarged by 20 to 50 times the actual size. Because each photo was not perfectly aligned in the slide jacket, the image was projected on a large piece of graph paper and aligned separately for each photo. Drawdown in the pure water column was calculated by measuring the relative change in height of the liquid-gas meniscus for each successive slide taken during an experiment. Changes in the position of the meniscus in the projected image could be measured to within 0.5 mm, corresponding to a volume change of ± 0.2 mm^3 (or 1% of the average mass transferred) in the upstream reservoir at the lowest enlargement. Pure water drawdown data (and draw-up in the LiCl solution

when measured) for the gas-filled pore-throat experiments is presented in Appendix C. The rate of drawdown in the pure water reservoir was effectively constant after an initial equilibration period of approximately 8 hours for the gas-filled pore-throat experiments. The solution-level rise (drawup) in the LiCl column was difficult to observe due to low interfacial tension and non-uniform wettability.

The liquid-island experiments had the same upgradient and downgradient solutions as the gas-filled pore-throat experiments, creating the same gradient from source to sink. The pore-throat, however, was filled with a $Ca(NO_3)_2$ solution, which was injected into the pore-throat by a syringe with a curved needle. The vapor pressure of a saturated calcium nitrate solution (approximately 51%) was nearly midway between those of the two end members.

The liquid-island length was controlled by the mass of the calcium nitrate in solution. A range of different molality $Ca(NO_3)_2$ solutions (3.3, 3.0, 2.8, 2.6, and 1.5 M) were injected in different volumes to control the solute mass and initial liquid-island size. The liquid-island then adjusted its size and concentration to a steady state through evaporation and condensation. The 2.6 M solution was used in most of the experiments, with varying volumes injected into the pore-throat. A greater mass of solute resulted in a longer liquid-island. Liquid-island lengths were measured between the center of its two meniscii. The drawdown in the liquid-island experiments took between 8 and 16 hours to reach an equilbrium rate and the data is presented in Appendix D. Generally, with a larger initial island volume (and length), the equilibration time was also longer. However, for

most experiments, the liquid-island was at, or at least close to, its steady state length after 16 hours. After this time, vapor flux was constant. Vapor flux calculations for the single-pore-throat apparatus are presented in Appendix E. Appendix F presents a table of solute mass and liquid volume of the liquid-island.

The constant rate of drawdown during each experiment, both with and without a liquid-island, suggested that small fluctuations in ambient conditions, such as temperature and atmospheric pressure, had a negligible effect on the sealed diffusion cell. Because the vapor flux through the gas-filled pore-throats did not significantly vary with repetition, we can conclude that the diffusion rate is insensitive to small differences in total length from source to sink caused by slightly different initial solution volumes, and hence initial heights, in each reservoir. Only three tests were required to establish repeatability for the gas-filled pore-throat experiment.

A simple experiment was performed using pure water as the liquid-island. With no vapor pressure gradient between the upgradient source and the liquid-island, the island simply evaporated towards the LiCl solution while the water level in the pure water column remained static. Eventually the liquid-island disappeared. Results from this experiment are presented in Appendix G

The inner diameter of the cell was calibrated by removing known amounts of water from the upgradient reservoir, the downgradient reservoir and the pore-throat (details are given in Appendix G). Since the reservoir column has a uniform cross sectional area and mass was conserved over the course of the experiment (see below), the drawdown in the pure water reservoir provided a

direct estimate of vapor flux. Repeated measurements of steady-state drawdown during the same experiments yielded a total vapor flux estimated error of less than 2%.

The tops of both vertical columns were sealed with rubber septa during the experiments to preserve mass balance. After sealing the diffusion cells with the septa, the gas pressure inside was equilibrated with atmospheric pressure by puncturing the septum momentarily using a hollow needle. Equation (2) shows that without this equilibration, any increased pressure within the diffusion cell caused by the assembly would result in a slower rate of vapor diffusion. This effect could be seen in the results of several preliminary experiments shown in Appendix H. During the liquid-island experiments the vapor spaces on either side of the island were connected by a thin tube that was forced through both septa, illustrated in Figure 2b. This tube served to equalize the gas pressure on either side of the liquid-island. The inner diameter of this equilibration needle was sufficiently small that the amount of vapor diffusion through the needle was negligible. This was quantified in an experiment described below.

A dual-pore-throat diffusion cell was designed to determine whether water preferentially passes through a gas or a liquid-filled pore-throat, when both are available. Figure 3 shows the dual-pore-throat diffusion cell where the top pore-throat is gas-filled and the bottom one is liquid-filled. The pore-throat geometry was difficult to determine since it could not be easily calibrated. Upon visual inspection, however, it appeared that the top pore-throat was slightly larger than the bottom pore-throat, and the flux experiments confirmed this. The dual-pore-

throat experiments were run for several combinations of gas and liquid-filled pore-throats: liquid/liquid (the states i/j refer to the top and bottom pores respectively), gas/gas, gas/liquid, liquid/gas. Drawdown data for the dual-pore-throat apparatus is presented in Appendix I. To determine the vapor diffusion rates through each gas-filled pore separately, experiments were performed where the top (or the bottom) pore was filled with non-reactive, non-volatile mineral oil. This was repeated with mineral oil and water-filled pore-throat experiments to see if the sum of the rates during the gas/mineral-oil experiment and the mineral-oil/liquid-island experiment equaled the vapor flux through the gas/liquid-island experiment. Vapor flux calculations for the dual-pore-throat apparatus are presented in Appendix J.

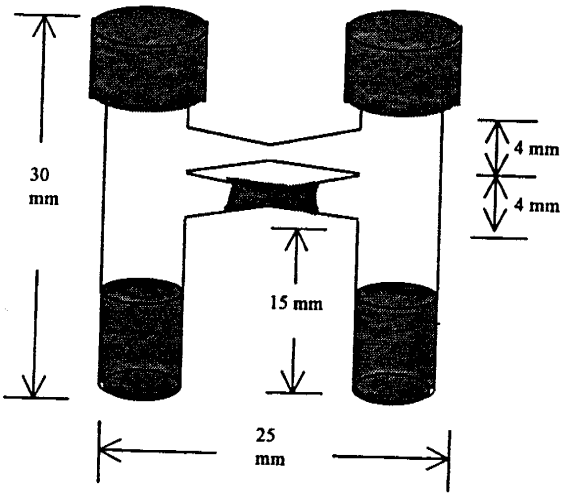

Figure 3. Dual-pore-throat (inner diameters are equal to the single-pore cell).

A preliminary experiment was conducted using the single-pore-throat apparatus with a mineral oil liquid-island in order to verify that that no vapor could be transported through the oil, and, since the length of the island remained

constant over the experiment, the oil also did not volatilize. The small diameter needle used to equilibrate total pressure on both sides of the liquid-island was also used for this experiment to verify that any water-vapor diffusion through the needle was negligible. No drawdown was observed in the pure water reservoir. The detailed results from these experiments can be found in Appendix H.

The last set of experiments used deuterium (D) as a non-reactive, stable isotope tracer to determine if EVD enhanced solute transport. Using a D enriched upgradient reservoir solution and a D depleted downgradient reservoir and intermittent sampling, we could track the D flux from source to sink in the presence and absence of a liquid-island (designated liquid-island D experiment and gas D experiment). The same vapor pressure gradient was used as the earlier experiments, but with a D enriched deionized (DI) water in the upgradient source and a saturated LiCl solution made with D depleted water (from melted Antarctic ice) in the downgradient sink. The liquid-island calcium nitrate solution (2.9 M) was also made with the D depleted water. Data from the deuterium tracer experiments is included in Appendix K. A simple explanatory model, which calculates D enrichment of the downgradient solution over time, is presented in Appendix L.

The gas and liquid-island D experiments proceeded for 120 and 72 hours respectively. It took a few hours for the water vapor flux to reach steady state, but this did not appear to significantly effect the D breakthrough to the downstream LiCl reservoir. To minimize equilibration time (which was slightly longer for liquid-island experiments) the initial volume and concentration of the liquid-

island solution was chosen based on an earlier experiment that examined liquid-island length change as a function of solute mass.

In both deuterium tracer experiments the LiCl reservoir was sampled at 12 hour intervals, removing between 6 and 10 μL of solution depending on how many 3 μL sample replicates were desired. The upgradient solution was periodically sampled over the course of the experiments to show that it also became more deuterium-enriched over time, inasmuch as deuterium preferentially remains in the liquid phase due to its higher mass than ^{1}H. To minimize the disturbance to the system, samples were removed without uncapping the septa. However, repeated puncturing of the septum required their occasional replacement. After the solution was removed by syringe, it was imbibed into a 3 microliter capillary tube, which was subsequently sealed in a larger capillary tube and stored until analysis. The deuterium samples were analyzed at the New Mexico Tech Stable Isotope Laboratory. Deuterium is reported in delta (δ) notation as per mille (‰) differences relative to the V-SMOW (Vienna-Standard Mean Ocean Water) standard,

$$\delta D = \left[\frac{R_{sample} - R_{SMOW}}{R_{SMOW}} \right] \times 1000 \qquad (13)$$

where R is the D/H ratio. Measurements were made on a Finnegan-Mat Delta-E stable-isotope-ratio mass spectrometer using OZ-Tech gas standards. For the δD analysis, hydrogen was extracted using the zinc method of Kendall and Coplen (1985) with 3 μL of solution and 300 mg of zinc reacted at 450 °C. The analyses were corrected using a linear regression ($\delta D_{actual} = 0.9507 \times \delta D_{measured} - 24.444$, R^2

= 0.998) based on V-SMOW, GISP (Greenland Ice and Snow Precipitation) and SLAP (Standard Light Antarctic Precipitate) standards. For a detailed account of the procedure used during both isotope experiments, see Appendix A.

All experiments were performed in a temperature-controlled cabinet at approximately 29 degrees Celsius. The temperature was recorded every 10 minutes over the duration of each experiment. Minimum, maximum and average temperatures are included with the drawdown data for each experiment. No condensation was observed on the inside of the diffusion cell. The septa effectively sealed the diffusion cell from the atmosphere, but, in any event, atmospheric pressure varied by less than 3% over 5 months. Internal cell pressure was also monitored with a tensimeter at the onset and conclusion of several experiments to ensure constant atmospheric pressure. Appendix H includes a discussion on atmospheric pressure and internal cell pressure during the experiments. The temperature and pressure fluctuations were not large enough to influence the experiments.

The mass of both septa, the diffusion cell with all the liquid, and the cell with all liquids and the septa were measured at the onset and conclusion of each experiment to ensure mass conservation. The average mass loss for each experiment was approximately 3% of the total mass of vapor transferred. Some mass loss was expected since the septa can transmit small amounts of vapor to less humid surrounding air. Mass conservation data for each experiment is given in Appendix H.

Results and Discussion

This section of the paper is divided by group of experiments, beginning with the single-pore-throat experiments, followed by dual-pore-throat experiments, and finishing with deuterium tracer experiments. The single-pore-throat experiments section is further subdivided into three sections: gas-filled pore-throat, liquid-filled pore-throat, and enhancement factor. Following the results for each group of experiments is a detailed discussion.

Single-pore-throat experiment results

Gas-filled pore-throat

Figure 4 shows typical drawdown curves in the pure water column over time for several representative experiments, including one gas-filled pore-throat experiment, two liquid-filled pore-throat experiments, and one dual-pore-throat (gas/gas) experiment. For the gas-filled pore-throat experiments, drawdown rates of the pure water did not vary after an initial equilibration period (approx. 8 hrs), after which time the curves can be fit with a straight line. The water vapor flux is given by the slope of the linear regression to this part of the curve. Table 1 shows the calculated water vapor flux for three experiments for the gas-filled single-pore-throat diffusion cell, and three similar experiments for the gas/gas dual-pore-throat cell. Each experiment shows excellent repeatability, with a maximum difference in the calculated rate of less than 4% for each set of three experiments.

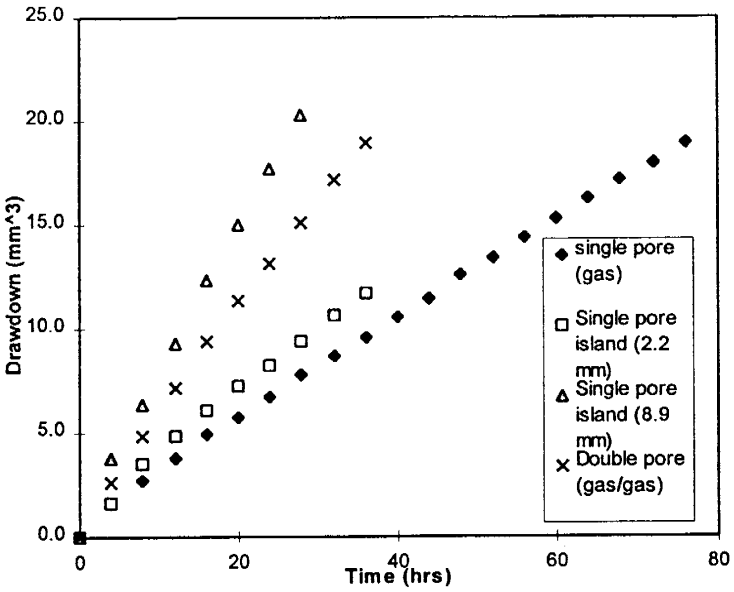

Figure 4. Drawdown versus time in upgradient reservoir.

Table 1. Vapor flux through the single and dual gas-filled pore-throat diffusion cells.

	Vapor Flux (mm^3/hr) -- No Island		
	Experiment 1	Experiment 2	Experiment 3
Single Pore	0.24	0.24	0.24
Dual-pore	0.48	0.49	0.47

Liquid-island filled pore-throat experiments

Similar to the gas-filled pore-throat experiments, drawdown rates during the liquid-island experiments were consistent after an initial equilibration period of approximately 8-16 hours. The vapor flux in each liquid-island experiment was faster than in the gas-filled pore-throat experiments. Table 2 shows the vapor flux values for the single-pore-throat cell experiments. The validity of the primary hypothesis is confirmed by these results; the presence of liquid-islands in a pore-throat enhances the rate of vapor transport.

Table 2. Vapor fluxes and enhancement values for gas and liquid-filled single pore-throat experiments.

Island length (mm)	Water vapor flux (mm^3/hr)	Enhancement, E
0.0	0.24	1.00
2.2	0.30	1.26
8.9	0.68	2.85

Figure 5 shows a graph of liquid-island length versus time for the single-pore-throat apparatus. In all but one experiment, the liquid-island length decreased from the initial length. That one experiment corresponded with the highest mass of solute (also the highest molality) in the liquid-island solution. For reference, a figure showing the almost linear relationship between steady state liquid-island length (L) and solute mass in the liquid-island (M) is subset in Figure 5. The length at which the island stopped increasing or decreasing is the steady state length. After the steady state length was reached, the drawdown in the pure water reservoir was constant.

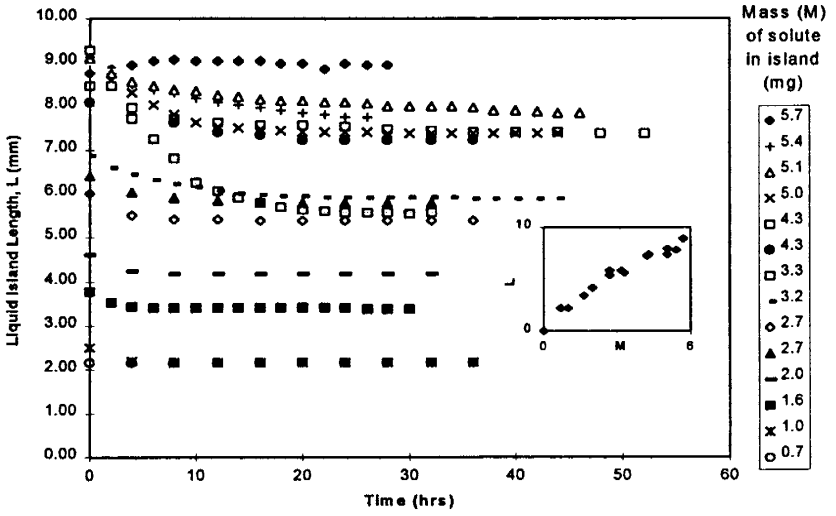

Figure 5. Liquid-island length over time in the single-pore-throat cell.

Enhancement

Dividing the vapor diffusion rate through a liquid-filled pore by the rate through a gas-filled pore gives the relative enhancement. An enhancment value of 1 indicates no enhancment relative to the gas-filled pore-throat scenario. Table 2 shows enhancment values for several representative experiments. Figure 6 shows enhancement as a function of steady state liquid-island length for the liquid-island experiments. The experimental data can be represented by a second-order polynomial equation, with excellent correlation.

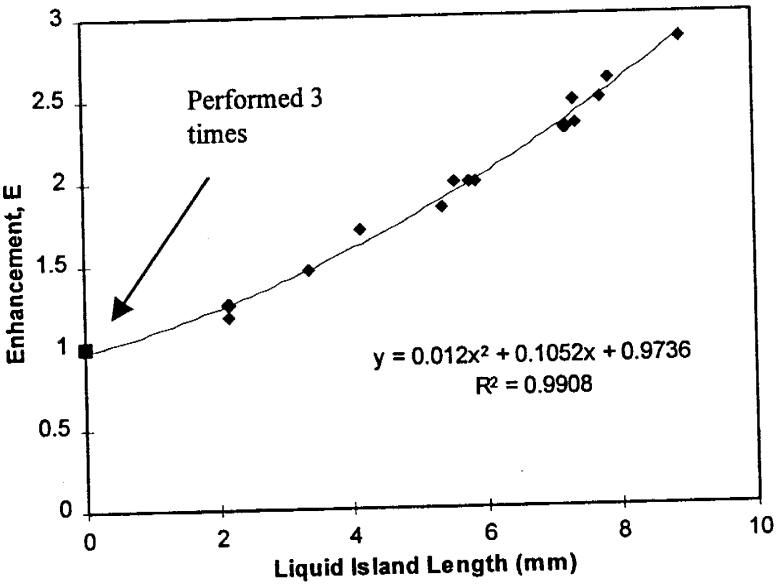

Figure 6. Enhancement versus liquid-island length in the single-pore-throat apparatus.

The relationships between solute mass in the island and island length is examined as a function of enhancement in Appendix G. Although these comparisons are interesting to observe, liquid-island length remains the most

useful parameter for predicting enhancement since it is not specific to the type of solute, which determines the activity of the solution.

Single-pore-throat discussion

The consistent rate of pure water drawdown and the stability of the liquid-island at steady state help confirm our primary hypothesis: Water vapor flux through a liquid-filled pore-throat is enhanced relative to the flux through a gas-filled pore-throat. Further, enhancement is proportional to liquid-island length. Figure 6 shows that enhancement can be described by a quadratic function of liquid-island length where slope increases with island length. This data shows that liquid-islands do not act as a barrier to vapor transport, but function to reduce the total flow distance from source to sink. The results also confirm that a concentration differential can result in EVD; a temperature gradient was not necessary. Although it was difficult to repeat the conditions of any one liquid-island experiment, the correlation between the data over a range of different island lengths was excellent, and the fitted second order polynomial has a high R^2 value.

A model of enhancement for two separate pore-throat geometries is presented in Appendix L. The model, derived by J. L. Wilson, shows that enhancement (in terms of E in this model), can be calculated as a function of pore throat area and liquid island length. The model examines enhancement under two different pore-throat geometries, one where the inner diameter is uniform and one where the taper is described by a cosine function.

Dual-pore-throat experiment results

The water vapor flux and liquid-island length for each pore-throat (if liquid-filled) is presented in Table 3 for each combination of liquid, gas, and mineral oil (L,G, and M respectively) for the dual-pore-throat apparatus. Figure 7 shows the same results presented in a more comparable format. The gas/gas experiment was performed three times and the rate of vapor diffusion varied by only 4% as shown in Table 1. For comparison of vapor fluxes under the different conditions of gas or liquid-filled pore-throats, the liquid-island lengths in the gas/liquid and liquid/gas experiments were intended to have the same lengths as in the liquid/liquid experiments. However, some difference in steady state length was inevitable. The steady state length of the top pore varied by 0.7 mm (8%) between runs while the island length in the bottom pore varied by only 0.3 mm (4%) between runs.

Table 3. Diffusion rates and liquid-island lengths for the dual-pore-throat diffusion cell. G=gas, L=liquid-island, and M=mineral oil.

Experiment	Top Pore Steady State Island Length (mm)	Bottom Pore Island Length (mm)	Diffusion Rate (mm^3/hr)
G/G*	--	--	0.48±0.01
L/L	8.1	7.5	0.92
G/L	--	7.4	0.73
L/G	8.3	--	0.67
G/M	--	--	0.32
M/G	--	--	0.29
M/L	--	7.7	0.66
L/M	7.6	--	0.57

*This experiment was performed three times.

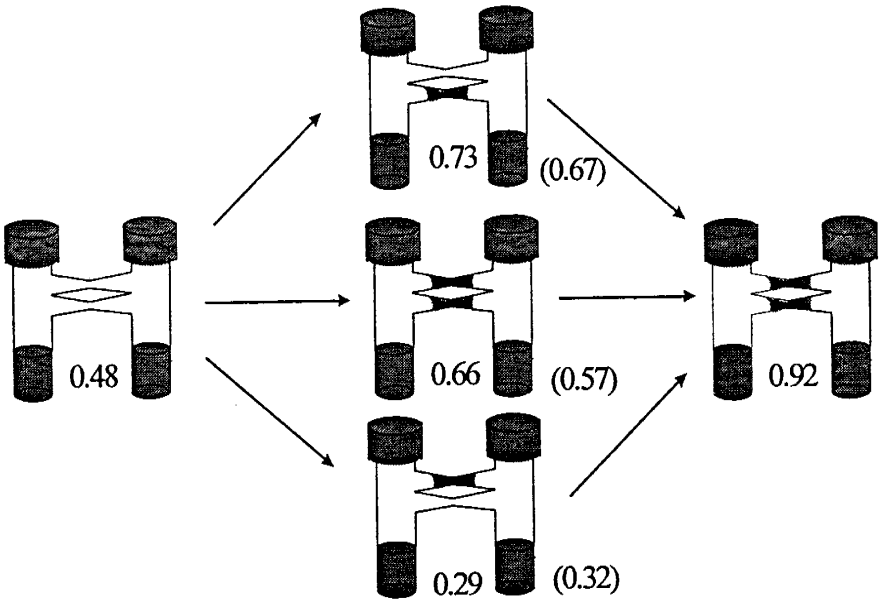

Figure 7. Flow diagram of dual-pore-throat experimental results. The numbers between columns represent the vapor flux for the pictured condition. The numbers in parenthesis represent the inverse case. Gray pore-throats = liquid; black pore-throats = mineral oil; and white pore-throats = gas.

Dual-pore-throat discussion

Figure 4 shows that similar to the single-pore-throat experiments, drawdown rates for the dual-pore-throat experiments were consistent after an initial equilibration period. Notice in Table 1 that the water vapor flux through the dual-pore-throat diffusion cell under gas-filled conditions (G/G) is approximately double the flux through the single pore-throat when gas-filled. This suggests that the effective area in the dual-pore-throats is approximately double that of the single pore-throat. By examining both pore-throats of the dual-pore-throat cell individually, however, we see that the vapor flux in the G/M and the M/G experiments is 33% and 21% higher respectively than in the gas-filled

single-pore-throat experiments. These results suggest that both pore-throats in the dual cell have a larger effective flow area than the pore-throat on the single cell.

The sum of the vapor fluxes in the G/M and the M/G experiments is 27% greater than when both pores throats are gas-filled (G/G). These results suggests that the total resistance in the pore-throats of the dual cell was not high enough to dominate vapor fluxes. If the resistance in the pore-throats completely dominated diffusion rates, the sum of the fluxes through the G/M and the M/G experiments should approximately equal the vapor flux when both pore-throats are gas filled (G/G). A model of pore-throat resistance is presented in Appendix L that relates resistance to flow distance and effective flow area. This model shows quantitatively that the effective area of each pore-throat separately is higher than the effective area of the pore-throat in the single-pore-throat diffusion cell.

In the G/M experiment, the vapor flux is 10% higher than the vapor flux through only the gas-filled bottom pore (M/G) despite a longer path distance from source to sink reservoir. This suggests a higher effective area for vapor flux in the top pore-throat than in the bottom pore-throat. The model presented in Appendix L suggests that the effective area in the top pore was nearly 35% larger than the bottom pore.

When one pore is gas-filled and one liquid-filled, as in the G/L experiment, the vapor transfer rate is observed to be higher than in the M/L experiment, suggesting that water vapor is transported simultaneously through a gas and liquid-filled pore-throat if both are available. A similar comparison can be made for the rate of diffusion through the L/M experiments compared to the

L/G experiment. The difference in liquid-island lengths between experiments was not enough to significantly affect these relationships.

Deuterium tracer experiment results

Figure 7 shows the δD values for each liquid reservoir for the gas and liquid-island experiments. Samples from the liquid-island solution were taken at the onset and conclusion of the experiment. The volume of the liquid-island was approximately constant at 7 mm^3 for the duration of the experiment. The δD values in each liquid reservoir increased over time for both experiments. Figure 8 shows a comparison plot of only the downgradient reservoir δD values for the gas and liquid-filled pore-throat experiments. Notice the approximately linear variations of δD over time for both experiments. The δD flux is approximated by the slope of the linear trend line: 0.72 δD/hr and 1.08 δD/hr for the gas and liquid-island deuterium experiments respectively.

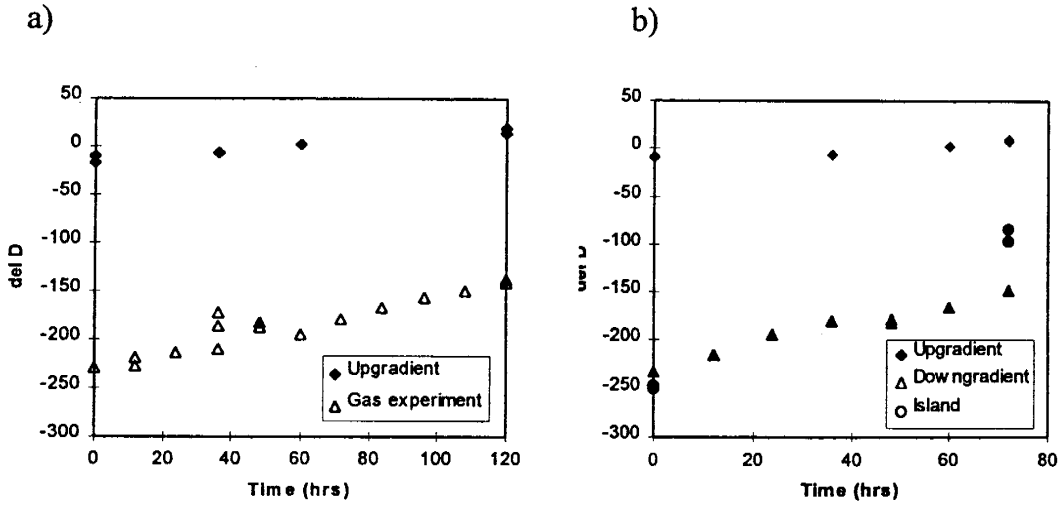

Figure 8. Upgradient, downgradient, and liquid-island (when present) δD values in a) the gas-filled pore-throat experiment, and b) the liquid-island experiment.

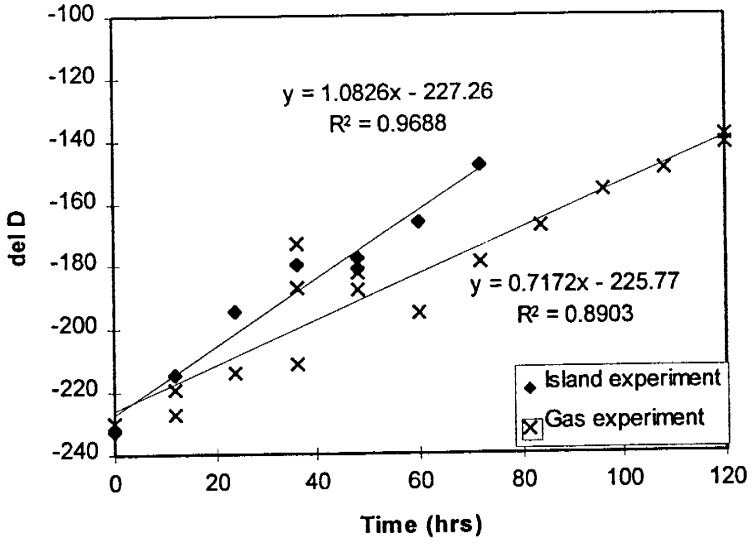

Figure 9. D enrichment in the downgradient reservoir over time for the gas and liquid-filled pore-throat experiments.

Deuterium tracer experiments discussion

Although Figure 7a has some anomalous replicate δD values at the 36 hour mark, the trends in deuterium enrichment for both the gas and liquid-island experiments are both approximately linear. The δD in the downgradient reservoir increases by approximately 50% faster in the presence of a liquid-island than when the pore-throat is gas-filled, or E=1.5. This suggests that liquid-phase advection through the island may be quite rapid relative to the vapor diffusion across an equivalent gas-filled pore-throat. No initial lag in deuterium transfer, caused by the slower deuterium diffusion rate through liquid, was observed in the liquid-island experiment.

A lumped parameter model of deuterium transfer under gas-filled and liquid-filled pore-throat conditions is presented in Appendix L. This model explains the trends seen in the experimental results. Both the model and

experimental results show that the liquid-filled pore-throat does not inhibit deuterium transport despite a two order of magnitude slower diffusion coefficient through liquid than through air.

Although neither the model nor experimental results show the expected lag in deuterium transfer in the presence of a liquid-island, a 12 hour experiment with frequent sampling may reveal this effect. Such an experiment, however, seems impractical with the current experimental design which takes between 8 and 16 hours to reach steady state vapor (and presumably deuterium) flux. The flow geometry in the pore-throat may also preclude any noticeable lag in deuterium breakthrough. The relatively fast diffusion time within the liquid-island compared to absolute vapor flux through the island most likely masks any noticeable lag in deuterium breakthrough. This is verified by a simple calculation of the Peclet number for the liquid-island (using experimentally derived values) which describes the relative importance of advective transport to diffusive transport within the liquid-island. The value of this number, given an island length (d) of 7.2 mm and a vapor flux F_v of 0.55 mm^3/hr. Using an average area of the pore throat of radius 0.75 mm (area, A = 1.77 mm^2), we calculate a velocity from the expression $v = F_v/A$ = 0.31 mm/hr. Using a self diffusion coefficient (D_D) of deuterium in water of approximately 2.3 x10^{-5} cm^2/s we calculate the Peclet number, P, defined as $P = vd/D_D$ is approximately 0.27. A Peclet number below 1 indicates diffusion-dominated flow. A visualization experiment using blue food coloring in the liquid-island solution supported this calculation. We did

not observe any accumulation of dye on the downstream side of the liquid-island, which would be expected if flow were advection dominated.

Conclusions

Under a brine-induced vapor pressure gradient, the rate of vapor transport through a liquid-filled pore-throat is enhanced relative to the rate through a gas-filled pore-throat. The enhancement is shown to be a quadratic function of liquid-island length. The effect of a liquid-island is a net reduction in travel distance from source to sink. The effect of an alternative vapor pathway on EVD yielded inconclusive results. Given two parallel pore throats, one gas-filled, and one liquid-filled, water vapor will simultaneously travel through both pores throats. Attempts to determine the degree to which water vapor travels through either pore, however, were unsuccessful due to insufficiencies in the design of the diffusion cell.

Finally, the deuterium tracer experiments showed that the rate of solute transfer is enhanced by the presence of a liquid island. This enhancement is likely a result of pore throat geometry. From a simple calculation of Peclet number and a visualization experiment with a dyed liquid island solution, transport in the liquid island was shown to be diffusion dominated.

References

Bird, R.B., W.E. Stewart, and E.L. Lightfoot, (1960), Transport Phenomena, Wiley, New York.

Cary, J.W. (1963), "Onsager's relation and the non-isothermal diffusion of water vapor," Journal of Physical Chemistry, v. 67, p. 126-129.

Cary, J.W., (1979), "Soil Heat Transducers and Water Vapor Flow," *Soil Science Society of America Journal*, v. 43 p. 835-839.

Cass , A., G.S. Campbell, and T.L. Jones, (1984), "Enhancement of thermal water vapor diffusion in soil," *Soil Science Society of America Journal*, v. 48, p. 25-32.

Cunningham, R.E., and R.J.J. Williams (1980), Diffusion in Gases and Porous Media, Plenum Press, New York.

De Vries, D.A., and A.J. Kruger (1967), Phenomenes de Transport, "On the value of the diffusion coefficient of water vapour in air," Proccrs. Symp. 160; Collogques Internationaux du Centre National de la Recherche Scientifique, Paris, p 61-72.

Friedman, I., and J.R O'Neil (1977), Data of Geochemistry: Sixth Edition. United States Government Printing Office, Washington.

Gurr, C.G., T.J. Marshall, and J.T. Hutton, (1952), "Movement of Water in Soil Due to a Temperature Gradient," *Soil Science*, v. 74, p. 335-345.

Ho, C.K. and S.W. Webb, (1998), "Review of Porous Media Enhanced Vapor-Phase Diffusion Mechanisms, Models and Data - Does Enhanced Vapor-Phase Diffusion Exist?," *Journal of Porous Media*, v. 1, p. 71-92.

Jackson, R.D., (1964), "Water vapor diffusion in a relatively dry soil: I. Theoretical considerations and sorption experiments," *Soil Science Society of America Proceedings*, v. 28, p. 172-176.

Jury, W.A. and J. Letey Jr., (1979), "Water Vapor Movement in Soil: Reconciliation of Theory and Experiment," *Soil Science Society of America Journal*, v. 43, p. 823-827.

Kendall C. and T.B. Coplen, (1985), "Multisample Conversion of Water to Hydrogen by Zinc for Stable Isotope Determination," *Analytical Chemistry*, v. 57, p. 1437-1440.

Philip, J.R., and D. A. de Vries, (1957), "Moisture Movement in Porous Materials under Temperature Gradients," *Tran. Am. Geophys.* Union, v. 38, p. 222-232.

Taylor, S.A. and L. Cavazza (1954), "The Movement of Soil Moisture in Response to Temperature Gradients," *Soil Sci. Soc. Am. Proceedings*," v. 18, p. 351-358.

Webb, S.W. and C.K. Ho, (1997), Pore-Scale Modeling of Enhanced Vapor Diffusion in Porous Media," 1997 ASME International Mechanical Engineering Congress and Exposition, Sixth Symposium on Multiphase Transport in Porous Media.

Wexler, A. (editor), (1965), Humidity and Moisture: Measurement and Control in Science and Industry, Reinhold Publishing Co., New York.

Appendix A – Procedures

Appendix A details the procedures for cell cleaning, experimental set-up of both the gas-filled pore-throat, the liquid-filled pore-throat, and the isotope experiments.

Cell Cleaning

The diffusion cell was cleaned before the first use and after each mineral oil experiment by rinsing with a sequence of solvents presented below:

N-hexane → Ethyl acetate → Ethanol → Water

where each solvent is miscible with the solvent immediately left. After each experiment cells are rinsed thoroughly with only deionized water.

Experimental Set-up

1. Remove solid LiCl from supersaturated LiCl solution using B-D 3cc disposable syringe and gently add to the right column of the clean dry diffusion cell.
2. Add LiCl solution to the same column.
3. Add pure water solution to the other vertical column and weigh the entire apparatus.
4. For liquid-island experiments, add $Ca(NO_3)_2$ solution to the pore-throat with a curved needle syringe and weigh the diffusion cell again to determine the initial mass of the liquid-island.
5. Puncture pre-weighed septa with 23 gauge needle. (Needles are hollow to allow pressure equilibration between the diffusion cell and the atmosphere after the experiment is sealed).
6. Gently cap both columns with septa and carefully remove the needles.
7. For the liquid-island experiments, insert one end of the 15 cm hollow 26 s gauge needle through each septa. This allows for internal pressure equilibration in both vapor reservoirs on either side of the liquid-island.
8. Weigh entire apparatus together and place diffusion cell in front of camera.
9. Photograph every 4 hours for gas diffusion experiments and every 2 hours for liquid-island experiments.

At the conclusion of each experiment:

10. Weigh the diffusion cell to determine mass loss.
11. Puncture septa with hollow needles and remove septa.
12. Weigh the septa and diffusion cell separately again to check mass balance.
13. Thoroughly rinse the diffusion cell in deionized water and oven dry.

The same general procedures apply for the dual-pore-throat experiments.

Isotope Experiment Procedure

Gas-filled pore-throat experiment
Use the same set-up procedure described for the non-isotope experiments, but using deuterium depleted LiCl solution and deuterium enriched pure water.

Liquid-filled pore-throat
Use the same set-up procedure described for the non-isotope experiments, but using deuterium depleted LiCl solution, deuterium enriched pure water, and deuterium depleted calcium nitrate solution in the liquid-island.

Sampling procedure
1. Remove connecting needle from the septum above the downgradient reservoir if present.
2. Puncture the septum with a pointed-needle 10 microliter syringe and remove the desired volume of LiCl solution.
3. Remove the syringe needle from the apparatus and expurge the solution into a small dish.
4. Using a suction bulb, fill the 3 uL capillary tube
5. Seal the filled 3 uL capillary tube in the 7.5 cm capillary tube by melting both ends shut.
6. Replace septum after 3 to 4 separate punctures.
7. While replacing septa, sample upgradient reservoir simply by immersing the capillary tube in the liquid.
8. Seal these samples in the 7.5 cm capillary tubes as described above.

Sampling schedule
1. Sample the downgradient reservoir at 12 hour intervals beginning at time zero.
2. Sample the upgradient liquid every 36 to 48 hours.
3. Take at least 2 samples at every sampling event.

Appendix B – Materials

Appendix B contains a list of the materials used in the experiments and pictures of the experimental apparatus. Table B1 lists the general equipment, camera equipment, syringes, and needles used. Table B2 lists the solution concentrations used in each liquid reservoir. Figures B1, B2, and B3 show photographs of the glass diffusion cells with a gas-filled pore-throat, a liquid-filled pore-throat, and a gas/gas pore-throat respectively. The last two pages of Appendix B show the manufacturer's design specifications of the single pore-throat and dual pore-throat diffusion cell.

Table B1. General equipment, camera equipment, syringes and needles.

General equipment
Glass diffusion cells were made by Ace Glass Inc., Vineland, New Jersey. Mettler AT400 Balance 1-Fss Septa (1888 gray) from The West Company, Lionville, Pennsylvania Fisher Isotemp Oven, Model 230G Soil Measurement Systems Tensimeter
Camera equipment, film and developing
Nikon 8008 and 8008s cameras with MF-21 Nikon Control Back 60 mm AF Micro Nikkor lenses (2) Tiffen fluorescent light filters (2) Kodak Gold film, ISO 100 Film developed by Dale Laboratories, Hollywood, Florida.
Syringes and needles
B-D 3cc disposable sterile syringes B-D Precision glide needles (16 and 23 gauge) Hamilton 15 cm 26s gauge 304 ss hollow needle Hamilton 10 µL glass syringe #701 3 µL Drummond Microcaps Capillary tubes (4.2 cm) VWR Micro-Hematocrit capillary tubes (7.5 cm, 1.1 to 1.2 mm ID)

Table B2. Solutions used in regular and isotope experiments.

Solutions
(Each solution is made with 18Ω deionized water.)
Upgradient solution = 1 µM LiCl solution
Downgradient solution = supersaturated LiCl solution
Liquid-island solution = 1.5, 2. 6, 2.8, 2.9, and 3.3 M $Ca(NO_3)_2$ solution
Sigma heavy white mineral oil, catalog # 400-5
Deuterium depleted water from melted Antarctic ice (δ deuterium ≅-230)
Deuterium enriched water from evaporated DI water (δ deuterium ≅-10)
Liquid-island deuterium depleted $Ca(NO_3)_2$ solution ≅ 2.8 M.

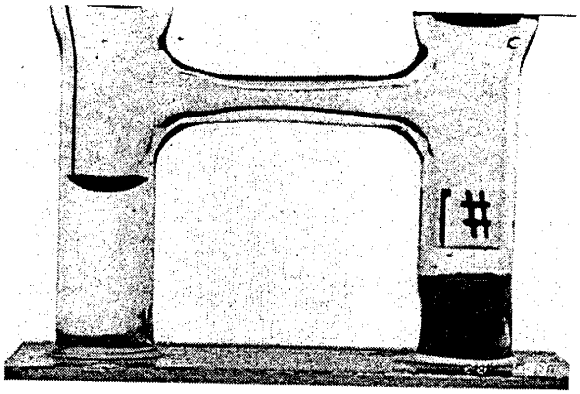

Figure B1. Gas-filled single pore-throat diffusion cell.

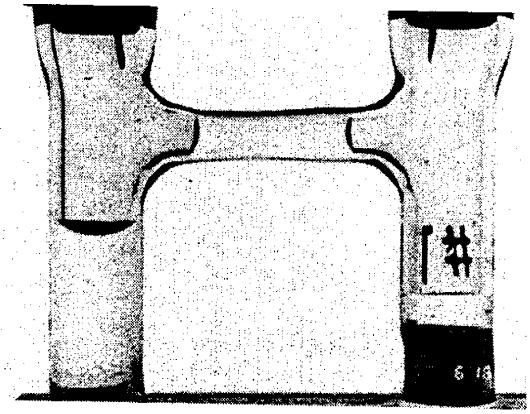

Figure B2. Liquid-filled single pore-throat diffusion cell.

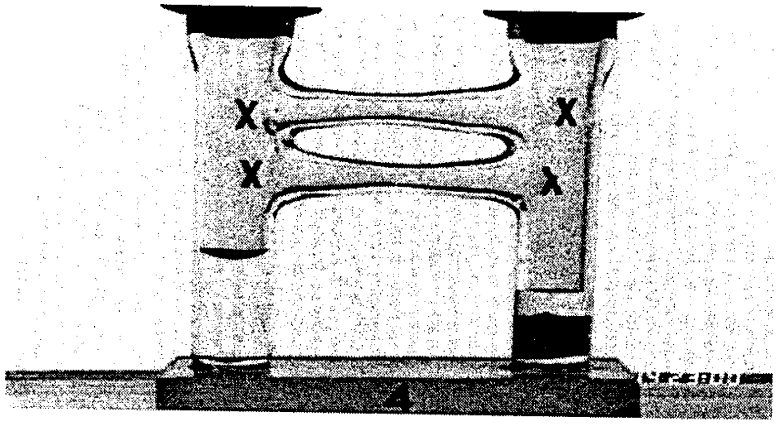

Figure B3. Gas-filled dual-pore-throat diffusion cell.

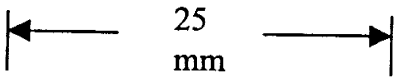

DRAWING NUMBER
D103676
CATALOG NUMBER

NOTES:

1. ALL DIMENSIONS ARE IN MILLIMETERS UNLESS OTHERWISE NOTED.
2. DECAL NO.S SEQUENTIALLY
3. LAMP CUTTER:
   3 PCS. – 5 OD SW – 6 INCHES
   2 PCS. – 7 OD SW – 6 INCHES
   1 PC. – PLATE GLASS 15MM X 150MM
   (NO HOLES IN PLATE)

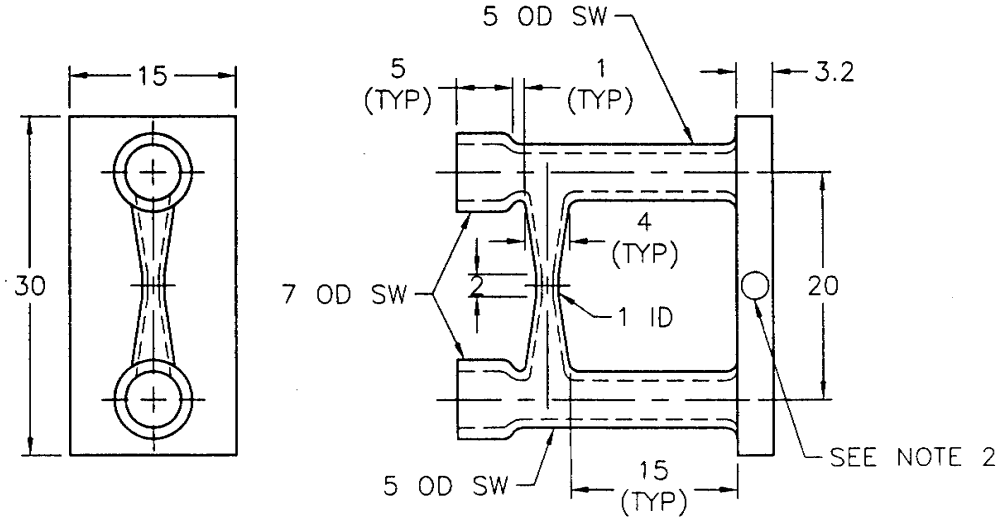

REVISIONS			
REV	DATE	BY	DESCRIPTION
A	3/98	JJR	PER – ECR0294
A	3/98	JJR	PER – ECR0399

TOLERENCES UNLESS OTHERWISE NOTED

STANDARD

FRACTION	±1/64
.XX	±.010
.XXX	±.005
.XXXX	±.0005
ANGULAR	±15'

METRIC (MM)

X.	±1.
X.X	±0.1
X.XX	±0.01

FINISH 63 RMS

ACE GLASS INC.
VINELAND, NJ

TITLE:
GLASS APPARTUS, DOUBLE SEPTUM PORT

		SCALE:	SHEET NO.	DATE:	DRAWN BY:
A		2:1	1 OF 1	2/11/98	JJR

NOTES:

1. ALL DIMENSIONS ARE IN MILLIMETERS UNLESS OTHERWISE NOTED.
2. DECAL NO.S SEQUENTIALLY
3. LAMP CUTTER:
   3 PCS. – 5 OD SW – 6 INCHES
   2 PCS. – 7 OD SW – 6 INCHES
   1 PC. – PLATE GLASS 15MM X 30MM (NO HOLES IN PLATE)

DRAWING NUMBER
D103913
CATALOG NUMBER

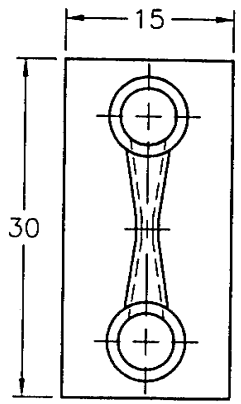

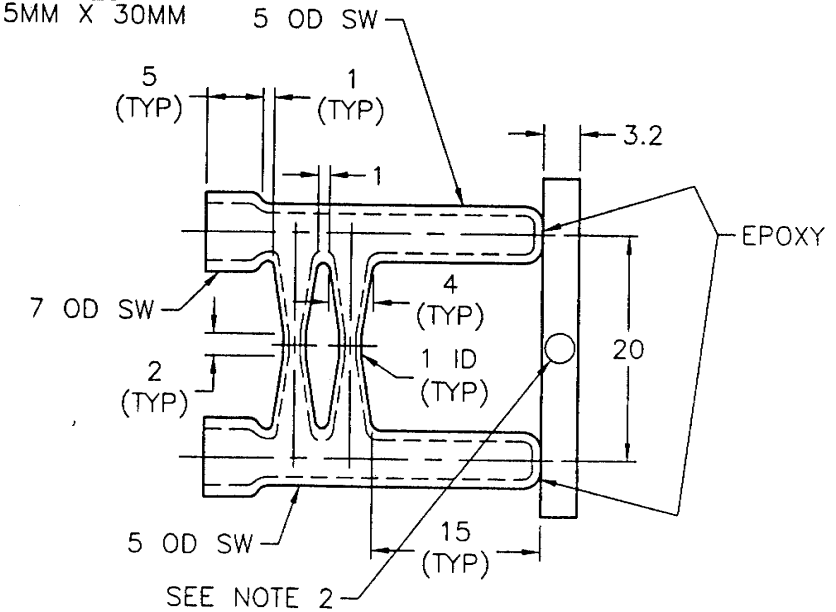

REVISIONS			
REV	DATE	BY	DESCRIPTION

TOLERENCES UNLESS OTHERWISE NOTED
STANDARD
FRACTION ±1/64
.XX ±.010
.XXX ±.005
.XXXX ±.0005
ANGULAR ±15'
METRIC (MM)
X. ±1.
X.X ±0.1
X.XX ±0.01
FINISH 63 RMS

ACE GLASS INC.
VINELAND, NJ

TITLE:
GLASS APPARTUS, DOUBLE SEPTUM PORT

A		SCALE: 2:1	SHEET NO. 1 OF 1	DATE: 3/20/98	DRAWN BY: JJR

Appendix C – Gas-filled single pore-throat drawdown data

Appendix C contains all drawdown data for the gas-filled single pore-throat experiments. The experiment name and date is found at the top of each table. The tables include the drawdown data measured on the projected image and corrected to millimeters. In addition, a figure of drawdown versus time can be found on each page. Also included on each page is the minimum, maximum, and average temperature next to the diffusion cell for each day over the duration of the experiment.

Single Pore -- Gas Diffusion Experiment

Begin Date 6/1/98
Begin Time 16:30
Interval 4 hr

	Temperature (C)			
	6/1/98	6/2/98	6/3/98	6/4/98
Min	28.91	28.59	28.60	28.47
Max	29.31	29.32	28.75	28.75
Ave	29.21	28.97	28.66	28.66

	Actual OD (mm)	Actual ID (mm)	Projected OD
left column	5.22	3.5	45.7
right column	5.18	3.5	44.5

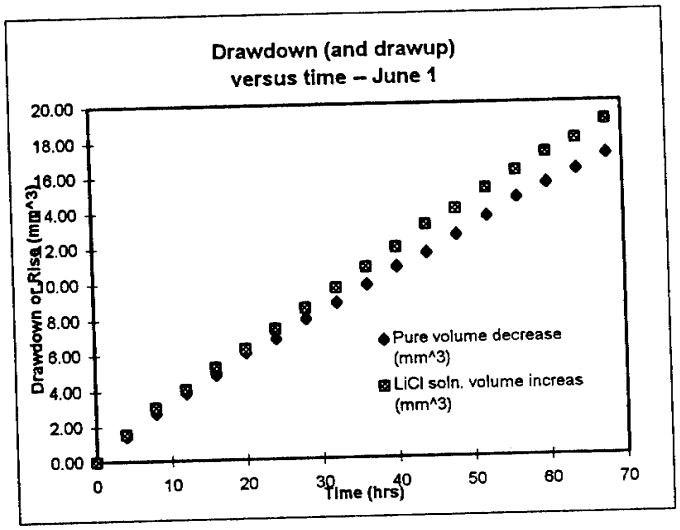

Photo	Date	Time	Hour	Projected pure drawdown	Projected LiCl soln. rise	Actual pure drawdown (mm)	Actual LiCl soln rise (mm)	Pure volume decrease (mm^3)	LiCl soln. volume increase (mm^3)
1	6/1/98	16:30	0	0.0	0.0	0.00	0.00	0.00	0.00
2		20:30	4	1.3	1.4	0.15	0.16	1.43	1.57
3	6/2/98	0:30	8	2.5	2.7	0.29	0.31	2.75	3.02
4		4:30	12	3.5	3.6	0.40	0.42	3.85	4.03
5		8:30	16	4.4	4.7	0.50	0.55	4.84	5.26
6		12:30	20	5.5	5.6	0.63	0.65	6.04	6.27
7		16:30	24	6.2	6.6	0.71	0.77	6.81	7.39
8		20:30	28	7.2	7.6	0.82	0.88	7.91	8.51
9	6/3/98	0:30	32	8.0	8.6	0.91	1.00	8.79	9.63
10		4:30	36	8.9	9.6	1.02	1.12	9.78	10.75
11		8:30	40	9.8	10.6	1.12	1.23	10.77	11.87
12		12:30	44	10.5	11.7	1.20	1.36	11.54	13.10
13		16:30	48	11.4	12.5	1.30	1.46	12.53	14.00
14		20:30	52	12.3	13.5	1.40	1.57	13.52	15.12
15	6/4/98	0:30	56	13.3	14.4	1.52	1.68	14.62	16.13
16		4:30	60	14.0	15.3	1.60	1.78	15.39	17.14
17		8:30	64	14.7	16.0	1.68	1.86	16.15	17.92
18		12:30	68	15.5	16.9	1.77	1.97	17.03	18.93

Sinlge Pore -- Gas Diffusion Experiment

Begin Date 6/5/98
Begin Time 12:00
Interval 4 hr

	Temperature (C)			
	6/5/98	6/6/98	6/7/98	6/8/98
Min	28.05	27.83	28.63	28.64
Max	28.74	29.09	28.89	28.95
Ave	28.67	28.43	28.76	28.75

	Actual OD (mm)	Actual ID (mm)	Projected OD
left column	5.22	3.5	46.4
right column	5.18	3.5	45.5

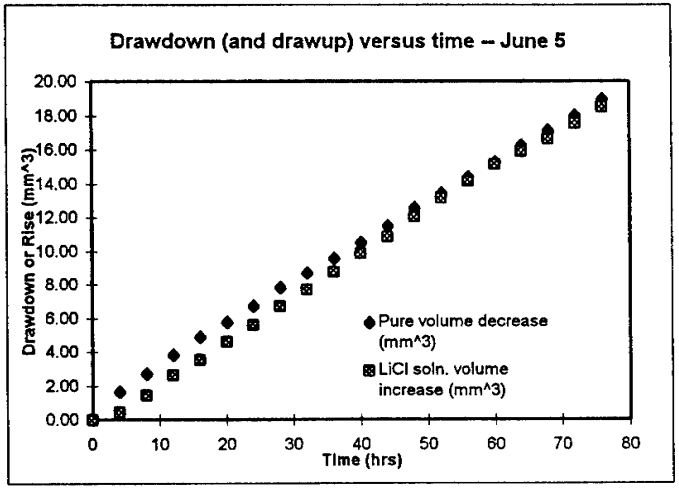

Photo	Date	Time	Hour	Projected pure drawdown	Projected LiCl soln. rise	Actual pure drawdown (mm)	Actual LiCl soln rise (mm)	Pure volume decrease (mm^3)	LiCl soln. volume increase (mm^3)
1	6/5/98	12:00	0	0.0	0.0	0.00	0.00	0.00	0.00
2		16:00	4	1.5	0.4	0.17	0.05	1.62	0.44
3		20:00	8	2.5	1.3	0.28	0.15	2.71	1.42
4	6/6/98	0:00	12	3.5	2.4	0.39	0.27	3.79	2.63
5		4:00	16	4.5	3.2	0.51	0.36	4.87	3.51
6		8:00	20	5.3	4.2	0.60	0.48	5.74	4.60
7		12:00	24	6.2	5.1	0.70	0.58	6.71	5.59
8		16:00	28	7.2	6.1	0.81	0.69	7.79	6.68
9		20:00	32	8.0	7.0	0.90	0.80	8.66	7.67
10	6/7/98	0:00	36	8.8	8.0	0.99	0.91	9.52	8.76
11		4:00	40	9.7	9.0	1.09	1.02	10.50	9.86
12		8:00	44	10.6	9.9	1.19	1.13	11.47	10.84
13		12:00	48	11.6	11.0	1.31	1.25	12.56	12.05
14		16:00	52	12.4	12.0	1.40	1.37	13.42	13.14
15		20:00	56	13.3	12.9	1.50	1.47	14.40	14.13
16	6/8/98	0:00	60	14.1	13.8	1.59	1.57	15.26	15.12
17		4:00	64	15.0	14.5	1.69	1.65	16.24	15.88
18		8:00	68	15.8	15.2	1.78	1.73	17.10	16.65
19		12:00	72	16.6	16.0	1.87	1.82	17.97	17.53
20		16:00	76	17.5	16.9	1.97	1.92	18.94	18.51

Sinlge Pore -- Gas Diffusion Experiment

Begin Date 6/9/98
Begin Time 21:00
Interval 4 hr

	Temperature (C)		
	6/9/98	6/10/98	6/11/98
Min	27.77	28.64	28.75
Max	28.84	28.84	28.88
Ave	28.69	28.75	28.82

	Actual OD (mm)	Actual ID (mm)	Projected OD
left column	5.22	3.5	46.5
right column	5.18	3.5	45.8

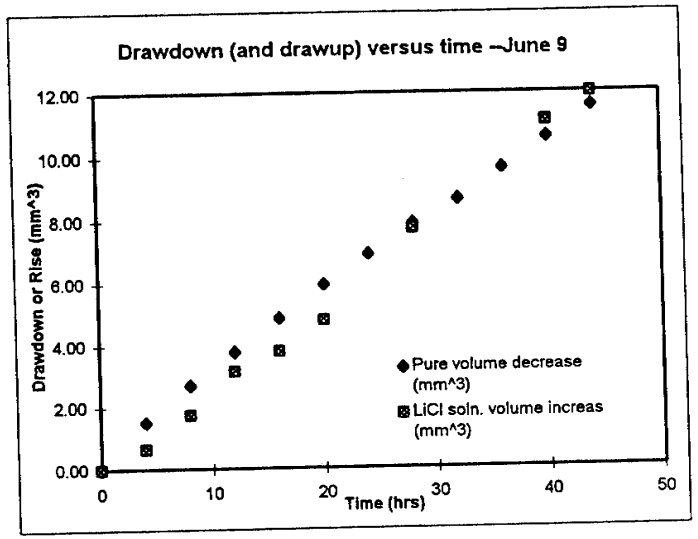

Photo	Date	Time	Hour	Projected pure drawdown	Projected LiCl soln. rise	Actual pure drawdown (mm)	Actual LiCl soln rise (mm)	Pure volume decrease (mm^3)	LiCl soln. volume increase (mm^3)
1	6/9/98	14:10	0	0.0	0.0	0.00	0.00	0.00	0.00
2		18:10	4	1.4	0.6	0.16	0.07	1.51	0.65
3		22:10	8	2.5	1.6	0.28	0.18	2.70	1.74
4	6/10/98	2:10	12	3.5	2.9	0.39	0.33	3.78	3.16
5		6:10	16	4.5	3.5	0.51	0.40	4.86	3.81
6		10:10	20	5.5	4.4	0.62	0.50	5.94	4.79
7		14:10	24	6.4		0.72		6.91	
8		18:10	28	7.3	7.1	0.82	0.80	7.88	7.73
9		22:10	32	8.0		0.90		8.64	
10	6/11/98	2:10	36	8.9		1.00		9.61	
11		6:10	40	9.8	10.2	1.10	1.15	10.58	11.10
12		10:10	44	10.7	11.0	1.20	1.24	11.56	11.97

Note: Missing LiCl solution data due to non-uniform rise.

Appendix D – Liquid-filled single pore-throat drawdown data

Appendix D includes all drawdown data for the liquid-filled single pore-throat experiments. Similar to the tables in Appendix C, these tables include the measured and corrected drawdown data as well as a figure of drawdown versus time. Minimum, maximum, and average temperature adjacent to the diffusion cell is shown on each page.

Sinige Pore -- Liquid Island Experiment

Begin Date 4/2/98
Begin Time 22:30
Interval 2 hr

	Temperature (C)		
	4/2/98	4/3/98	4/4/98
Min	*	29.12	28.10
Max	*	29.19	29.17
Ave	*	29.16	29.05

	Actual OD (mm)	Actual ID (mm)	Projected OD
left column	5.22	3.5	52.5
right column	5.18	3.5	49.9

Initial Island Motility
2.6

Horizontal width 24.84 mm

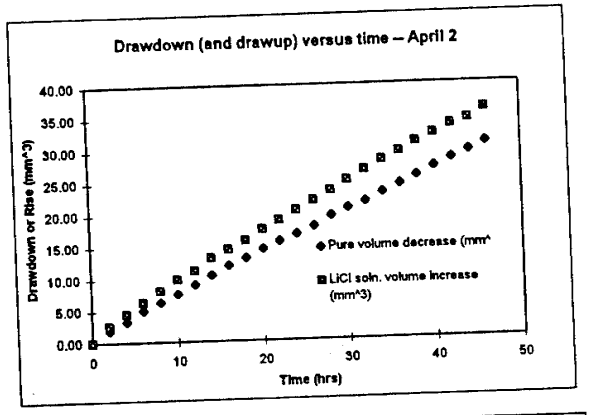

Photo	Date	Time	Hour	Projected pure drawdown	Projected LiCl soln. rise	Actual pure drawdown (mm)	Actual LiCl soln rise (mm)	Pure volume decrease (mm^3)	LiCl soln. volume increase (mm^3)	Projected distance from left side	Projected distance from right side	Actual distance from left side (mm)	Actual Distance from right side (mm)	Length of Island (mm)
1	4/2/98	22:30	0	0.0	0.0	0.00	0.00	0.00	0.00	81.3	73.7	8.08	7.65	9.11
2	4/3/98	0:30	2	2.0	2.5	0.20	0.26	1.91	2.50	82.7	75.7	8.22	7.86	8.76
3		2:30	4	3.4	4.5	0.34	0.47	3.25	4.49	83.6	76.7	8.31	7.96	8.57
4		4:30	6	5.2	6.3	0.52	0.65	4.97	6.29	84.2	77.1	8.37	8.00	8.46
5		6:30	8	6.5	8.0	0.65	0.83	6.22	7.99	84.5	77.7	8.40	8.07	8.37
6		8:30	10	7.9	9.9	0.79	1.03	7.56	9.89	85.0	77.4	8.45	8.03	8.35
7		10:30	12	9.4	11.2	0.93	1.16	8.99	11.19	85.5	77.9	8.50	8.09	8.25
8		12:30	14	11.0	13.2	1.09	1.37	10.52	13.18	85.9	77.9	8.54	8.09	8.21
9		14:30	16	12.5	14.5	1.24	1.51	11.96	14.48	86.1	78.1	8.56	8.11	8.17
10		16:30	18	13.7	15.9	1.36	1.65	13.11	15.88	86.4	78.1	8.59	8.11	8.14
11		18:30	20	15.2	17.6	1.51	1.83	14.54	17.58	86.4	78.1	8.59	8.11	8.14
12		20:30	22	16.4	19.0	1.63	1.97	15.69	18.98	86.6	78.3	8.61	8.13	8.10
13		22:30	24	17.5	20.5	1.74	2.13	16.74	20.47	86.6	78.3	8.61	8.13	8.10
14	4/4/98	0:30	26	18.7	21.9	1.86	2.27	17.89	21.87	86.8	78.3	8.63	8.13	8.08
15		2:30	28	20.3	23.4	2.02	2.43	19.42	23.37	87.2	78.6	8.67	8.16	8.01
16		4:30	30	21.6	25.0	2.15	2.60	20.66	24.97	87.2	78.6	8.67	8.16	8.01
17		6:30	32	22.6	26.6	2.25	2.76	21.62	26.57	87.2	78.6	8.67	8.16	8.01
18		8:30	34	24.0	28.1	2.39	2.92	22.96	28.06	87.4	78.6	8.69	8.16	7.99
19		10:30	36	25.3	29.4	2.52	3.05	24.20	29.36	87.6	78.6	8.71	8.16	7.97
20		12:30	38	26.7	30.8	2.65	3.20	25.54	30.76	87.9	78.8	8.74	8.18	7.92
21		14:30	40	28.1	32.1	2.79	3.33	26.88	32.06	87.9	78.8	8.74	8.18	7.92
22		16:30	42	29.5	33.5	2.93	3.48	28.19	33.46	88.1	79.0	8.76	8.20	7.88
23		18:30	44	30.6	34.3	3.04	3.56	29.27	34.26	88.3	79.0	8.78	8.20	7.86
24		20:30	46	32.0	35.9	3.18	3.73	30.61	35.85	88.3	79.0	8.78	8.20	7.86

* Denotes temperature not taken on this day (only 1.5 hours missing).

Single Pore – Liquid Island Experiment

Begin Date 4/6/98
Begin Time 14:45
Interval 4 hr

	Temperature (C)			
	4/6/98	4/7/98	4/8/98	4/9/98
Min	28.89	28.96	28.98	28.97
Max	29.04	29.10	29.08	29.03
Ave	29.01	29.03	29.01	28.99

	Actual OD (mm)	Actual ID (mm)	Projected OD
left column	5.22	3.5	51.3
right column	5.18	3.5	50.3

Initial Island Molality
2.6

Horizontal width 24.84 mm

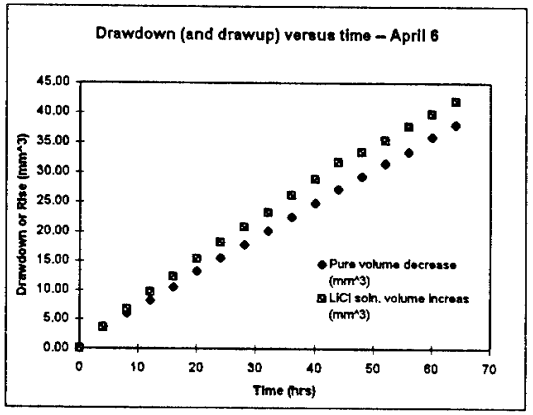

Photo	Date	Time	Hour	Projected pure drawdown	Projected LiCl soln. rise	Actual pure drawdown (mm)	Actual LiCl soln rise (mm)	Pure volume decrease (mm^3)	LiCl soln. volume increase (mm^3)	Projected distance from left side	Projected distance from right side	Actual distance from left side (mm)	Actual Distance from right side (mm)	Length of island (mm)
1	4/6/98	14:45	0	0.0	0.0	0.00	0.00	0.00	0.00	81.6	78.4	8.30	8.07	8.46
2		16:45	2											
3		18:45	4	3.7	3.5	0.38	0.36	3.62	3.47	82.8	82.1	8.43	8.45	7.96
4		20:45	6											
5		22:45	8	6.0	6.8	0.61	0.70	5.87	6.74	83.7	83.6	8.52	8.61	7.71
6		0:45	10											
7	4/7/98	2:45	12	8.3	9.7	0.84	1.00	8.13	9.61	83.7	84.4	8.52	8.69	7.63
8		4:45	14											
9		6:45	16	10.7	12.4	1.09	1.28	10.48	12.29	84.1	84.7	8.56	8.72	7.56
10		8:45	18											
11		10:45	20	13.4	15.5	1.36	1.60	13.12	15.36	84.1	84.7	8.56	8.72	7.56
12		12:45	22											
13		14:45	24	15.8	18.3	1.61	1.88	15.47	18.13	84.3	84.7	8.58	8.72	7.54
14		16:45	26											
15		18:45	28	18.1	20.9	1.84	2.15	17.72	20.71	84.8	84.7	8.63	8.72	7.49
16		20:45	30											
17		22:45	32	20.5	23.5	2.09	2.42	20.07	23.28	85.1	84.7	8.66	8.72	7.46
18		0:45	34											
19	4/8/98	2:45	36	22.9	26.4	2.33	2.72	22.42	26.16	85.4	84.7	8.69	8.72	7.43
20		4:45	38											
21		6:45	40	25.4	29.2	2.58	3.01	24.87	28.93	85.4	84.7	8.69	8.72	7.43
22		8:45	42											
23		10:45	44	27.8	32.0	2.83	3.30	27.22	31.71	85.4	84.7	8.69	8.72	7.43
24		12:45	46											
25		14:45	48	30.0	33.8	3.05	3.48	29.37	33.49	85.8	84.7	8.73	8.72	7.39
26		16:45	50											
27		18:45	52	32.2	35.7	3.28	3.68	31.52	35.37	85.8	84.7	8.73	8.72	7.39
28		20:45	54											
29		22:45	56	34.2	38.1	3.48	3.92	33.48	37.75	86.1	84.9	8.76	8.74	7.34
30		0:45	58											
31	4/9/98	2:45	60	36.7	40.2	3.73	4.14	35.93	39.83	86.1	84.9	8.76	8.74	7.34
32		4:45	62											
33		6:45	64	38.8	42.3	3.95	4.36	37.98	41.91	86.1	84.9	8.76	8.74	7.34

Note: Solid salt crystals dissolved at hour 40. Experiment was run for 24 hours after solid LiCl dissolved to observe effect

Single Pore -- Liquid Island Experiment

Begin Date 4/24/98
Begin Time 21:00
Interval 2 hr

	Temperature (C)		
	4/24/98	4/25/98	4/26/98
Min	29.21	29.21	*
Max	29.30	29.29	*
Ave	29.24	29.24	*

	Actual OD (mm)	Actual ID (mm)	Projected OD
left column	5.22	3.5	50.7
right column	5.18	3.5	49.7

Initial Island Molality
2.6

Horizontal width 24.84 mm

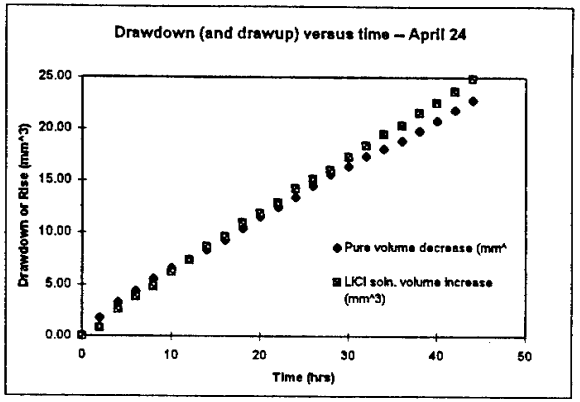

Photo	Date	Time	Hour	Projected pure drawdown	Projected LiCl soln. rise	Actual pure drawdown (mm)	Actual LiCl soln rise (mm)	Pure volume decrease (mm^3)	LiCl soln. volume increase (mm^3)	Projected distance from left side	Projected distance from right side	Actual distance from left side (mm)	Actual Distance from right side (mm)	Length of Island (mm)
1	4/24/98	21:00	0	0.0	0.0	0.00	0.00	0.00	0.00	85.7	87.6	8.82	9.13	6.89
2		23:00	2	1.8	0.8	0.19	0.08	1.78	0.80	87.6	88.4	9.02	9.21	6.61
3	4/25/98	1:00	4	3.3	2.6	0.34	0.27	3.27	2.61	89.0	88.4	9.16	9.21	6.46
4		3:00	6	4.4	3.8	0.45	0.40	4.36	3.81	89.9	88.7	9.26	9.24	6.34
5		5:00	8	5.6	4.8	0.58	0.50	5.55	4.81	90.6	89.1	9.33	9.29	6.23
6		7:00	10	6.6	6.2	0.68	0.65	6.54	6.22	91.3	89.1	9.40	9.29	6.15
7		9:00	12	7.5	7.3	0.77	0.76	7.43	7.32	92.0	89.1	9.47	9.29	6.08
8		11:00	14	8.4	8.6	0.86	0.90	8.32	8.62	92.4	89.3	9.51	9.31	6.02
9		13:00	16	9.4	9.6	0.97	1.00	9.31	9.63	92.6	89.5	9.53	9.33	5.98
10		15:00	18	10.5	10.9	1.08	1.14	10.40	10.93	92.8	89.5	9.55	9.33	5.96
11		17:00	20	11.6	11.8	1.19	1.23	11.49	11.83	92.8	89.5	9.55	9.33	5.96
12		19:00	22	12.5	12.8	1.29	1.33	12.38	12.84	92.9	89.7	9.56	9.35	5.93
13		21:00	24	13.5	14.2	1.39	1.48	13.37	14.24	92.9	89.7	9.56	9.35	5.93
14		23:00	26	14.6	15.1	1.50	1.57	14.46	15.14	92.9	89.9	9.56	9.37	5.91
15	4/26/98	1:00	28	15.7	15.9	1.62	1.66	15.55	15.94	92.9	89.9	9.56	9.37	5.91
16		3:00	30	16.5	17.2	1.70	1.79	16.34	17.25	92.9	89.9	9.56	9.37	5.91
17		5:00	32	17.5	18.3	1.80	1.91	17.34	18.35	92.9	89.9	9.56	9.37	5.91
18		7:00	34	18.2	19.4	1.87	2.02	18.03	19.45	92.9	89.9	9.56	9.37	5.91
19		9:00	36	19.0	20.3	1.96	2.12	18.82	20.36	92.9	90.2	9.56	9.40	5.87
20		11:00	38	20.0	21.5	2.06	2.24	19.81	21.56	92.9	90.2	9.56	9.40	5.87
21		13:00	40	21.0	22.5	2.16	2.35	20.80	22.56	92.9	90.2	9.56	9.40	5.87
22		15:00	42	22	23.6	2.27	2.46	21.79	23.67	92.9	90.2	9.56	9.40	5.87
23		17:00	44	23	24.8	2.37	2.58	22.78	24.87	92.9	90.2	9.56	9.40	5.87

* Denotes temperature not taken on this day (only 1.5 hours missing).

Single Pore -- Liquid Island Experiment

Begin Date 4/27/98
Begin Time 17:45
Interval 2 hr

Notes: air bubbles release from LiCl soln.

	Temperature (C)		
	4/27/98	4/28/98	4/29/98
Min	29.05	28.49	29.00
Max	29.08	29.08	29.06
Ave	29.06	29.02	29.02

	Actual OD (mm)	Actual ID (mm)	Projected OD
left column	5.22	3.5	52.0
right column	5.18	3.5	50.7

Horizontal width 24.84 mm

Initial Island Molality
2.6

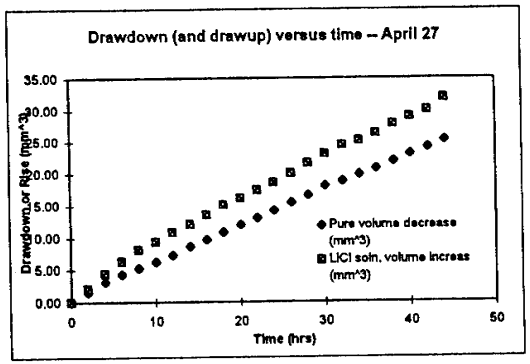

Photo	Date	Time	Hour	Projected pure drawdown	Projected LiCl soln. rise	Actual pure drawdown (mm)	Actual LiCl soln rise (mm)	Pure volume decrease (mm^3)	LiCl soln. volume increase (mm^3)	Projected distance from left side	Projected distance from right side	Actual distance from left side (mm)	Actual Distance from right side (mm)	Length of Island (mm)
1	4/27/98	17:45	0	0.0	0.0	0.00	0.00	0.00	0.00	80.9	74.3	8.12	7.59	9.13
2		19:45	2	1.6	2.1	0.16	0.21	1.55	2.06	83.5	76.9	8.38	7.86	8.60
3		21:45	4	3.3	4.5	0.33	0.46	3.19	4.42	85.8	77.3	8.61	7.90	8.33
4		23:45	6	4.5	6.4	0.45	0.65	4.35	6.29	88.6	77.3	8.89	7.90	8.05
5	4/28/98	1:45	8	5.4	8.2	0.54	0.84	5.22	8.06	90.4	77.9	9.07	7.96	7.81
6		3:45	10	6.4	9.5	0.64	0.97	6.18	9.34	90.6	79.4	9.09	8.11	7.63
7		5:45	12	7.5	11.0	0.75	1.12	7.24	10.81	90.6	80.3	9.09	8.20	7.54
8		7:45	14	8.9	12.3	0.89	1.26	8.60	12.09	90.6	80.7	9.09	8.25	7.50
9		9:45	16	10.0	13.8	1.00	1.41	9.66	13.57	90.6	81.0	9.09	8.28	7.47
10		11:45	18	11.2	15.3	1.12	1.56	10.82	15.04	90.6	81.3	9.09	8.31	7.44
11		13:45	20	12.4	16.4	1.24	1.68	11.98	16.12	90.6	81.5	9.09	8.33	7.42
12		15:45	22	13.5	17.7	1.36	1.81	13.04	17.40	90.6	81.5	9.09	8.33	7.42
13		17:45	24	14.6	18.9	1.47	1.93	14.10	18.58	90.6	81.5	9.09	8.33	7.42
14		19:45	26	15.9	20.4	1.60	2.08	15.36	20.05	90.6	81.5	9.09	8.33	7.42
15		21:45	28	17.1	22.0	1.72	2.25	16.52	21.63	90.6	81.7	9.09	8.35	7.40
16		23:45	30	18.6	23.4	1.87	2.39	17.99	23.00	90.6	81.7	9.09	8.35	7.40
17	4/29/98	1:45	32	19.4	24.8	1.95	2.53	18.74	24.38	90.6	81.7	9.09	8.35	7.40
18		3:45	34	20.5	25.6	2.06	2.62	19.80	25.16	90.6	81.7	9.09	8.35	7.40
19		5:45	36	21.5	26.8	2.16	2.74	20.76	26.34	90.6	81.7	9.09	8.35	7.40
20		7:45	38	22.7	28.3	2.28	2.89	21.92	27.82	90.6	81.7	9.09	8.35	7.40
21		9:45	40	23.9	29.4	2.40	3.00	23.08	28.90	90.6	81.7	9.09	8.35	7.40
22		11:45	42	25.0	30.5	2.51	3.12	24.15	29.98	90.6	81.8	9.09	8.36	7.39
23		13:45	44	26.1	32.4	2.62	3.31	25.21	31.85	90.6	81.8	9.09	8.36	7.39

Single Pore -- Liquid Island Experiment

Begin Date 5/21/98
Begin Time 14:45
Interval 2 hr

	Temperature (C)	
	5/21/98	5/22/98
Min	27.63	27.97
Max	28.21	28.18
Ave	27.90	28.10

	Actual OD (mm)	Actual ID (mm)	Measured OD
left column	5.22	3.5	46
right column	5.18	3.5	44.4

	actual (mm)	Measured
Total length	24.84	183.3

Initial Island Molality
3.3

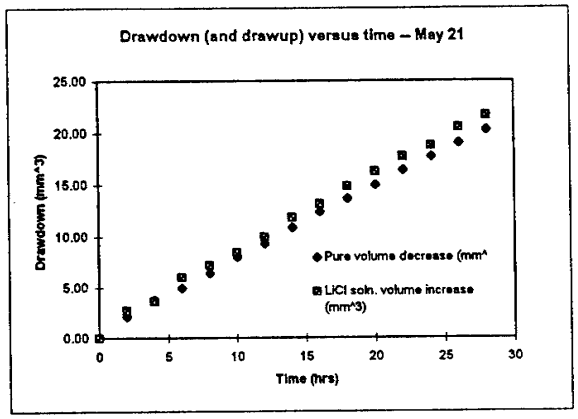

Picture #	Date	Time	Hour	Measured pure drawdown	Measured LiCl soln. rise	Actual pure drawdown (mm)	Actual LiCl soln rise (mm)	Pure volume decrease (mm^3)	LiCl soln. volume increase (mm^3)	Measured distance from left side	Measured distance from right side	Actual distance from left side (mm)	Actual Distance from right side (mm)	Length of Island (mm)
1	5/21/98	14:45	0	0.0	0.0	0.00	0.00	0.00	0.00	62.3	56.5	8.44	7.66	8.74
2		16:45	2	1.9	2.4	0.22	0.28	2.07	2.69	61.7	56.2	8.36	7.62	8.86
3		18:45	4	3.4	3.2	0.39	0.37	3.71	3.59	61.7	55.6	8.36	7.53	8.94
4		20:45	6	4.5	5.3	0.51	0.62	4.91	5.95	61.1	55.6	8.28	7.53	9.03
5		22:45	8	5.8	6.4	0.66	0.75	6.33	7.18	61.1	55.4	8.28	7.51	9.05
6	5/22/98	0:45	10	7.3	7.5	0.83	0.88	7.97	8.42	61.1	55.6	8.28	7.53	9.03
7		2:45	12	8.5	8.8	0.96	1.03	9.28	9.88	61.1	55.6	8.28	7.53	9.03
8		4:45	14	9.9	10.5	1.12	1.23	10.81	11.79	61.1	55.6	8.28	7.53	9.03
9		6:45	16	11.3	11.7	1.28	1.37	12.34	13.13	61.1	55.6	8.28	7.53	9.03
10		8:45	18	12.5	13.2	1.42	1.54	13.65	14.82	61.7	55.4	8.36	7.51	8.97
11		10:45	20	13.7	14.5	1.55	1.69	14.96	16.28	61.7	55.4	8.36	7.51	8.97
12		12:45	22	15.0	15.8	1.70	1.84	16.38	17.73	61.7	56.2	8.36	7.62	8.86
13		14:45	24	16.2	16.7	1.84	1.95	17.69	18.75	61.7	55.4	8.36	7.51	8.97
14		16:45	26	17.4	18.3	1.97	2.14	19.00	20.54	61.7	55.6	8.36	7.53	8.94
15		18:45	28	18.6	19.3	2.11	2.25	20.31	21.66	61.7	55.6	8.36	7.53	8.94

Single Pore – Liquid Island Experiment

Begin Date 5/26/98
Begin Time 11:30
Interval 2 hr

	Temperature (C)	
	5/26/98	5/27/98
Min	27.52	27.48
Max	27.78	28.38
Ave	27.63	27.86

	Actual OD (mm)	Actual ID (mm)	Projected OD
left column	5.22	3.5	41.3
right column	5.18	3.5	40.7

Initial Island Motility
2.9

Horizontal Width 24.84 mm

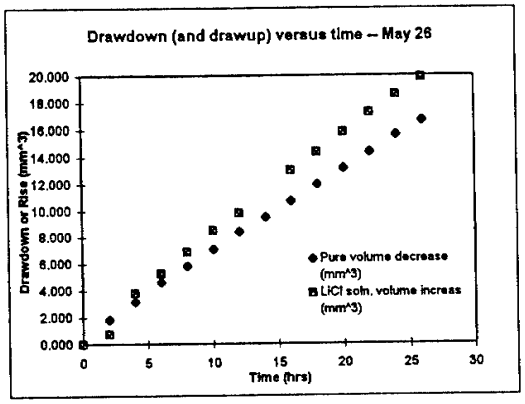

Photo	Date	Time	Hour	Projected pure drawdown	Projected LiCl soln. rise	Actual pure drawdown (mm)	Actual LiCl soln rise (mm)	Pure volume decrease (mm^3)	LiCl soln. volume increase (mm^3)	Projected distance from left side	Projected distance from right side	Actual distance from left side (mm)	Actual Distance from right side (mm)	Length of island (mm)
1	5/26/98	11:30	0	0	0	0.000	0.000	0.000	0.000	63.5	60.5	8.026	7.700	9.114
2		13:30	2	1.5	0.6	0.190	0.076	1.824	0.735	65	61.8	8.215	7.865	8.759
3		15:30	4	2.6	3.1	0.329	0.395	3.162	3.796	66.5	62.3	8.405	7.929	8.506
4		17:30	6	3.8	4.3	0.480	0.547	4.621	5.265	67.5	62.3	8.531	7.929	8.379
5		19:30	8	4.8	5.6	0.607	0.713	5.837	6.857	68	62.3	8.595	7.929	8.316
6		21:30	10	5.8	6.9	0.733	0.878	7.053	8.449	68.8	62.5	8.696	7.955	8.190
7		23:30	12	6.9	8	0.872	1.018	8.391	9.796	69.6	62.5	8.797	7.955	8.089
8	5/27/98	1:30	14	7.8		0.986		9.485		70	62.5	8.847	7.955	8.038
9		3:30	16	8.8	10.6	1.112	1.349	10.701	12.980	70.6	62.5	8.923	7.955	7.962
10		5:30	18	9.8	11.7	1.239	1.489	11.917	14.327	71	62.5	8.974	7.955	7.912
11		7:30	20	10.8	12.9	1.365	1.642	13.133	15.796	71.4	62.7	9.024	7.980	7.836
12		9:30	22	11.8	14.1	1.491	1.795	14.349	17.266	71.6	62.7	9.050	7.980	7.810
13		11:30	24	12.8	15.2	1.618	1.935	15.565	18.613	71.7	62.9	9.062	8.005	7.772
14		13:30	26	13.7	16.2	1.732	2.062	16.660	19.837	71.8	62.9	9.075	8.005	7.760

bland cell denotes missing data due to non-uniform rise in LiCl solution

Single Pore -- Liquid Island Experiment

Begin Date 5/30/98
Begin Time 13:15
Interval 2 hr

	Temperature (C)	
	5/30/98	5/31/98
Min	28.44	28.24
Max	28.86	28.66
Ave	28.75	28.52

	Actual OD (mm)	Actual ID (mm)	Projected OD
left column	5.22	3.5	45.9
right column	5.18	3.5	44.9

Horizontal Width 24.84 mm

Initial Island Molality
1.5

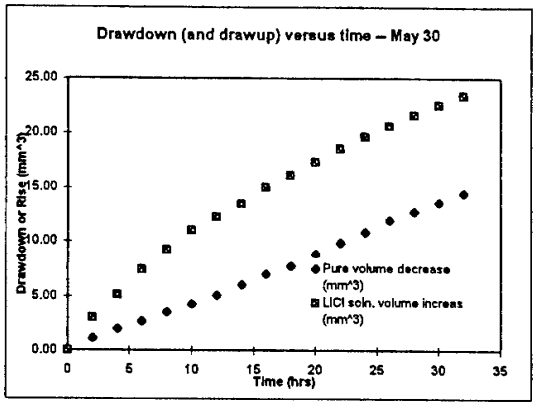

Photo	Date	Time	Hour	Projected pure drawdown	Projected LiCl soln. rise	Actual pure drawdown (mm)	Actual LiCl soln rise (mm)	Pure volume decrease (mm^3)	LiCl soln. volume increase (mm^3)	Projected distance from left side	Projected distance from right side	Actual distance from left side (mm)	Actual Distance from right side (mm)	Length of Island (mm)
1	5/30/98	13:15	0	0.0	0.0	0.00	0.00	0.00	0.00	67.2	68.5	7.64	7.90	9.29
2		15:15	2	1.0	2.7	0.11	0.31	1.09	3.00	71.8	71.2	8.17	8.21	8.46
3		17:15	4	1.8	4.6	0.20	0.53	1.97	5.11	73.5	75.9	8.36	8.76	7.72
4		19:15	6	2.4	6.7	0.27	0.77	2.63	7.44	75.7	77.8	8.61	8.98	7.26
5		21:15	8	3.2	8.3	0.36	0.96	3.50	9.21	79.3	78.1	9.02	9.01	6.81
6		23:15	10	3.9	9.9	0.44	1.14	4.27	10.99	81.1	81.1	9.22	9.36	6.26
7	5/31/98	1:15	12	4.6	11.0	0.52	1.27	5.03	12.21	81.6	82.2	9.28	9.48	6.08
8		3:15	14	5.5	12.1	0.63	1.40	6.02	13.43	82.1	83.2	9.34	9.60	5.90
9		5:15	16	6.4	13.5	0.73	1.56	7.00	14.98	82.4	83.8	9.37	9.67	5.80
10		7:15	18	7.1	14.5	0.81	1.67	7.77	16.09	82.7	84.5	9.41	9.75	5.69
11		9:15	20	8.0	15.6	0.91	1.80	8.75	17.32	82.9	84.8	9.43	9.78	5.63
12		11:15	22	9.0	16.7	1.02	1.93	9.85	18.54	82.9	85.1	9.43	9.82	5.59
13		13:15	24	9.9	17.7	1.13	2.04	10.83	19.65	82.9	85.3	9.43	9.84	5.57
14		15:15	26	10.9	18.6	1.24	2.15	11.93	20.65	82.9	85.3	9.43	9.84	5.57
15		17:15	28	11.6	19.5	1.32	2.25	12.69	21.64	82.9	85.3	9.43	9.84	5.57
16		19:15	30	12.4	20.3	1.41	2.34	13.57	22.53	82.9	85.5	9.43	9.86	5.55
17		21:15	32	13.2	21.1	1.50	2.43	14.44	23.42	82.7	85.5	9.41	9.86	5.57

Single Pore – Liquid Island Experiment

Begin Date 6/11/98
Begin Time 13:15
Interval 2 hr

	Temperature (C)		
	6/11/98	6/12/98	6/13/98
Min	28.78	28.79	28.78
Max	28.83	28.89	28.87
Ave	28.81	28.83	28.81

	Actual OD (mm)	Actual ID (mm)	Projected OD
left column	5.22	3.5	44.9

Initial Island Molality
2.8

Horizontal width 24.84 mm

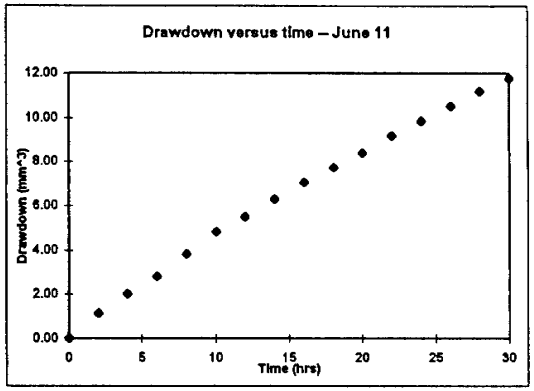

Picture #	Date	Time	Hour	Projected pure drawdown	Actual pure drawdown (mm)	Pure volume decrease (mm^3)	Projected distance from left side	Projected distance from right side	Actual distance from left side (mm)	Actual Distance from right side (mm)	Length of Island (mm)
1	6/11/98	22:15	0	0.0	0.00	0.00	87.4	93.8	10.16	10.90	3.78
2	6/12/98	0:15	2	1.0	0.12	1.12	88.5	94.9	10.29	11.03	3.52
3		2:15	4	1.8	0.21	2.01	88.9	95.3	10.34	11.08	3.43
4		4:15	6	2.5	0.29	2.80	88.9	95.7	10.34	11.12	3.38
5		6:15	8	3.4	0.40	3.80	88.9	95.7	10.34	11.12	3.38
6		8:15	10	4.3	0.50	4.81	88.9	95.7	10.34	11.12	3.38
7		10:15	12	4.9	0.57	5.48	88.9	95.7	10.34	11.12	3.38
8		12:15	14	5.6	0.65	6.26	88.9	95.7	10.34	11.12	3.38
9		14:15	16	6.3	0.73	7.05	88.9	95.7	10.34	11.12	3.38
10		16:15	18	6.9	0.80	7.72	88.9	95.7	10.34	11.12	3.38
11		18:15	20	7.5	0.87	8.39	88.9	95.7	10.34	11.12	3.38
12		20:15	22	8.2	0.95	9.17	88.9	95.7	10.34	11.12	3.38
13		22:15	24	8.8	1.02	9.84	88.9	95.7	10.34	11.12	3.38
14	6/13/98	0:15	26	9.4	1.09	10.51	88.9	95.9	10.34	11.14	3.36
15		2:15	28	10.0	1.16	11.19	88.9	95.9	10.34	11.14	3.36
16		4:15	30	10.5	1.22	11.74	88.9	95.9	10.34	11.14	3.36

Single Pore – Liquid Island Experiment

Begin Date 6/13/98
Begin Time 17:15
Interval 4 hr

	Temperature (C)		
	6/13/98	6/14/98	6/15/98
Min	28.75	28.79	28.77
Max	28.88	28.90	28.93
Ave	28.84	28.84	28.84

	Actual OD (mm)	Actual ID (mm)	Projected OD
left column	5.22	3.5	37.4

Initial Island Molalty
2.8

Horizontal width 24.84 mm

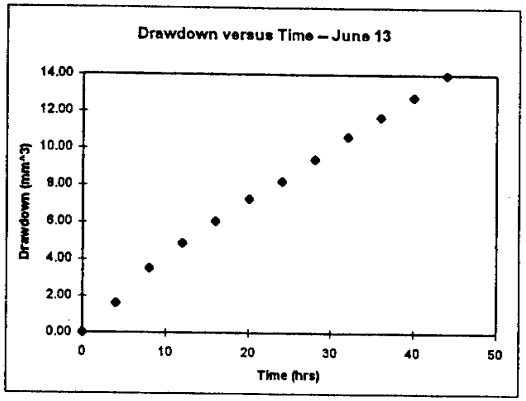

Picture #	Date	Time	Hour	Projected pure drawdown	Actual pure drawdown (mm)	Pure volume decrease (mm^3)	Projected distance from left side	Projected distance from right side	Actual distance from left side (mm)	Actual Distance from right side (mm)	Length of Island (mm)
1	6/13/98	17:15	0	0.0	0.00	0.00	78.5	81.6	10.96	11.39	2.49
2		21:15	4	1.2	0.17	1.61	78.9	83.4	11.01	11.64	2.19
3	6/14/98	1:15	8	2.6	0.36	3.49	79.1	83.4	11.04	11.64	2.16
4		5:15	12	3.6	0.50	4.83	79.1	83.4	11.04	11.64	2.16
5		9:15	16	4.5	0.63	6.04	79.1	83.4	11.04	11.64	2.16
6		13:15	20	5.4	0.75	7.25	79.1	83.4	11.04	11.64	2.16
7		17:15	24	6.1	0.85	8.19	79.1	83.4	11.04	11.64	2.16
8		21:15	28	7.0	0.98	9.40	79.1	83.4	11.04	11.64	2.16
9	6/15/98	1:15	32	7.9	1.10	10.61	79.1	83.4	11.04	11.64	2.16
10		5:15	36	8.7	1.214	11.683	79.1	83.4	11.040	11.640	2.160
11		9:15	40	9.5	1.326	12.757	79.1	83.4	11.040	11.640	2.160
12		13:15	44	10.4	1.452	13.966	79.1	83.4	11.040	11.640	2.160

Single Pore -- Liquid Island Experiment

Begin Date 6/15/98
Begin Time 20:15
Interval 2 hr

	Temperature (C)		
	6/15/98	6/16/98	6/17/98
Min	28.78	28.77	28.80
Max	28.93	29.02	28.88
Ave	28.83	28.87	28.84

	Actual OD (mm)	Actual ID (mm)	Projected OD
left column	5.22	3.5	35.4

Initial Island Molality
2.6

Horizontal width 24.84 mm

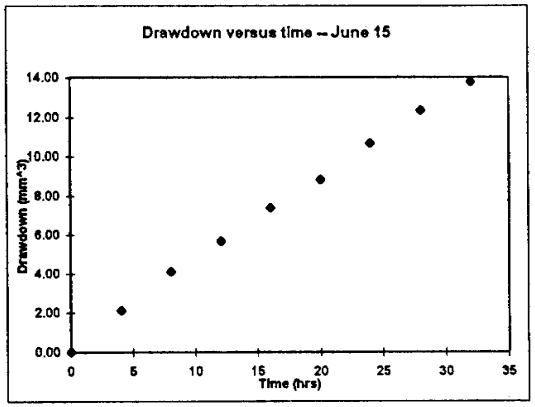

Picture #	Date	Time	Hour	Projected pure drawdown	Actual pure drawdown (mm)	Pure volume decrease (mm^3)	Projected distance from left side	Projected distance from right side	Actual distance from left side (mm)	Actual Distance from right side (mm)	Length of island (mm)
1	6/15/98	20:15	0	0.0	0.00	0.00	68.2	68.9	10.06	10.16	4.62
2		22:15	2								
3	6/16/98	0:15	4	1.5	0.22	2.13	68.9	70.8	10.16	10.44	4.24
4		2:15	6								
5		4:15	8	2.9	0.43	4.11	69.1	71.1	10.19	10.48	4.17
6		6:15	10								
7		8:15	12	4.0	0.59	5.67	69.1	71.1	10.19	10.48	4.17
8		10:15	14								
9		12:15	16	5.2	0.77	7.38	69.1	71.1	10.19	10.48	4.17
10		14:15	18								
11		16:15	20	6.2	0.91	8.80	69.1	71.1	10.19	10.48	4.17
12		18:15	22								
13		20:15	24	7.5	1.11	10.64	69.1	71.1	10.19	10.48	4.17
14		22:15	26								
15	6/17/98	0:15	28	8.7	1.28	12.34	69.1	71.1	10.19	10.48	4.17
16		2:15	30								
17		4:15	32	9.7	1.43	13.76	69.1	71.1	10.19	10.48	4.17

Sinlge Pore –Liquid Island Experiment

Begin Date 6/17/98
Begin Time 22:00
Interval 2 hr

	Temperature (C)		
	6/17/98	6/18/98	6/19/98
Min	28.64	28.77	28.78
Max	28.83	28.93	28.90
Ave	28.75	28.83	28.84

	Actual OD (mm)	Actual ID (mm)	Projected OD
left column	5.22	3.5	34.9

Initial Island Molalty
2.6

	Actual (mm)	Projected
Total length	24.84	164.3

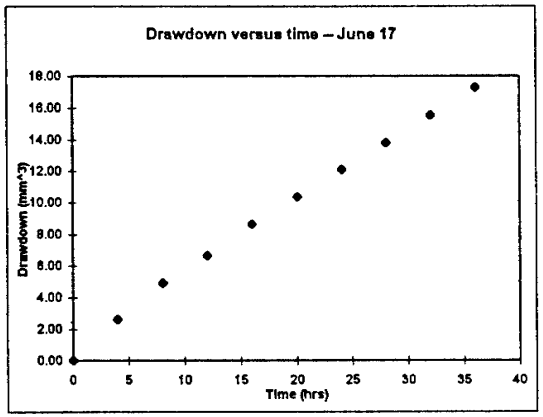

Picture #	Date	Time	Hour	Projected pure drawdown	Actual pure drawdown (mm)	Pure volume decrease (mm^3)	Projected distance from left side	Projected distance from right side	Actual distance from left side (mm)	Actual Distance from right side (mm)	Length of island (mm)
1	6/17/98	22:00	0	0.0	0.00	0.00	63.9	60.6	9.66	9.16	6.02
2	6/18/98	0:00	2								
3		2:00	4	1.8	0.27	2.59	64.6	63.2	9.77	9.56	5.52
4		4:00	6								
5		6:00	8	3.4	0.51	4.89	64.6	63.8	9.77	9.65	5.43
6		8:00	10								
7		10:00	12	4.6	0.69	6.62	64.6	63.9	9.77	9.66	5.41
8		12:00	14								
9		14:00	16	6.0	0.90	8.63	64.6	64.0	9.77	9.68	5.40
10		16:00	18								
11		18:00	20	7.2	1.08	10.36	64.7	64.0	9.78	9.68	5.38
12		20:00	22								
13		22:00	24	8.4	1.26	12.09	64.7	64.0	9.78	9.68	5.38
14	6/19/98	0:00	26								
15		2:00	28	9.6	1.44	13.81	64.7	64.0	9.78	9.68	5.38
16		4:00	30								
17		6:00	32	10.8	1.62	15.54	64.7	64.0	9.78	9.68	5.38
18		8:00	34								
19		10:00	36	12.0	1.79	17.27	64.7	64.0	9.78	9.68	5.38

Single Pore – Liquid Island Experiment

Begin Date 6/21/98
Begin Time 22:20
Interval 2 hr

	Temperature (C)		
	6/21/98	6/22/98	6/23/98
Min	28.69	28.69	28.71
Max	28.82	28.87	28.89
Ave	28.76	28.79	28.78

	Actual OD (mm)	Actual ID (mm)	Projected OD
left column	5.22	3.5	32

	Actual (mm)	Projected
Total length	24.84	150.6

Initial Island Molalty
2.6

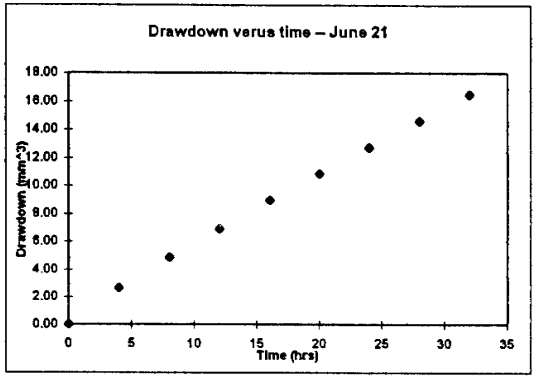

Picture #	Date	Time	Hour	Projected pure drawdown	Actual pure drawdown (mm)	Pure volume decrease (mm^3)	Projected distance from left side	Projected distance from right side	Actual distance from left side (mm)	Actual Distance from right side (mm)	Length of island (mm)
1	6/21/98	22:20	0	0.0	0.00	0.00	54.2	57.5	8.94	9.48	6.42
2	6/22/98	0:20	2								
3		2:20	4	1.7	0.28	2.67	55.5	58.4	9.15	9.63	6.05
4		4:20	6								
5		6:20	8	3.1	0.51	4.87	56	58.7	9.24	9.68	5.92
6		8:20	10								
7		10:20	12	4.4	0.72	6.91	56.3	58.7	9.29	9.68	5.87
8		12:20	14								
9		14:20	16	5.7	0.93	8.95	56.6	58.7	9.34	9.68	5.82
10		16:20	18								
11		18:20	20	6.9	1.13	10.83	56.6	58.9	9.34	9.71	5.79
12		20:20	22								
13		22:20	24	8.1	1.32	12.71	56.6	58.9	9.34	9.71	5.79
14	6/23/98	0:20	26								
15		2:20	28	9.3	1.52	14.60	56.6	58.9	9.34	9.71	5.79
16		4:20	30								
17		6:20	32	10.5	1.71	16.48	56.6	58.9	9.34	9.71	5.79

Single Pore – Liquid Island Experiment

Begin Date 7/13/98
Begin Time 22:20
Interval 4 hr

	Temperature (C)		
	7/13/98	7/14/98	7/15/98
Min	28.75	28.75	28.79
Max	28.86	28.86	28.84
Ave	28.82	28.81	28.82

	Actual OD (mm)	Actual ID (mm)	Projected OD
left column	5.22	3.5	29.5

Initial Island Molality
2.6

Horizontal width 24.84 mm

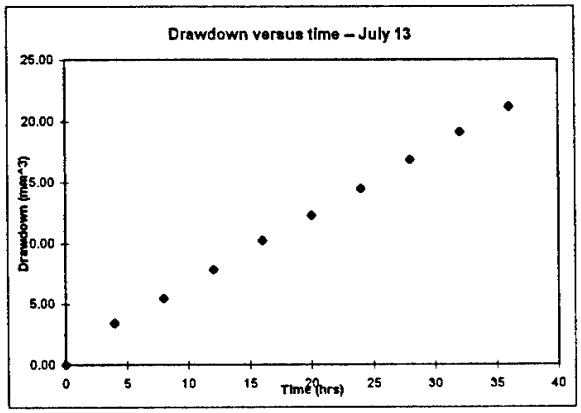

Picture #	Date	Time	Hour	Projected pure drawdown	Actual pure drawdown (mm)	Pure volume decrease (mm^3)	Projected distance from left side	Projected distance from right side	Actual distance from left side (mm)	Actual Distance from right side (mm)	Length of island (mm)
1	7/13/98	22:20	0	0.0	0.00	0.00	46.6	48	8.25	8.49	8.10
2	7/14/98	2:20	4	2.0	0.35	3.40	47.8	48.5	8.46	8.58	7.80
3		6:20	8	3.2	0.57	5.45	48.3	48.9	8.55	8.65	7.64
4		10:20	12	4.6	0.81	7.83	49	49.5	8.67	8.76	7.41
5		14:20	16	6.0	1.06	10.21	49.4	49.5	8.74	8.76	7.34
6		18:20	20	7.2	1.27	12.26	49.6	49.9	8.78	8.83	7.23
7		22:20	24	8.5	1.50	14.47	49.6	49.9	8.78	8.83	7.23
8	7/15/98	2:20	28	9.9	1.75	16.85	49.6	49.9	8.78	8.83	7.23
9		6:20	32	11.2	1.98	19.07	49.6	50	8.78	8.85	7.22
10		10:20	36	12.4	2.19	21.11	49.6	50	8.78	8.85	7.22

Single Pore -- Liquid Island Experiment

Begin Date 7/18/98
Begin Time 19:10
Interval 4 hr

	Temperature (C)		
	7/18/98	7/19/98	7/20/98
Min	28.88	28.87	28.85
Max	28.92	28.91	28.91
Ave	28.89	28.89	28.88

	Actual OD (mm)	Actual ID (mm)	Projected OD
left column	5.22	3.5	27.8

Initial Island Molality
2.6

Horizontal width 24.84 mm

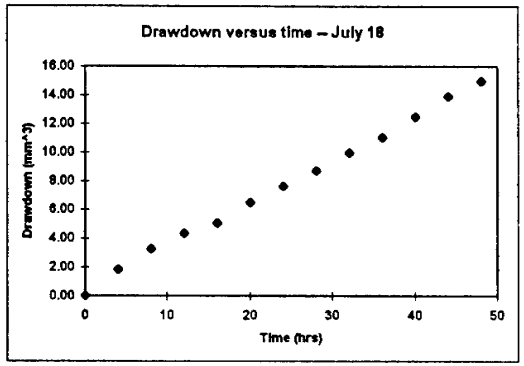

Picture #	Date	Time	Hour	Projected pure drawdown	Actual pure drawdown (mm)	Pure volume decrease (mm^3)	Projected distance from left side	Projected distance from right side	Actual distance from left side (mm)	Actual Distance from right side (mm)	Length of Island (mm)
1	7/18/98	19:10	0	0.0	0.00	0.00	54.3	66.5	10.20	12.49	2.16
2		23:10	4	1.0	0.19	1.81	54.3	66.5	10.20	12.49	2.16
3	7/19/98	3:10	8	1.8	0.34	3.25	54.3	66.5	10.20	12.49	2.16
4		7:10	12	2.4	0.45	4.34	54.3	66.5	10.20	12.49	2.16
5		11:10	16	2.8	0.53	5.06	54.3	66.5	10.20	12.49	2.16
6		15:10	20	3.6	0.68	6.50	54.3	66.5	10.20	12.49	2.16
7		19:10	24	4.2	0.79	7.59	54.3	66.5	10.20	12.49	2.16
8		23:10	28	4.8	0.90	8.67	54.3	66.5	10.20	12.49	2.16
9	7/20/98	3:10	32	5.5	1.03	9.94	54.3	66.5	10.20	12.49	2.16
10		7:10	36	6.1	1.15	11.02	54.3	66.5	10.20	12.49	2.16
11		11:10	40	6.9	1.30	12.47	54.3	66.5	10.20	12.49	2.16
12		15:10	44	7.7	1.45	13.91	54.3	66.5	10.20	12.49	2.16
13		19:10	48	8.3	1.56	14.99	54.3	66.5	10.20	12.49	2.16

Appendix E – Liquid-island chemistry

Appendix E presents a table of calcium nitrate mass in the liquid-island solution and approximate liquid-island volumes for each experiment. Two Excel graphs are included as well, which show the relationship between enhancement versus island volume and enhancement versus island solute mass.

Experiment Start Date	Initial Liquid Island Mass (g)	Density of Liquid Island (g/ml)	Initial Volume (ul)	Molarity (mol/L)	Mass of solute in island (g)	Final Island Length (mm)	Approx Final Volume (uL)	Enhancement
4/2/98	0.0175	1.471	11.90	2.6	0.00507	7.86	8.9	2.67
4/6/98	0.0149	1.471	10.13	2.6	0.00432	7.34	8.1	2.51
4/24/98	0.0109	1.471	7.41	2.6	0.00316	5.87	5.9	2.02
4/27/98	0.0174	1.471	11.83	2.6	0.00504	7.39	8.4	2.36
5/21/98	0.0168	1.596	10.53	3.3	0.00570	8.94	11.0	2.94
5/26/98	0.0172	1.504	11.44	2.9	0.00544	7.76	9.0	2.54
5/30/98	0.0169	1.258	13.43	1.5	0.00330	5.57	5.6	1.97
6/11/98	0.0050	1.397	3.58	2.8	0.00164	3.36	2.9	1.51
6/13/98	0.0031	1.397	2.22	2.8	0.00102	2.16	1.7	1.21
6/15/98	0.0069	1.471	4.69	2.6	0.00200	4.17	3.8	1.72
6/17/98	0.0094	1.471	6.39	2.6	0.00272	5.38	5.5	1.87
6/21/98	0.0093	1.471	6.32	2.6	0.00270	5.79	5.8	2.03
7/13/98	0.0147	1.471	9.99	2.6	0.00426	7.22	7.9	2.36
7/15/98	0.0024	1.471	1.63	2.6	0.00070	2.16	1.7	1.25
gas pore	0		0		0	0	0.0	1

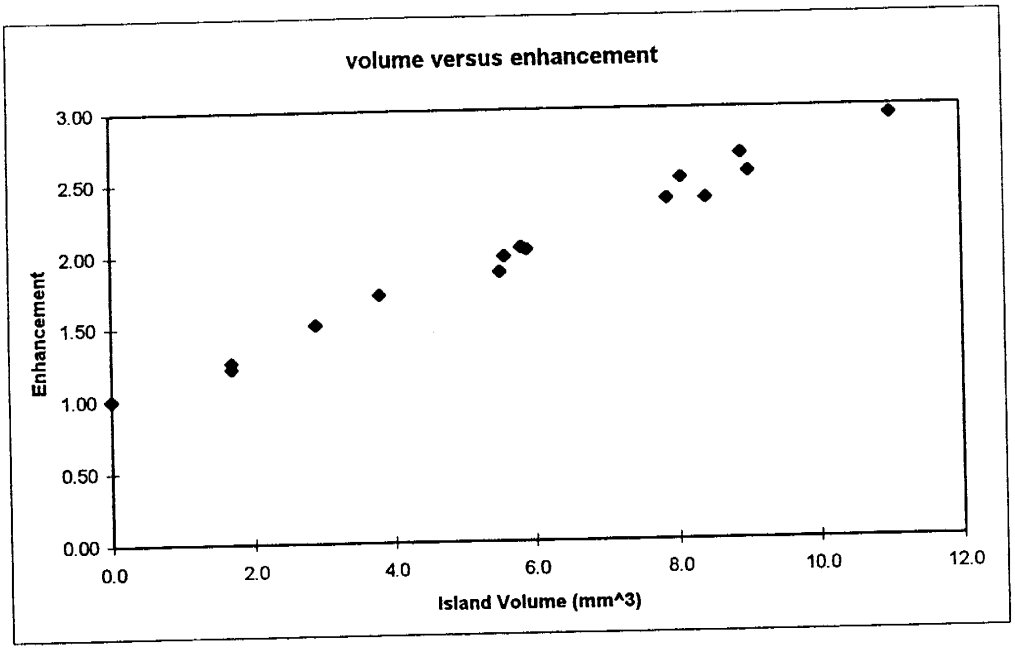
volume versus enhancement
Enhancement
3.00
2.50
2.00
1.50
1.00
0.50
0.00
0.0
2.0
4.0
6.0
8.0
10.0
12.0
Island Volume (mm^3)

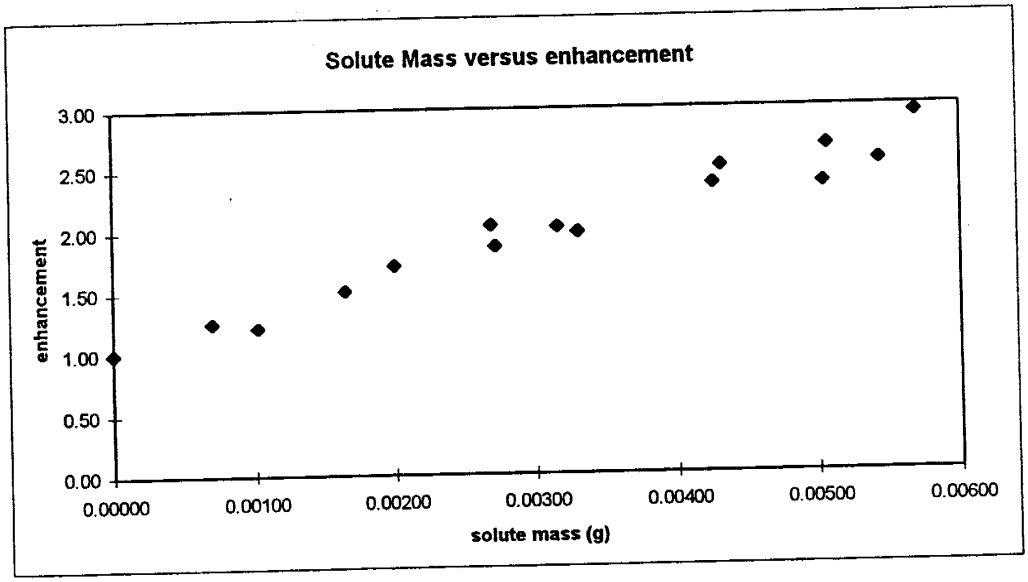
Solute Mass versus enhancement
enhancement
3.00
2.50
2.00
1.50
1.00
0.50
0.00
0.00000
0.00100
0.00200
0.00300
0.00400
0.00500
0.00600
solute mass (g)

Appendix F –Vapor flux calculations: single pore-throat

Appendix F includes the vapor flux calculations for each single-pore-throat experiment. The experiments are grouped by month and the rate for each experiment is given next to each curve. Rates are determined by a linear regression fit using the drawdown over time data after an equilibration period of about 12 hours.

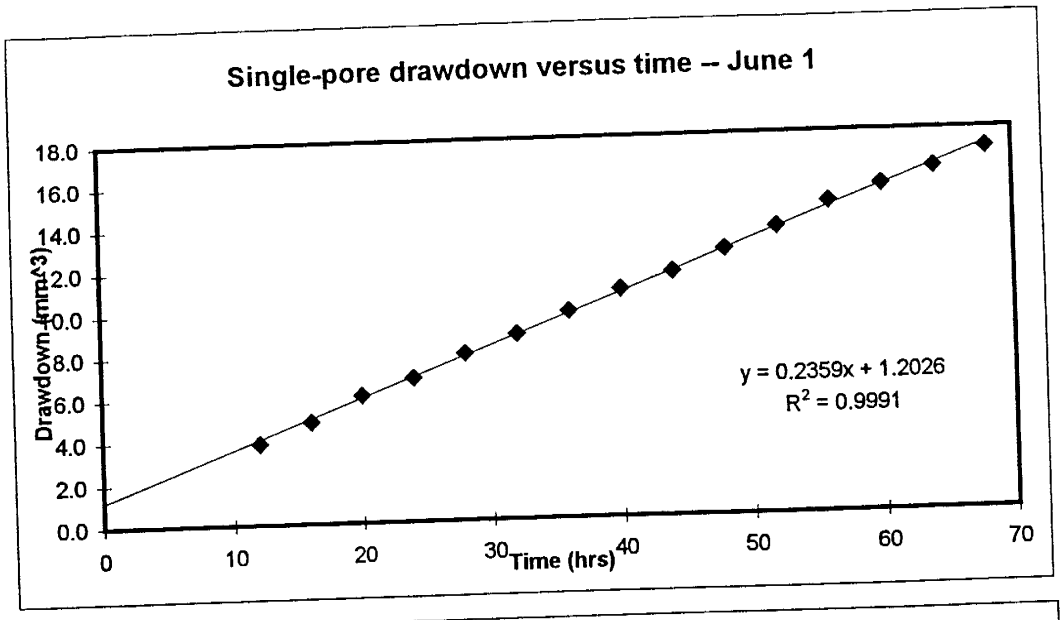
Single-pore drawdown versus time -- June 1
Drawdown (mm^3)
Time (hrs)
y = 0.2359x + 1.2026
R2 = 0.9991

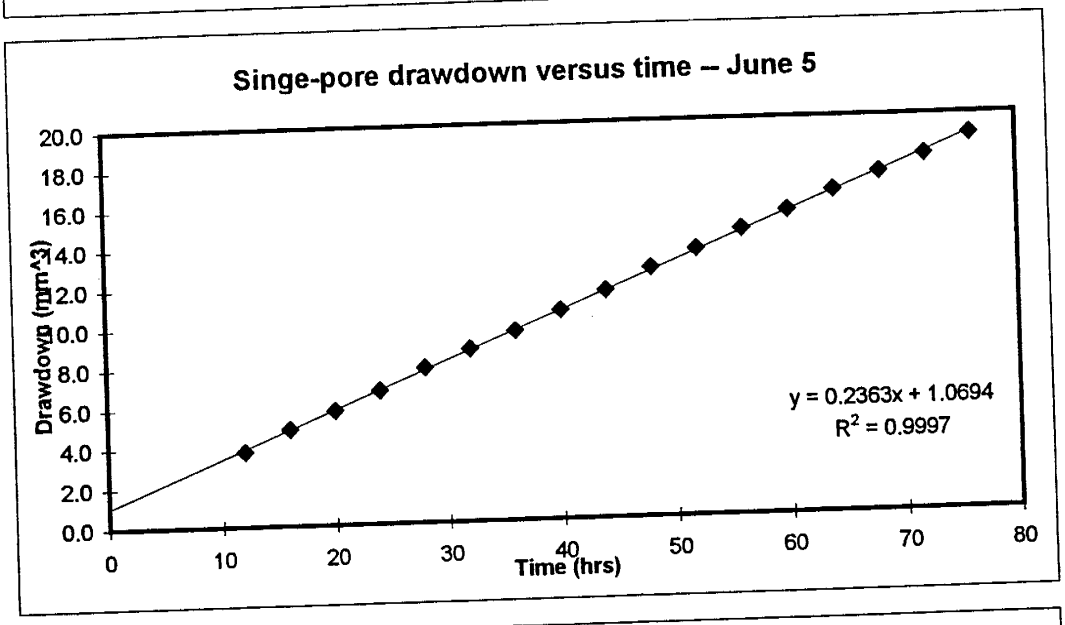
Singe-pore drawdown versus time -- June 5
Drawdown (mm^3)
Time (hrs)
y = 0.2363x + 1.0694
R2 = 0.9997

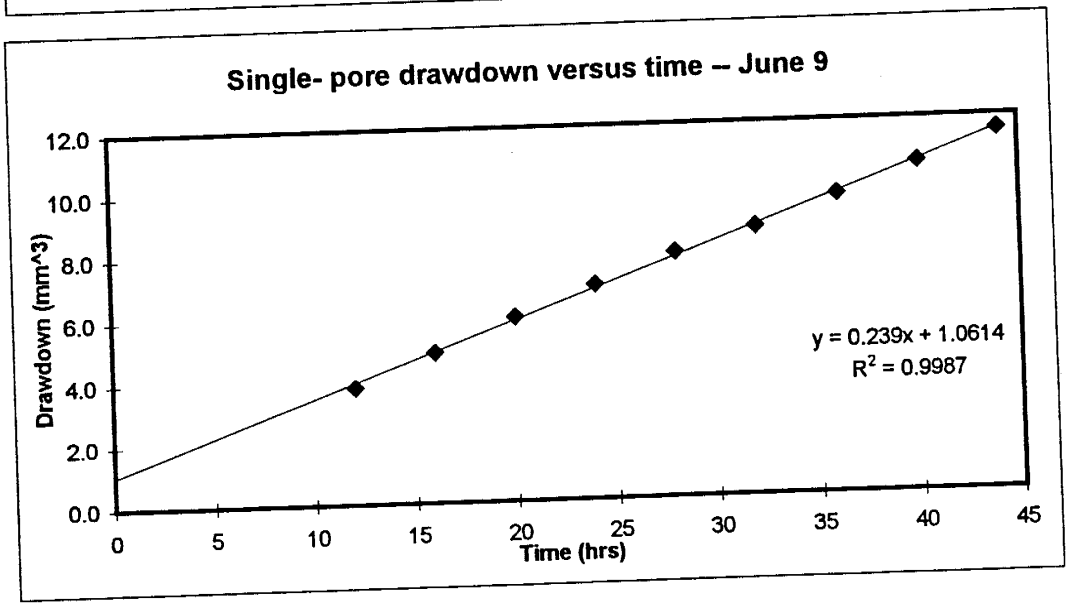
Single- pore drawdown versus time -- June 9
Drawdown (mm^3)
Time (hrs)
y = 0.239x + 1.0614
R2 = 0.9987

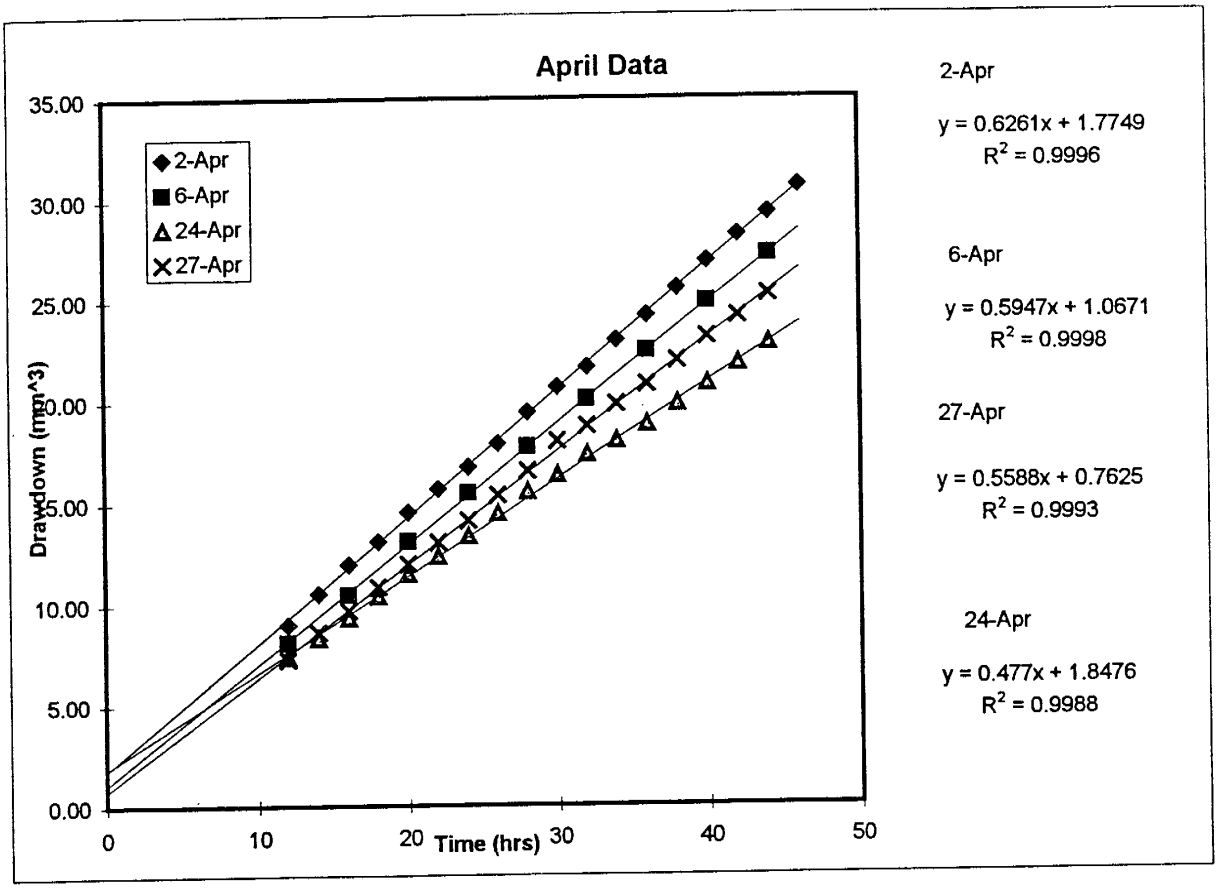
April Data
2-Apr
6-Apr
24-Apr
27-Apr
Drawdown (mm^3)
Time (hrs)
35.00
30.00
25.00
20.00
15.00
10.00
5.00
0.00
0
10
20
30
40
50
2-Apr
y = 0.6261x + 1.7749
R2 = 0.9996
6-Apr
y = 0.5947x + 1.0671
R2 = 0.9998
27-Apr
y = 0.5588x + 0.7625
R2 = 0.9993
24-Apr
y = 0.477x + 1.8476
R2 = 0.9988

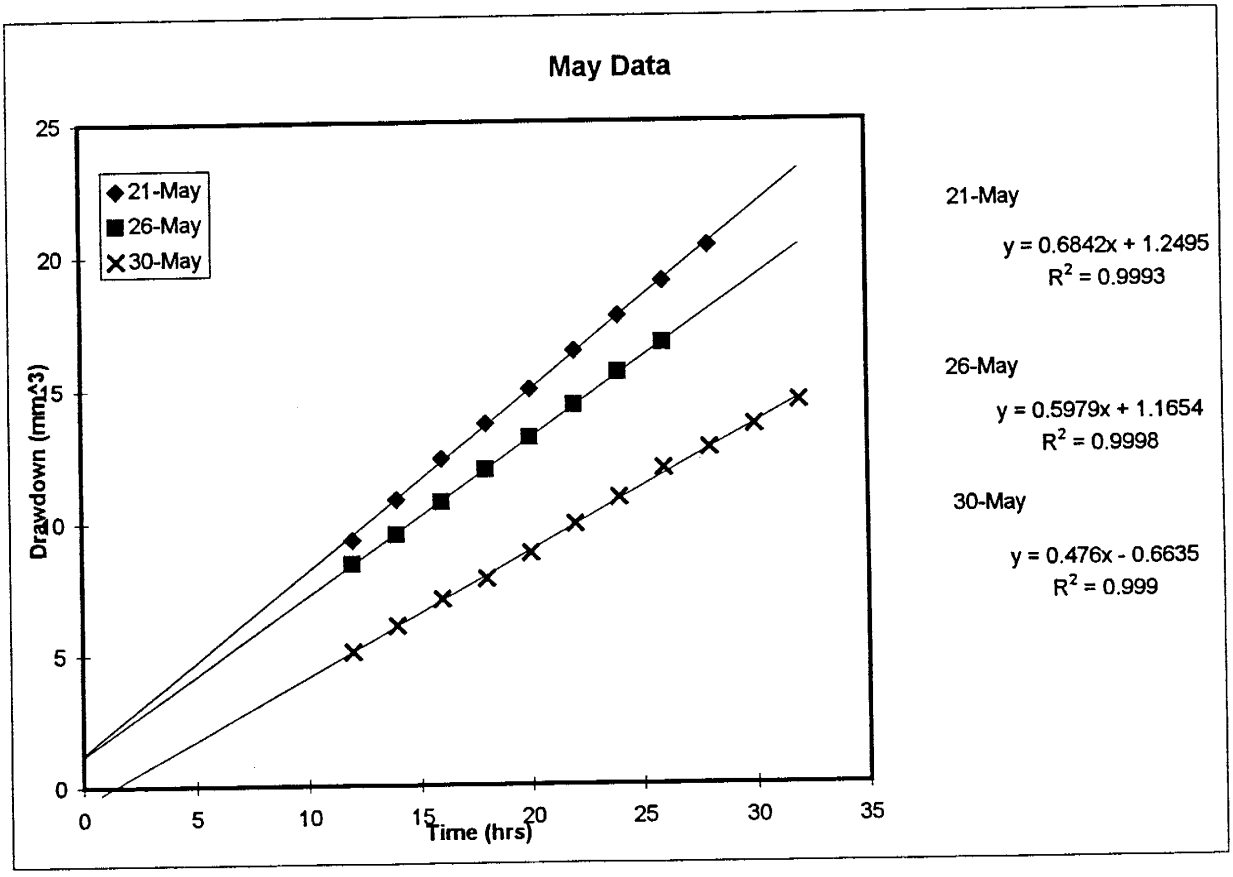
May Data
21-May
26-May
30-May
Drawdown (mm^3)
Time (hrs)
25
20
15
10
5
0
0
5
10
15
20
25
30
35
21-May
y = 0.6842x + 1.2495
R2 = 0.9993
26-May
y = 0.5979x + 1.1654
R2 = 0.9998
30-May
y = 0.476x - 0.6635
R2 = 0.999

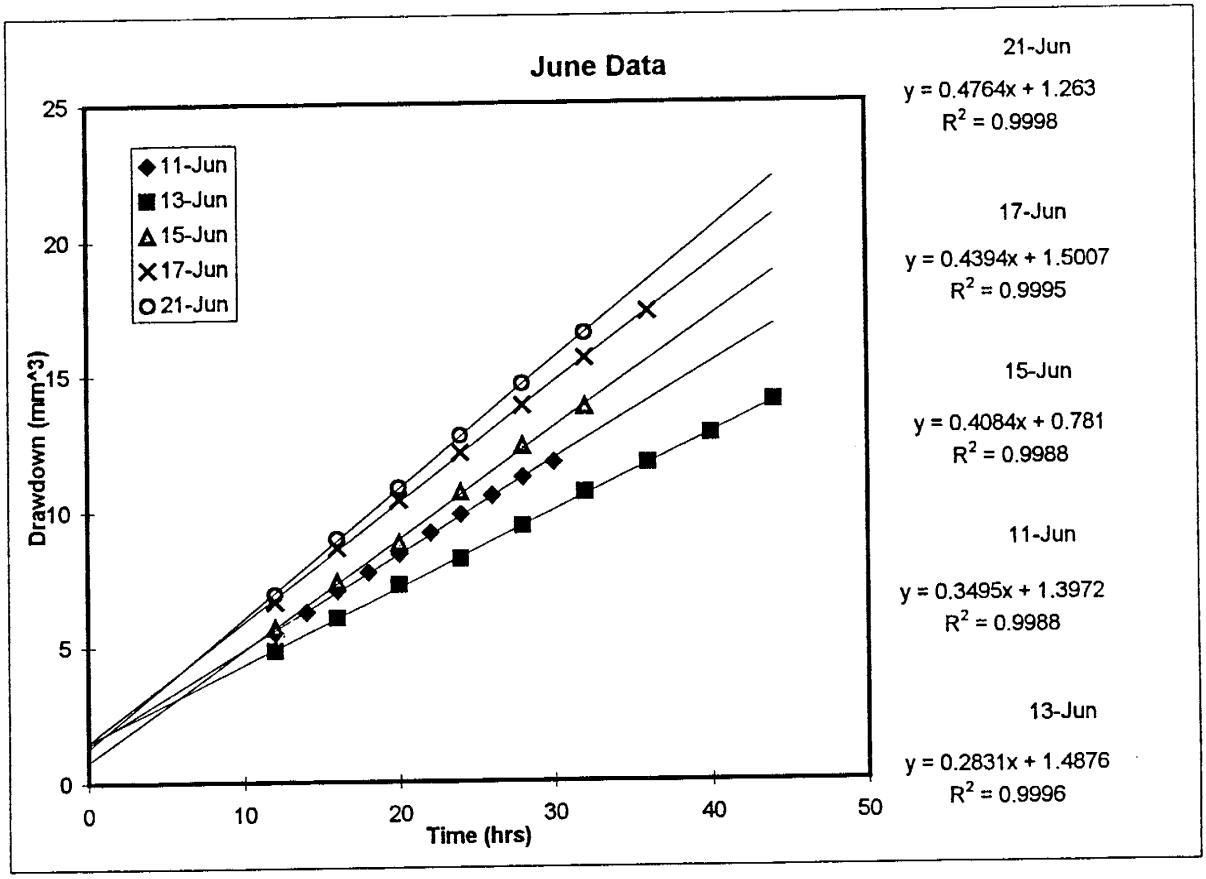
June Data
11-Jun
13-Jun
15-Jun
17-Jun
21-Jun
Drawdown (mm^3)
Time (hrs)
0
5
10
15
20
25
0
10
20
30
40
50
21-Jun
y = 0.4764x + 1.263
R2 = 0.9998
17-Jun
y = 0.4394x + 1.5007
R2 = 0.9995
15-Jun
y = 0.4084x + 0.781
R2 = 0.9988
11-Jun
y = 0.3495x + 1.3972
R2 = 0.9988
13-Jun
y = 0.2831x + 1.4876
R2 = 0.9996

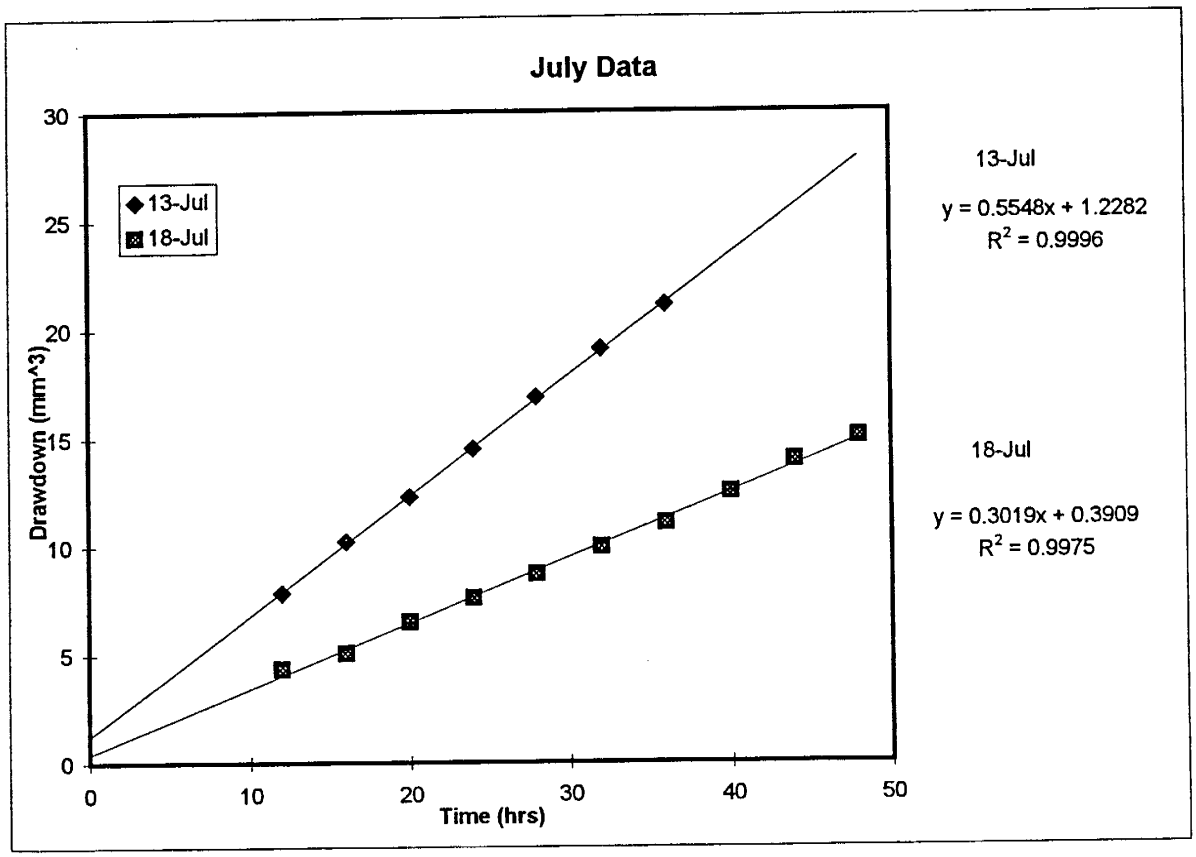
July Data
13-Jul
18-Jul
Drawdown (mm^3)
Time (hrs)
0
5
10
15
20
25
30
0
10
20
30
40
50
13-Jul
y = 0.5548x + 1.2282
R2 = 0.9996
18-Jul
y = 0.3019x + 0.3909
R2 = 0.9975

Appendix G – Experimental checks and Calibration

Appendix G contains data from the mineral oil liquid-island experiment and the pure water liquid-island experiment. A description of the vertical column calibration is included as well.

Single Pore – Mineral Oil Liquid Island Experiment

Begin Date 7/15/98
Begin Time 15:30
Interval 4 hr

	Temperature (C)		
	7/15/98	7/16/98	7/17/98
Min	28.69	28.81	28.83
Max	28.86	28.89	28.96
Ave	28.81	28.84	28.87

	Actual OD (mm)	Actual ID (mm)	Measured OD
left column	5.22	3.5	31

Total length 24.84

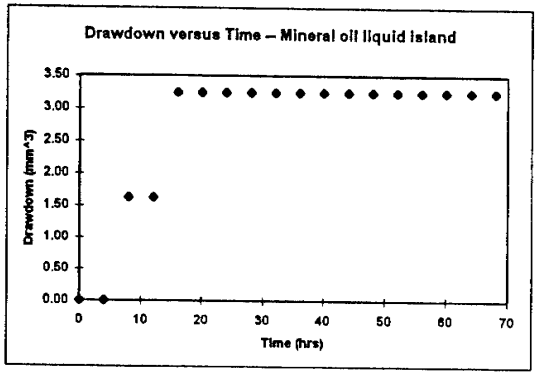

Picture #	Date	Time	Hour	Measured pure drawdown	Actual pure drawdown (mm)	Pure volume decrease (mm^3)	Measured distance from left side	Measured distance from right side	Actual distance from left side (mm)	Actual Distance from right side (mm)	Length of Island (mm)
1	7/15/98	15:30	0	0.0	0.00	0.00	54.2	57.5	9.13	9.68	6.03
2		19:30	4	0.0	0.00	0.00	54.2	57.5	9.13	9.68	6.03
3		23:30	8	1.0	0.17	1.62	54.2	57.5	9.13	9.68	6.03
4	07/16/98	3:30	12	1.0	0.17	1.62	54.2	57.5	9.13	9.68	6.03
5		7:30	16	2.0	0.34	3.24	54.2	57.5	9.13	9.68	6.03
6		11:30	20	2.0	0.34	3.24	54.2	57.5	9.13	9.68	6.03
7		15:30	24	2.0	0.34	3.24	54.2	57.5	9.13	9.68	6.03
8		19:30	28	2.0	0.34	3.24	54.2	57.5	9.13	9.68	6.03
9		23:30	32	2.0	0.34	3.24	54.2	57.5	9.13	9.68	6.03
10	07/17/98	3:30	36	2.0	0.34	3.24	54.2	57.5	9.13	9.68	6.03
11		7:30	40	2.0	0.34	3.24	54.2	57.5	9.13	9.68	6.03
12		11:30	44	2.0	0.34	3.24	54.2	57.5	9.13	9.68	6.03
13		15:30	48	2.0	0.34	3.24	54.2	57.5	9.13	9.68	6.03
14		19:30	52	2.0	0.34	3.24	54.2	57.5	9.13	9.68	6.03
15		23:30	56	2.0	0.34	3.24	54.2	57.5	9.13	9.68	6.03
16	07/18/98	3:30	60	2.0	0.34	3.24	54.2	57.5	9.13	9.68	6.03
17		7:30	64	2.0	0.34	3.24	54.2	57.5	9.13	9.68	6.03
18		11:30	68	2.0	0.34	3.24	54.2	57.5	9.13	9.68	6.03

Single Pore -- Pure Water Liquid Island Experiment

Begin Date 8/11/98
Begin Time 14:40
Interval 4 hr

	Temperature (C)	
	8/11/98	8/12/98
Min	28.70	29.10
Max	29.13	29.12
Ave	29.10	29.11

	Actual OD (mm)	Actual ID (mm)	Projected OD
left column	5.22	3.5	21

Initial Island Molality
0

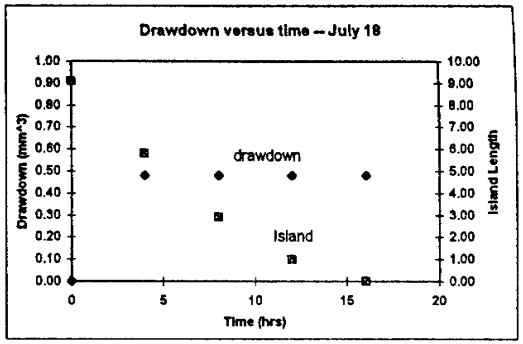

Picture #	Date	Time	Hour	Projected pure drawdown	Actual pure drawdown (mm)	Pure volume decrease (mm^3)	Projected Island Length	Length of Island (mm)
1	8/11/98	19:10	0	0.0	0.00	0.00	36.60	9.10
2		23:10	4	0.2	0.05	0.48	23.30	5.79
3	8/12/98	3:10	8	0.2	0.05	0.48	11.70	2.91
4		7:10	12	0.2	0.05	0.48	3.90	0.97
5		11:10	16	0.2	0.05	0.48	0.00	0.00

Vertical Column Calibration

The inner diameter of the upgradient vertical column was determined by removing 4 mm^3 aliquots from the liquid reservoir and photographing the new liquid level. Multiple samples were removed to show that the inner diameter was constant over the height of the column where drawdown measurements were made. This was performed for both the single and double pore throat diffusion cells.

The pore throat for the single pore throat cell was calibrated by filling up one vertical column and the pore throat with water. After sealing the top of the water-filled column with a septum, 0.2 mm^3 aliquots were removed and the new liquid level was photographed. This procedure was repeated for both sides of the pore throat since it was not symmetrical. This calibration gave a rough estimate of the liquid island volume. The dual pore throats could not be calibrated with the procedure described above. However, estimates of pore throat flux area are discussed in the dual pore throat resistance model in Appendix L.

Pure Water Column Calibration: Single and Dual Pore-Throat Cells					
Single Pore Throat			Dual Pore Throat		
Vol. removed (mm^3)	change in height (mm)	radius (mm)	Vol. removed (mm^3)	change in height (mm)	radius (mm)
4	0.104	3.499	4	0.103	3.516
4	0.103	3.516	4	0.103	3.516
4	0.104	3.499	4	0.104	3.499
4	0.104	3.499	4	0.104	3.499
4	0.104	3.499	4	0.104	3.499
4	0.103	3.516	4	0.103	3.516
4	0.104	3.499	4	0.104	3.499
average		3.504	average		3.506

Appendix H – Internal pressure effects on the diffusion and mass balance

Appendix H includes a discussion on internal pressure effects in the diffusion cell and mass balance.

Pressure Effects on Diffusion

This section details the effect of internal pressure in the diffusion cell on calculated diffusion rates. Early experiments of diffusion through a gas-filled pore-throat exhibited significantly different mass transfer rates. The cause of this was determined to be the internal pressure within the diffusion cell. When the septa are placed on the tops of both vertical columns they compress the air within the diffusion cell. From Equation (2) in the paper we see that pressure is inversely proportional to the diffusion coefficient. By simply puncturing the septum with a hollow needle before placing the septum in the top of the vertical column and removing both needles after the septa are in place, the internal pressure within the cell is equilibrated with the atmosphere. This procedure is necessary during the liquid-island experiments as well. The two experiments shown in this section exhibit a lower flux rate (2% and 5% respectively) than the later experiments where pressure inside the diffusion cell was equilibrated with the atmosphere with the hollow needle. The gas pressure within the diffusion cell was not measured. Vapor fluxes for three experiments, which were equilibrated with the atmosphere, varied by less than 1%.

Gas Diffusion Experiment

Begin Date	3/11/98
Begin Time	19:30
Interval	4 hr

	Actual OD (mm)	Actual ID (mm)	Projected OD
left	5.22	3.5	46.7
right	5.18	3.5	45.6

	Temperature (C)					
	3/11/98	3/12/98	3/13/98	3/14/98	3/15/98	3/16/98
Min	28.64	29.20	29.19	29.19	29.29	29.27
Max	29.22	29.25	29.24	29.28	29.37	29.37
Ave	29.06	29.22	29.21	29.22	29.34	29.35

Photo	Date	Time	Hour	Projected pure drawdown	Actual pure drawdown (mm)	Pure volume decrease (mm^3)
1	3/11/98	19:30	0	0	0.00	0.0
2	3/12/98	3:30	8	2.1	0.23	2.3
3		11:30	16	3.9	0.44	4.2
4		19:30	24	6.2	0.69	6.7
5	3/13/98	3:30	32	7.6	0.85	8.2
6		11:30	40	9.3	1.04	10.0
7		19:30	48	11	1.23	11.8
8	3/14/98	3:30	56	12.7	1.42	13.7
9		11:30	64	14.5	1.62	15.6
10		19:30	72	16.1	1.80	17.3
11	3/15/98	3:30	80	17.6	1.97	18.9
12		11:30	88	19.4	2.17	20.9
13		19:30	96	21.2	2.37	22.8
14	3/16/98	3:30	104	22.9	2.56	24.6
15		11:30	112	24.5	2.74	26.3

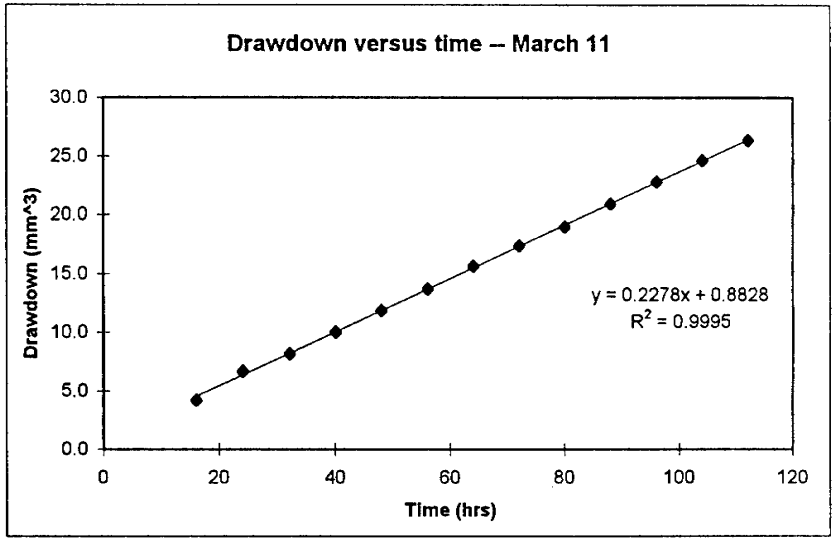

Single Pore –Gas Diffusion Experiment – High Internal Pressure

Begin Date	4/12/98
Begin Time	20:45
Interval	4 hr

	Actual OD (mm)	Actual ID (mm)	Projected OD
left	5.22	3.5	40.7
right	5.18	3.5	39.9

	Temperature (C)						
	4/12/98	4/13/98	4/14/98	4/15/98	4/16/98	4/17/98	4/18/98
Min	28.68	28.92	28.92	28.88	28.93	28.92	28.95
Max	29.08	29.08	29.07	29.04	29.07	29.11	29.15
Ave	29.01	28.99	28.98	28.97	29.00	29.01	29.04

Photo	Date	Time	Hour	Projected pure drawdown	Projected LiCl soln. rise	Actual pure drawdown (mm)	Actual LiCl soln rise (mm)	Pure volume decrease (mm^3)	LiCl soln. volume increase (mm^3)
1	4/12/98	20:45	0	0	0	0.00	0.00		0.0
2	4/13/98	0:45	4	1	0	0.13	0.00		0.0
3		4:45	8	1.7	0.3	0.22	0.04		0.4
4		8:45	12	2.2	1	0.28	0.13	2.7	1.2
5		12:45	16	2.9	1.7	0.37	0.22	3.6	2.1
6		16:45	20	3.6	2.4	0.46	0.31	4.4	3.0
7		20:45	24	4.5	3.2	0.58	0.42	5.6	4.0
8	4/14/98	0:45	28	5.2	3.8	0.67	0.49	6.4	4.7
9		4:45	32	5.7	4.7	0.73	0.61	7.0	5.9
10		8:45	36	6.2	5.2	0.80	0.68	7.7	6.5
11		12:45	40	6.8	5.8	0.87	0.75	8.4	7.2
12		16:45	44	7.4	6.5	0.95	0.84	9.1	8.1
13		20:45	48	8	7.1	1.03	0.92	9.9	8.9
14	4/15/98	0:45	52	8.5	7.9	1.09	1.03	10.5	9.9
15		4:45	56	9.2	8.5	1.18	1.10	11.4	10.6
16		8:45	60	9.7	9.3	1.24	1.21	12.0	11.6
17		12:45	64	10.2	9.8	1.31	1.27	12.6	12.2
18		16:45	68	10.9	10.4	1.40	1.35	13.5	13.0
19		20:45	72	11.4	11.2	1.46	1.45	14.1	14.0
20	4/16/98	0:45	76	12	11.8	1.54	1.53	14.8	14.7
21		4:45	80	12.6	12.3	1.62	1.60	15.5	15.4
22		8:45	84	13.4	13	1.72	1.69	16.5	16.2
23		12:45	88	14	13.5	1.80	1.75	17.3	16.9
24		16:45	92	14.7	14.1	1.89	1.83	18.1	17.6
25		20:45	96	15.2	14.8	1.95	1.92	18.8	18.5
26	4/17/98	0:45	100	15.8	15.4	2.03	2.00	19.5	19.2
27		4:45	104	16.5	16.4	2.12	2.13	20.4	20.5
28		8:45	108	17.1	16.3	2.19	2.12	21.1	20.4
29		12:45	112	17.8	17.3	2.28	2.25	22.0	21.6
30		16:45	116	18.4	17.9	2.36	2.32	22.7	22.4
31		20:45	120	18.9	18.4	2.42	2.39	23.3	23.0
32	4/18/98	0:45	124	19.4	19.2	2.49	2.49	23.9	24.0
33		4:45	128	20	19.9	2.57	2.58	24.7	24.9
34		8:45	132	20.6	20.5	2.64	2.66	25.4	25.6

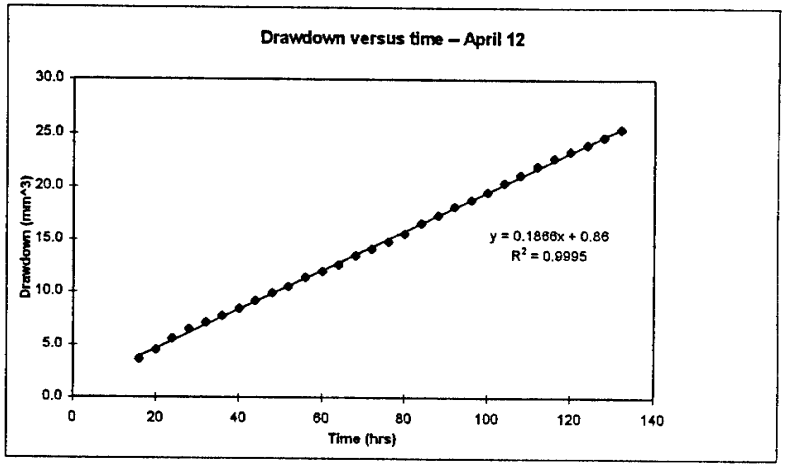

Mass Loss

The following section shows tabulated mass loss for each experiment. At the onset and conclusion of each experiment the mass of the following items was recorded: both septa, the diffusion cell with upgradient and downgradient solutions (and again with the liquid-island if present), the connecting needle when present, and the complete cell (which includes the all the liquid, both septa ,and the connecting needle when present). From these values we could calculate the mass loss over the duration of the experiment. Table B1 lists the mass loss for each item listed above. Individual averages for gas diffusion, liquid-island, and dual-pore experiments in addition to total averages are given as well.

From the operating manual, the repeatability of the Mettler AT400 balance is given as ±0.05 mg. The average mass of the septa actually increased over the course of each experiment. However, given the repeatability of the balance, this value is negligible. The results for the connecting needle are similar; virtually no mass was lost or gained over the duration of the experiments. This result became obvious after about eight experiments and hence, the needle was not weighed for each subsequent experiment. On average, the complete cell lost slightly more mass than the cell with only the liquid present, no septa or needle. However, the difference in these amounts is not significant given the repeatability of the balance. The average mass loss of the cell with only liquid present, therefore, was chosen as the most accurate measurement of mass loss for each experiment and was used for comparison to describe the percentage mass loss per amount of vapor transported in the paper.

Gas diffusion Experiments

Experiment Start Date	Mass loss/gain (mg)		
	2 septa	Apparatus, no septa	Total -- apparatus + septa
6/1/98	0.3	-0.3	-0.5
6/5/98	0.4	-0.5	-0.3
6/9/98	0.2	-0.3	-0.3
average	0.3	-0.4	-0.4

Liquid Island Experiments

Experiment Start Date	Mass loss/gain (mg)			
	2 septa	Apparatus, no septa	Total -- apparatus + septa	needle
4/2/98	0.4	-0.2	-0.4	
4/6/98	0.3	-0.3	-0.5	0.1
4/24/98	0.2	-0.2	-0.4	0.0
4/27/98	0.2	-0.4	-0.3	0.0
5/21/98	0.1	-0.3	-0.5	0.0
5/26/98	0.0	-0.2	-0.5	-0.1
5/28/98	0.4	0.0	-0.3	0.0
5/30/98	0.2	-0.5	-0.4	0.0
6/11/98		-0.3	-0.3	-0.1
6/13/98		-0.4	-0.6	
6/15/98	-0.4	-0.1	-0.3	
6/17/98	0.1	-0.9	-0.5	
6/21/98	0.1	-0.1	-0.5	
7/13/98	0.2	-0.4	-0.7	
7/15/98	0.2	-0.6	-0.7	
7/18/98	-0.9	-0.3	-0.4	
average	0.1	-0.3	-0.5	0.0

blank cells denote unrecorded data

Dual Pore Experiments

Experiment Start Date	Mass loss/gain (mg)		
	2 septa	Apparatus, no septa	Total -- apparatus + septa
6/9/98	0.1	-0.3	-0.2
6/11/98	0.1	-0.1	-0.3
6/13/98	-0.1	-0.1	-0.4
6/15/98	-0.2	-0.3	-0.2
6/17/98	0.2	-0.3	-0.4
6/19/98	0.0	-0.5	-0.4
6/21/98	0.1	-0.2	-0.4
7/15/98	0.0	-0.5	-0.7
7/18/98	-0.4	-0.3	-0.7
average	0.0	-0.3	-0.4

total average	0.1	-0.3	-0.4
std. deviation	0.3	0.2	0.1

Start Date	Mass of cell with solutions (g)	Mass of solutions (mg)	Mass Transported (mg)	Mass Lost (mg)	% of Total Mass	% of Mass Flux
Single Pore Throat						
6/1/98	5.1618	152.4	17.03	-0.3	0.20%	1.76%
6/5/98	5.1596	150.2	18.94	-0.5	0.33%	2.64%
6/9/98	5.1640	154.6	11.56	-0.3	0.19%	2.60%
4/2/98	5.2129	203.5	30.61	-0.2	0.10%	0.65%
4/6/98	5.2042	194.8	37.98	-0.3	0.15%	0.79%
4/24/98	5.1905	181.1	22.78	-0.2	0.11%	0.88%
4/27/98	5.1928	183.4	25.21	-0.4	0.22%	1.59%
5/21/98	5.2036	194.2	16.98	-0.3	0.15%	1.77%
5/26/98	5.1887	179.3	16.66	-0.2	0.11%	1.20%
5/28/98	5.1932	5.2	15.21	0.0	0.00%	0.00%
5/30/98	5.1955	186.1	14.44	-0.5	0.27%	3.46%
6/11/98	5.1722	162.8	11.74	-0.3	0.18%	2.56%
6/13/98	5.1570	147.6	13.96	-0.4	0.27%	2.87%
6/15/98	5.1786	169.2	13.76	-0.1	0.06%	0.73%
6/17/98	5.1834	174.0	17.27	-0.9	0.52%	5.21%
6/21/98	5.1749	165.5	16.48	-0.1	0.06%	0.61%
7/13/98	5.1889	179.5	21.11	-0.4	0.22%	1.89%
7/18/98	5.1966	187.2	14.99	-0.3	0.16%	2.00%
Dual Pore Throat						
6/9/98	6.1862	145.1	17.01	-0.3	0.21%	1.76%
6/11/98	6.1980	156.9	18.95	-0.1	0.06%	0.53%
6/13/98	6.1966	155.5	13.76	-0.1	0.06%	0.73%
6/17/98	6.2827	241.6	32.52	-0.3	0.12%	0.92%
6/19/98	6.2401	199.0	22.42	-0.5	0.25%	2.23%
6/21/98	6.2295	188.4	23.81	-0.2	0.11%	0.84%
7/15/98	6.2587	217.6	20.40	-0.5	0.23%	2.45%
7/18/98	6.2326	191.5	15.29	-0.3	0.16%	1.96%
			Average	-0.3077	0.17%	1.72%

Appendix I – Dual-pore-throat drawdown data

Appendix I contains all drawdown data for the dual-pore-throat experiments. Again, these tables include the measured and corrected drawdown data as well as a figure of drawdown versus time. Minimum, maximum, and average temperature adjacent to the diffusion cell is shown on each page.

Dual Pore -- Gas Diffusion Experiment

Begin Date 6/9/98
Begin Time 14:10
Interval 4 hr

	Temperature (C)	
	6/9/98	6/10/98
Min	27.57	28.50
Max	28.72	28.72
Ave	28.56	28.61

	Actual OD (mm)	Actual ID (mm)	Projected OD
left column	5.22	3.5	31

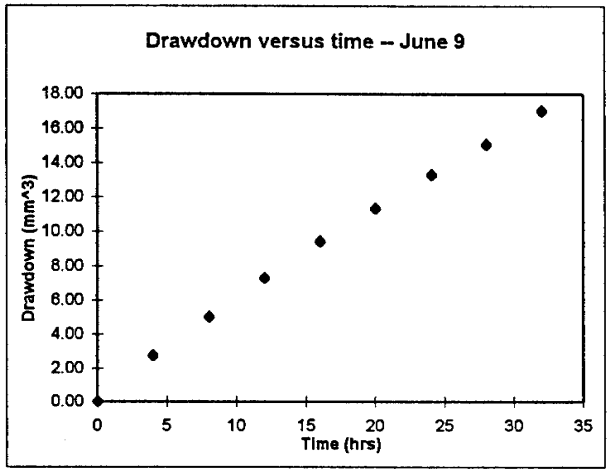

Photo	Date	Time	Hour	Projected pure drawdown	Actual pure drawdown (mm)	Pure volume decrease (mm^3)
1	6/9/98	14:10	0	0.0	0.00	0.00
2		18:10	4	1.7	0.29	2.75
3		22:10	8	3.1	0.52	5.02
4	6/10/98	2:10	12	4.5	0.76	7.29
5		6:10	16	5.8	0.98	9.40
6		10:10	20	7.0	1.18	11.34
7		14:10	24	8.2	1.38	13.28
8		18:10	28	9.3	1.57	15.07
9		22:10	32	10.5	1.77	17.01

Dual Pore -- Gas Diffusion Experiment

Begin Date 6/11/98
Begin Time 22:15
Interval 4 hr

	Temperature (C)		
	6/11/98	6/12/98	6/13/98
Min	28.63	28.63	28.62
Max	28.68	28.73	28.75
Ave	28.66	28.67	28.66

	Actual OD (mm)	Actual ID (mm)	Projected OD
left column	5.22	3.5	31

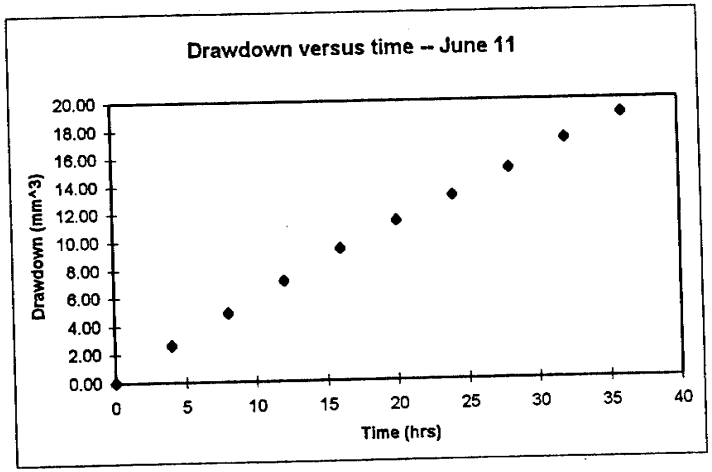

Photo	Date	Time	Hour	Projected pure drawdown	Actual pure drawdown (mm)	Pure volume decrease (mm^3)
1	6/11/98	22:15	0	0.0	0.00	0.00
2	6/12/98	2:15	4	1.6	0.27	2.59
3		6:15	8	3.0	0.51	4.86
4		10:15	12	4.4	0.74	7.13
5		14:15	16	5.8	0.98	9.40
6		18:15	20	7.0	1.18	11.34
7		22:15	24	8.1	1.36	13.12
8	6/13/98	2:15	28	9.3	1.57	15.07
9		6:15	32	10.6	1.78	17.17
10		10:15	36	11.7	1.97	18.95

Dual Pore -- Gas Diffusion Experiment

Begin Date 6/13/98
Begin Time 17:15
Interval 4 hr

	Temperature (C)	
	6/13/98	6/14/98
Min	28.61	28.63
Max	28.71	28.74
Ave	28.68	28.68

	Actual OD (mm)	Actual ID (mm)	Projected OD
left column	5.22	3.5	27

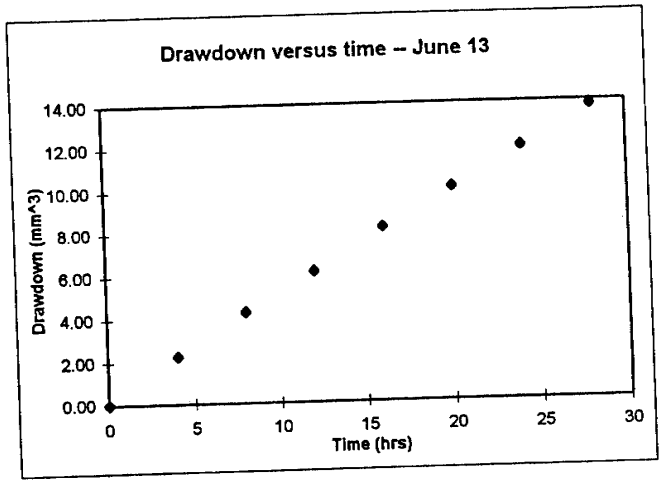

Photo	Date	Time	Hour	Projected pure drawdown	Actual pure drawdown (mm)	Pure volume decrease (mm^3)
1	6/13/98	17:15	0	0.0	0.00	0.00
2		21:15	4	1.2	0.23	2.23
3	6/14/98	1:15	8	2.3	0.44	4.28
4		5:15	12	3.3	0.64	6.14
5		9:15	16	4.4	0.85	8.18
6		13:15	20	5.4	1.04	10.04
7		17:15	24	6.4	1.24	11.90
8		21:15	28	7.4	1.43	13.76

Double Pore -- Liquid/Liquid

Begin Date 6/17/98
Begin Time 22:00
Interval 2 hr

	Temperature (C)		
	6/17/98	6/18/98	6/19/98
Min	28.55	28.58	28.60
Max	28.66	28.75	28.74
Ave	28.60	28.64	28.66

	Actual OD (mm)	Actual ID (mm)	Projected OD
left column	5.22	3.5	27.8

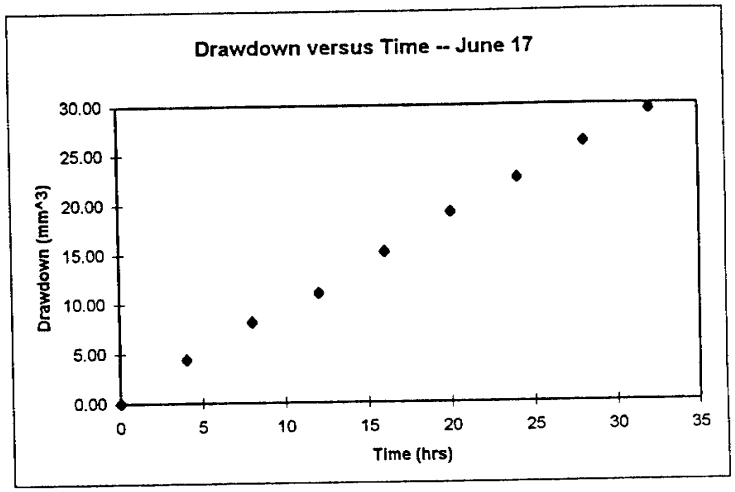

							Top Pore Throat					Bottom Pore Throat				
Photo	Date	Time	Hour	Projected pure drawdown	Actual pure drawdown (mm)	Pure volume decrease (mm^3)	Projected distance from center-left	Projected distance from center-right	Actual distance from center-left (mm)	Actual distance from center-right (mm)	Actual island length (mm)	Projected distance from center-left	Projected distance from center-right	Actual distance from center-left (mm)	Actual distance from center-right (mm)	Actual island length (mm)
1	6/17/98	22:00	0	0.0	0.00	0.00	24.2	23.7	4.54	4.45	8.99	19.6	25.9	3.68	4.86	8.54
2	6/18/98	0:00	2													
3		2:00	4	2.4	0.45	4.34	24.2	23.7	4.54	4.45	8.99	18.5	24.7	3.47	4.64	8.11
4		4:00	6													
5		6:00	8	4.5	0.84	8.13	23.8	23.4	4.47	4.39	8.86	18.0	24.1	3.38	4.53	7.91
6		8:00	10													
7		10:00	12	6.1	1.15	11.02	23.5	23.1	4.41	4.34	8.75	18.0	23.4	3.38	4.39	7.77
8		12:00	14													
9		14:00	16	8.4	1.58	15.18	23.1	22.7	4.34	4.26	8.60	17.7	23.1	3.32	4.34	7.66
10		16:00	18													
11		18:00	20	10.6	1.99	19.15	22.8	22.4	4.28	4.21	8.49	17.7	23.1	3.32	4.34	7.66
12		20:00	22													
13		22:00	24	12.5	2.35	22.58	22.5	22.1	4.22	4.15	8.37	17.5	22.9	3.29	4.30	7.59
14	6/19/98	0:00	26													
15		2:00	28	14.5	2.72	26.20	22.5	21.8	4.22	4.09	8.32	17.4	22.7	3.27	4.26	7.53
16		4:00	30													
17		6:00	32	16.3	3.06	29.45	22.2	21.5	4.17	4.04	8.21	17.4	22.7	3.27	4.26	7.53
18		8:00	34													
19		10:00	36	18.0	3.38	32.52	22.2	21.2	4.17	3.98	8.15	17.2	22.5	3.23	4.22	7.45

Double Pore -- Liquid/Gas

Begin Date 6/19/98
Begin Time 16:20
Interval 2 hr

	Temperature (C)		
	6/19/98	6/20/98	6/21/98
Min	28.59	28.62	28.64
Max	28.79	28.78	28.68
Ave	28.67	28.67	28.66

	Actual OD (mm)	Actual ID (mm)	projected OD
left column	5.22	3.5	28

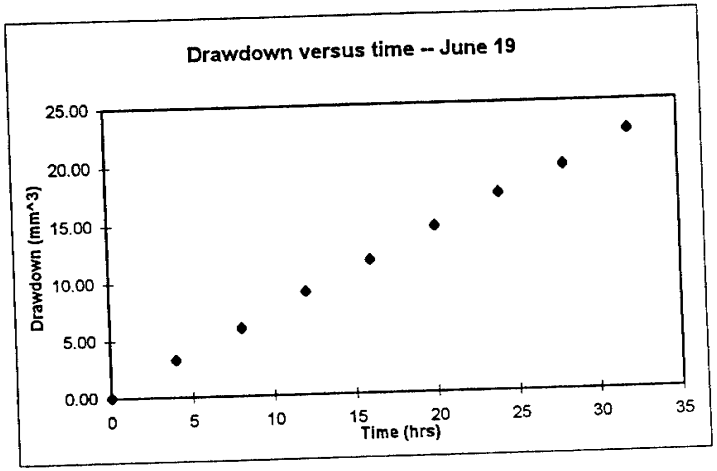

							Top Pore Throat					Bottom Pore Throat				
Photo	Date	Time	Hour	projected pure drawdown	Actual pure drawdown (mm)	Pure volume decrease (mm^3)	projected distance from center-left	projected distance from center-right	Actual distance from center-left (mm)	Actual distance from center-right (mm)	Actual island length (mm)	projected distance from center-left	projected distance from center-right	Actual distance from center-left (mm)	Actual distance from center-right (mm)	Actual island length (mm)
1	6/19/98	16:20	0	0.0	0.00	0.00	25.1	23.0	4.68	4.29	8.97					
2		18:20	2													
3		20:20	4	1.8	0.34	3.23	24.5	22.6	4.57	4.21	8.78					
4		22:20	6													
5	6/20/98	0:20	8	3.3	0.62	5.92	24.1	22.6	4.49	4.21	8.71					
6		2:20	10													
7		4:20	12	5.0	0.93	8.97	23.8	22.0	4.44	4.10	8.54					
8		6:20	14													
9		8:20	16	6.5	1.21	11.66	23.6	21.8	4.40	4.06	8.46					
10		10:20	18													
11		12:20	20	8.1	1.51	14.53	23.4	21.6	4.36	4.03	8.39					
12		14:20	22													
13		16:20	24	9.6	1.79	17.22	23.4	21.6	4.36	4.03	8.39					
14		18:20	26													
15		20:20	28	10.9	2.03	19.55	23.1	21.4	4.31	3.99	8.30					
16		22:20	30													
17	6/21/98	0:20	32	12.5	2.33	22.42	23.0	21.2	4.29	3.95	8.24					

Dual Pore -- Gas/Liquid

Begin Date 6/21/98
Begin Time 22:20
Interval 2 hr

	Temperature (C)		
	6/21/98	6/22/98	6/23/98
Min	28.45	28.54	28.57
Max	28.62	28.71	28.73
Ave	28.56	28.64	28.63

	Actual OD (mm)	Actual ID (mm)	Projected OD
left column	5.22	3.5	27

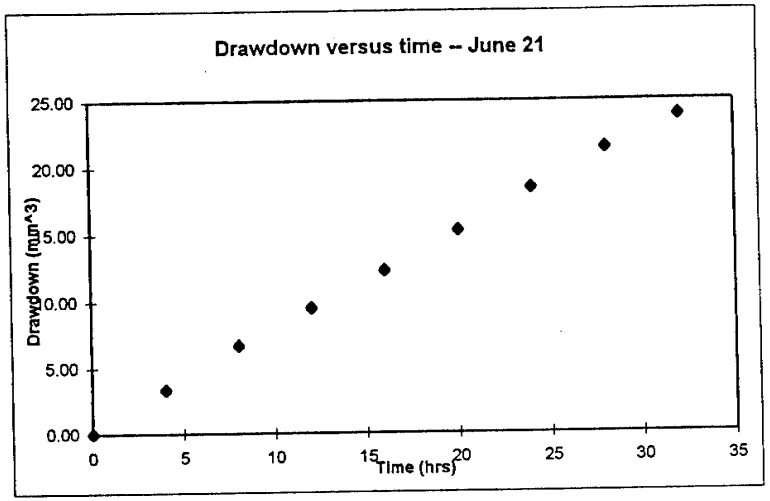

							Top Pore Throat					Bottom Pore Throat				
Photo	Date	Time	Hour	Projected pure drawdown	Actual pure drawdown (mm)	Pure volume decrease (mm^3)	Projected distance from center-left	Projected distance from center-right	Actual distance from center-left (mm)	Actual distance from center-right (mm)	Actual island length (mm)	Projected distance from center-left	Projected distance from center-right	Actual distance from center-left (mm)	Actual distance from center-right (mm)	Actual island length (mm)
1	6/21/98	22:20	0	0.0	0.00	0.00						20.1	24.4	3.89	4.72	8.60
2	6/22/98	0:20	2									18.8	23.1	3.63	4.47	8.10
3		2:20	4	1.8	0.35	3.35										
4		4:20	6									18.0	22.9	3.48	4.43	7.91
5		6:20	8	3.6	0.70	6.70										
6		8:20	10									17.5	22.6	3.38	4.37	7.75
7		10:20	12	5.1	0.99	9.49										
8		12:20	14									17.1	22.4	3.31	4.33	7.64
9		14:20	16	6.6	1.28	12.28										
10		16:20	18									16.8	22.2	3.25	4.29	7.54
11		18:20	20	8.2	1.59	15.25										
12		20:20	22									16.8	22.1	3.25	4.27	7.52
13		22:20	24	9.9	1.91	18.41										
14	6/23/98	0:20	26									16.5	22.1	3.19	4.27	7.46
15		2:20	28	11.5	2.22	21.39										
16		4:20	30									16.5	21.9	3.19	4.23	7.42
17		6:20	32	12.8	2.47	23.81										

Dual Pore -- Mineral Oil/Gas

Begin Date 7/15/98
Begin Time 15:30
Interval 4 hr

	Temperature (C)			
	7/15/98	7/16/98	7/17/98	7/18/98
Min	28.71	28.74	28.75	28.68
Max	28.84	28.84	28.91	28.87
Ave	28.77	28.78	28.80	28.83

	Actual OD (mm)	Actual ID (mm)	Projected OD
left column	5.22	3.5	22.4

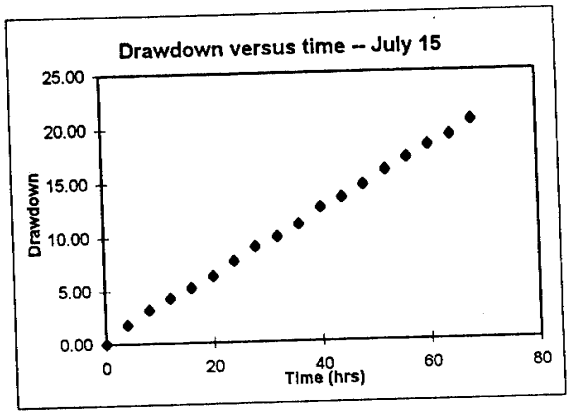

Photo	Date	Time	Hour	Projected pure drawdown	Actual pure drawdown (mm)	Pure volume decrease (mm^3)
1	7/15/98	15:30	0	0	0.00	0.00
2		19:30	4	0.8	0.19	1.79
3		23:30	8	1.4	0.33	3.14
4	16-Jul	3:30	12	1.9	0.44	4.26
5		7:30	16	2.3	0.54	5.16
6		11:30	20	2.8	0.65	6.28
7		15:30	24	3.4	0.79	7.62
8		19:30	28	4	0.93	8.97
9		23:30	32	4.4	1.03	9.87
10	17-Jul	3:30	36	4.9	1.14	10.99
11		7:30	40	5.6	1.31	12.56
12		11:30	44	6	1.40	13.45
13		15:30	48	6.5	1.51	14.57
14		19:30	52	7.1	1.65	15.92
15		23:30	56	7.6	1.77	17.04
16	18-Jul	3:30	60	8.1	1.89	18.16
17		7:30	64	8.5	1.98	19.06
18		11:30	68	9.1	2.12	20.40

Dual Pore -- Gas/Mineral Oil

Begin Date 7/18/98
Begin Time 19:10
Interval 4 hr

	Temperature (C)		
	7/18/98	7/19/98	7/20/98
Min	28.82	28.81	28.78
Max	28.86	28.87	28.87
Ave	28.83	28.84	28.82

	Actual OD (mm)	Actual ID (mm)	Projected OD
left column	5.22	3.5	23

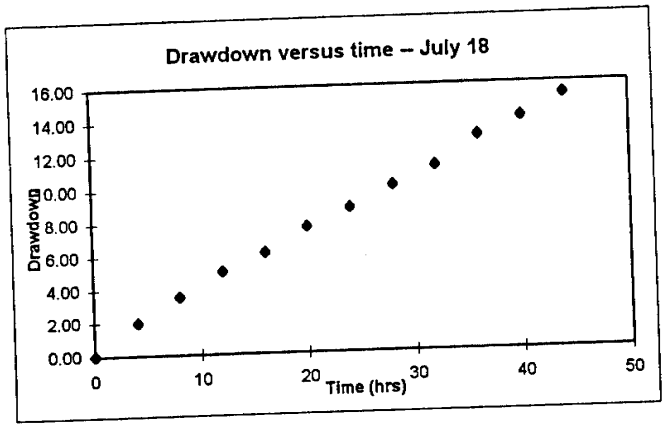

Photo	Date	Time	Hour	Projected pure drawdown	Actual pure drawdown (mm)	Pure volume decrease (mm^3)
1	7/18/98	19:10	0	0.0	0.00	0.00
2		23:10	4	0.9	0.20	1.97
3	7/19/98	3:10	8	1.6	0.36	3.49
4		7:10	12	2.3	0.52	5.02
5		11:10	16	2.8	0.64	6.11
6		15:10	20	3.5	0.79	7.64
7		19:10	24	4.0	0.91	8.73
8		23:10	28	4.6	1.04	10.04
9	7/20/98	3:10	32	5.1	1.16	11.14
10		7:10	36	5.9	1.34	12.88
11		11:10	40	6.4	1.45	13.97
12		15:10	44	7.0	1.59	15.29

Dual Pore -- Mineral Oil/Liquid

Begin Date 8/15/98
Begin Time 13:30
Interval 4 hr

	Temperature (C)		
	8/15/98	8/16/98	8/17/98
Min	28.22	28.20	28.96
Max	29.10	29.08	29.07
Ave	28.99	29.00	29.01

	Actual OD (mm)	Actual ID (mm)	Projected OD
left column	5.22	3.5	20.6

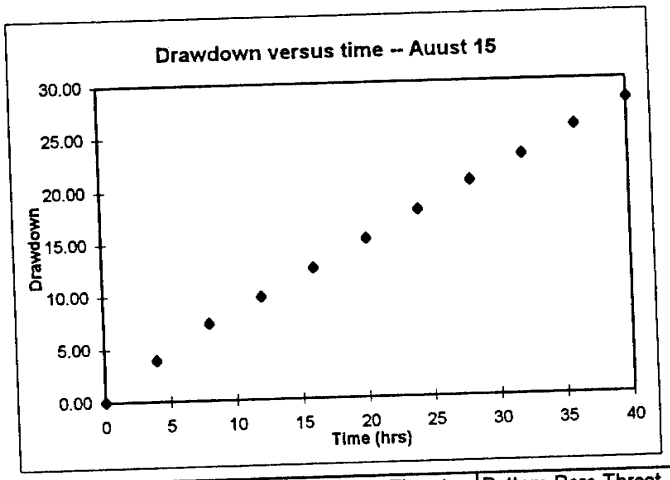

Photo	Date	Time	Hour	Projected pure drawdown	Actual pure drawdown (mm)	Pure volume decrease (mm^3)	Top Pore Throat		Bottom Pore Throat	
							Projected Isalnd length	Actual island length (mm)	Projected Isalnd length	Actual island length (mm)
1	8/15/98	13:30	0	0.0	0.00	0.00			33.0	8.36
2		17:30	4	1.6	0.41	3.90			32.6	8.26
3		21:30	8	3.0	0.76	7.31			32.0	8.11
4	8/16/98	1:30	12	4.0	1.01	9.75			31.6	8.01
5		5:30	16	5.1	1.29	12.43			31.2	7.91
6		9:30	20	6.2	1.57	15.12			30.9	7.83
7		13:30	24	7.3	1.85	17.80			30.9	7.83
8		17:30	28	8.4	2.13	20.48			30.7	7.78
9		21:30	32	9.4	2.38	22.92			30.5	7.73
10	8/19/98	1:30	36	10.5	2.66	25.60			30.5	7.73
11		5:30	40	11.5	2.91	28.04			30.5	7.73
12		9:30	44	12.5	3.17	30.47			30.5	7.73

Dual Pore -- Liquid/Mineral Oil

Begin Date 8/22/98
Begin Time 12:22
Interval 4 hr

	Temperature (C)		
	8/22/98	8/23/98	8/24/98
Min	28.19	28.83	28.88
Max	29.11	29.07	29.09
Ave	28.98	28.98	29.03

	Actual OD (mm)	Actual ID (mm)	Projected OD
left column	5.22	3.5	16

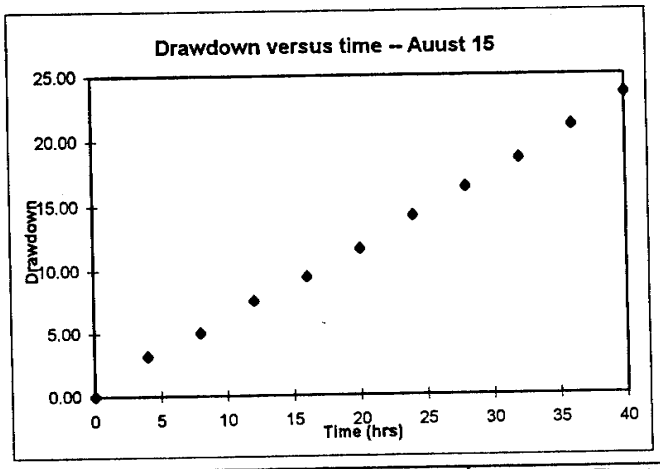

							Top Pore Throat		Bottom Pore Throat	
Photo	Date	Time	Hour	Projected pure drawdown	Actual pure drawdown (mm)	Pure volume decrease (mm^3)	Projected Isalnd length	Actual island length (mm)	Projected Isalnd length	Actual island length (mm)
1	8/22/98	12:22	0	0.0	0.00	0.00	27.4	8.94		
2		16:22	4	1.0	0.33	3.14	27.3	8.91		
3		20:22	8	1.6	0.52	5.02	25.7	8.38		
4	8/23/98	0:22	12	2.4	0.78	7.53	24.9	8.12		
5		4:22	16	3.0	0.98	9.42	24.1	7.86		
6		8:22	20	3.7	1.21	11.61	23.8	7.76		
7		12:22	24	4.5	1.47	14.13	23.5	7.67		
8		16:22	28	5.2	1.70	16.32	23.5	7.67		
9		20:22	32	5.9	1.92	18.52	23.5	7.67		
10	8/24/98	0:22	36	6.7	2.19	21.03	23.5	7.67		
11		4:22	40	7.5	2.45	23.54	23.4	7.63		
12		8:22	44	8.2	2.68	25.74	23.4	7.63		
13		12:22	48	9.0	2.94	28.25	23.4	7.63		

Appendix J – Vapor flux calculations: dual-pore-throat

Appendix J includes the vapor flux calculations for each dual-pore-throat experiment. The experiments are grouped by month and the rate for each experiment is given next to each curve. Rates are determined by a linear regression fit using the drawdown over time data after an equilibration period of about 12 hours.

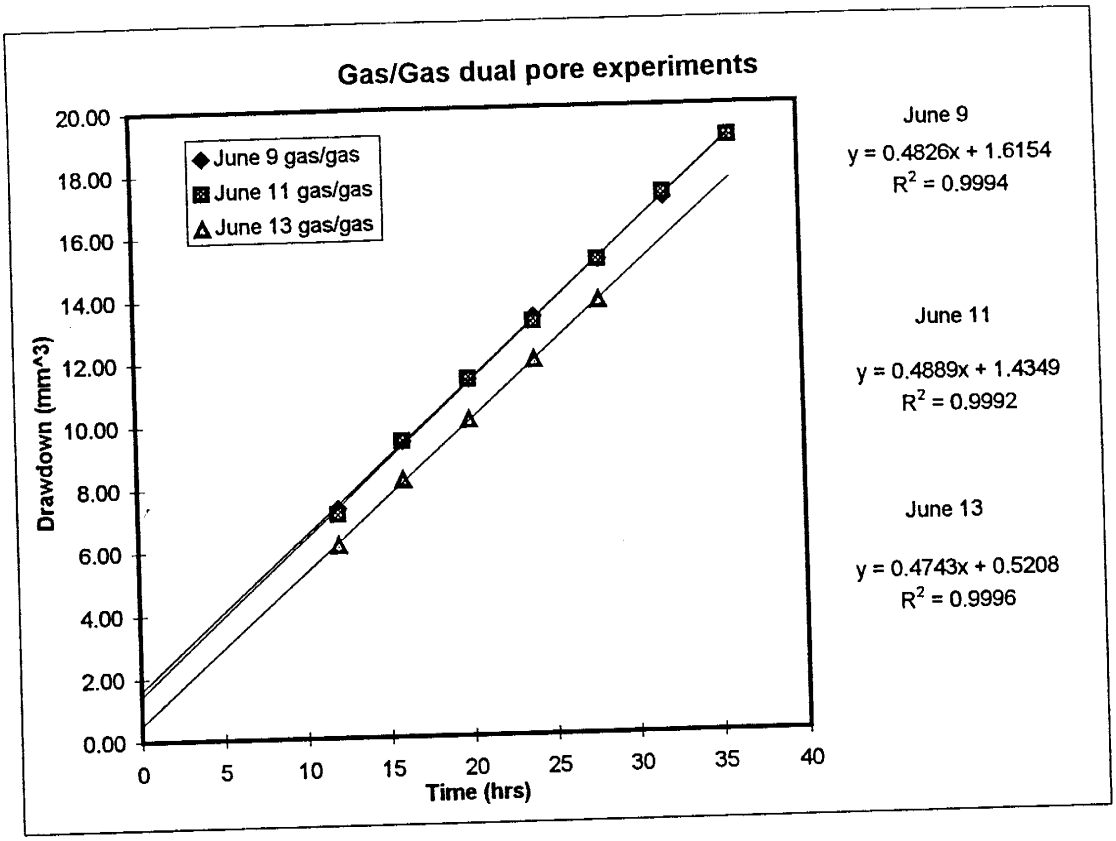
Gas/Gas dual pore experiments
June 9 gas/gas
June 11 gas/gas
June 13 gas/gas
Drawdown (mm^3)
Time (hrs)
20.00
18.00
16.00
14.00
12.00
10.00
8.00
6.00
4.00
2.00
0.00
0
5
10
15
20
25
30
35
40
June 9
y = 0.4826x + 1.6154
R2 = 0.9994
June 11
y = 0.4889x + 1.4349
R2 = 0.9992
June 13
y = 0.4743x + 0.5208
R2 = 0.9996

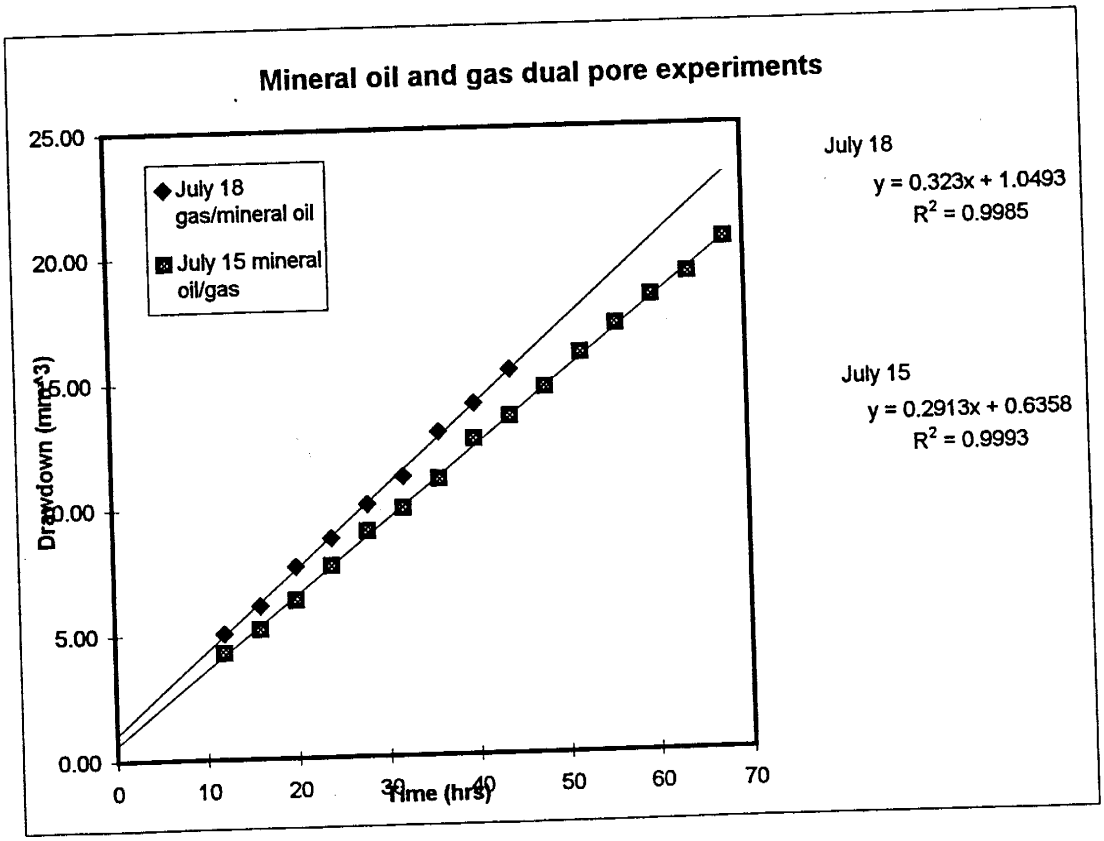
Mineral oil and gas dual pore experiments
July 18 gas/mineral oil
July 15 mineral oil/gas
Drawdown (mm^3)
Time (hrs)
25.00
20.00
15.00
10.00
5.00
0.00
0
10
20
30
40
50
60
70
July 18
y = 0.323x + 1.0493
R2 = 0.9985
July 15
y = 0.2913x + 0.6358
R2 = 0.9993

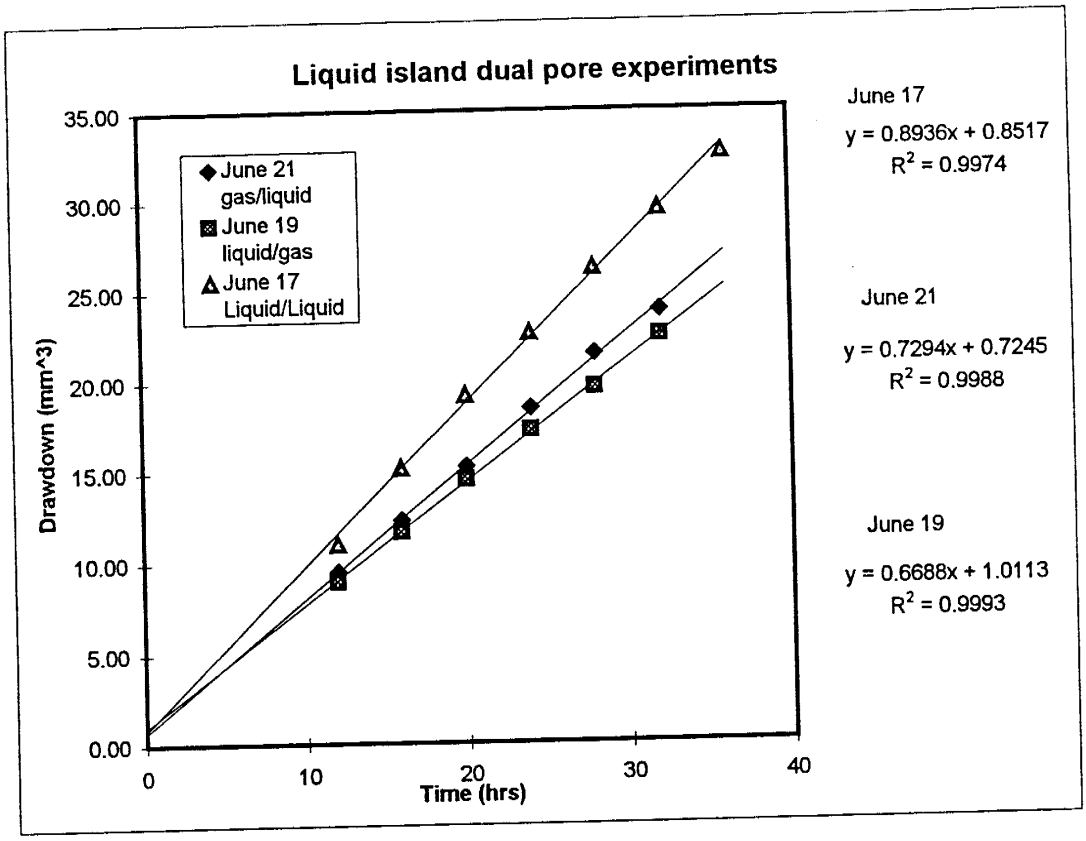
Liquid island dual pore experiments
June 21 gas/liquid
June 19 liquid/gas
June 17 Liquid/Liquid
Drawdown (mm^3)
Time (hrs)
0.00
5.00
10.00
15.00
20.00
25.00
30.00
35.00
0
10
20
30
40
June 17
y = 0.8936x + 0.8517
R2 = 0.9974
June 21
y = 0.7294x + 0.7245
R2 = 0.9988
June 19
y = 0.6688x + 1.0113
R2 = 0.9993

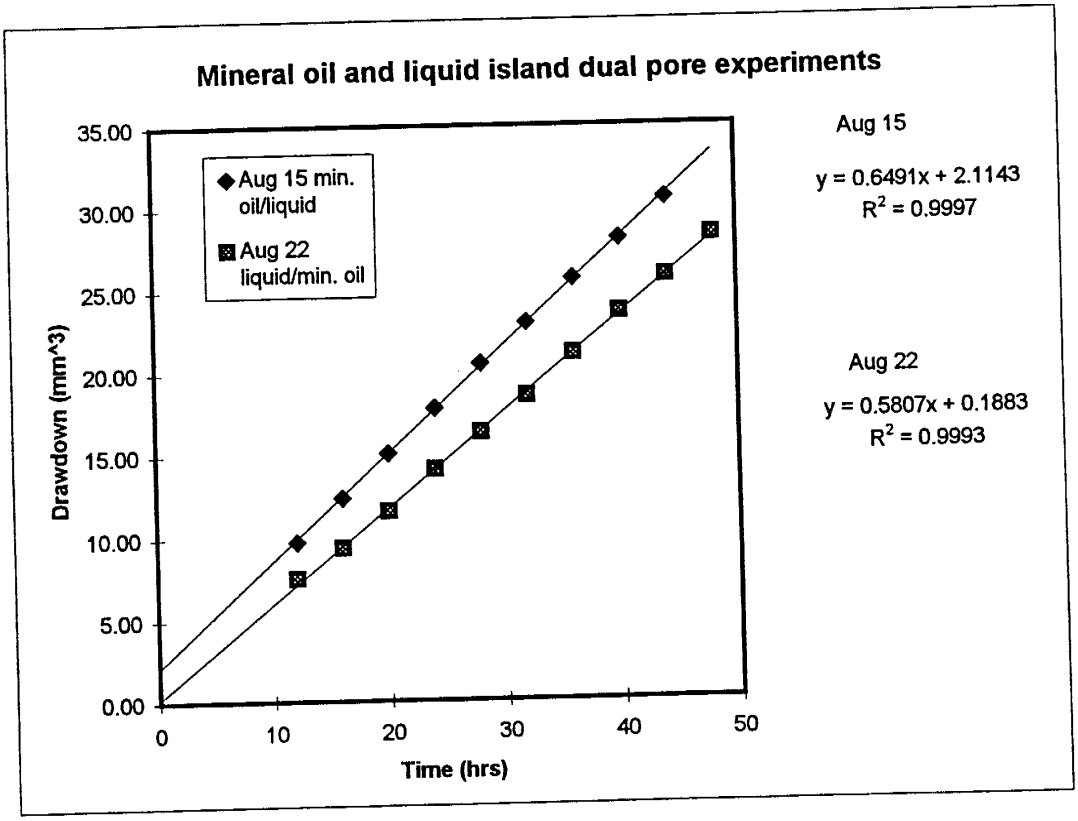
Mineral oil and liquid island dual pore experiments
Aug 15 min. oil/liquid
Aug 22 liquid/min. oil
Drawdown (mm^3)
Time (hrs)
0.00
5.00
10.00
15.00
20.00
25.00
30.00
35.00
0
10
20
30
40
50
Aug 15
y = 0.6491x + 2.1143
R2 = 0.9997
Aug 22
y = 0.5807x + 0.1883
R2 = 0.9993

Appendix K – Deuterium tracer experiment data

Appendix K contains the data from the deuterium tracer experiments, including all drawdown data for the gas and liquid-filled dual-pore-throat experiments. Again, these tables include the measured and corrected drawdown data as well as a figure of drawdown versus time. Minimum, maximum, and average temperature adjacent to the diffusion cell is shown on each page. The last page of Appedix K includes the raw mass spec data and the corrected values. The correction is based on a linear regression from the standards discussed in the text.

Deuterium -- Gas Diffusion Experiment

Begin Date 8/6/98
Begin Time 10:20
Interval 4 hr

	Temperature (C)					
	8/6/98	8/7/98	8/8/98	8/9/98	8/10/98	8/11/98
Min	28.32	27.43	26.46	28.46	27.56	28.60
Max	28.94	28.93	28.89	28.89	28.90	28.64
Ave	28.87	28.85	28.82	28.85	28.84	28.62

	Actual OD (mm)	Actual ID (mm)	Projected OD
left column	5.22	3.5	20.5

Photo	Date	Time	Hour	Projected pure drawdown	Actual pure drawdown (mm)	Pure volume decrease (mm^3)	Corrected volume decrease (mm^3)
1	8/6/98	10:20	0	0.0	0.00	0.00	0.0
2		14:20	4	0.7	0.178	1.71	1.7
3		18:20	8	1.2	0.31	2.94	2.9
4		22:20	12	1.7	0.43	4.16	4.2
5	8/7/98	2:20	16	2.2	0.56	5.39	5.4
6		6:20	20	2.4	0.61	5.88	5.9
7		10:20	24	2.9	0.74	7.10	7.1
8		14:20	28	3.4	0.87	8.33	8.3
9		18:20	32	3.8	0.97	9.31	9.3
10		22:20	36	6.7	1.71	16.41	10.4
11	8/8/98	2:20	40	7.2	1.83	17.64	11.6
12		6:20	44	7.7	1.96	18.86	12.9
13		10:20	48	8.1	2.06	19.84	13.8
14		14:20	52	8.5	2.16	20.82	14.8
15		18:20	56	8.9	2.27	21.80	15.8
16		22:20	60	11.5	2.93	28.17	16.2
17	8/9/98	2:20	64	12	3.06	29.40	17.4
18		6:20	68	12.4	3.16	30.38	18.4
19		10:20	72	12.9	3.28	31.60	19.6
20		14:20	76	13.3	3.39	32.58	20.6
21		18:20	80	13.7	3.49	33.56	21.6
22		22:20	84	14.1	3.59	34.54	22.5
23	8/10/98	2:20	88	14.6	3.72	35.77	23.8
24		6:20	92	14.9	3.79	36.50	24.5
25		10:20	96	15.3	3.90	37.48	25.5
26		14:20	100	15.6	3.97	38.22	26.2
27		18:20	104	16	4.07	39.20	27.2
28		22:20	108	16.4	4.18	40.18	28.2
29	8/11/98	2:20	112	16.9	4.30	41.40	29.4

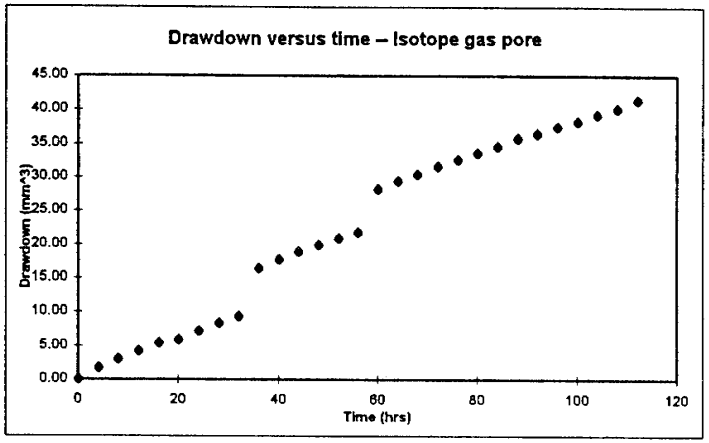

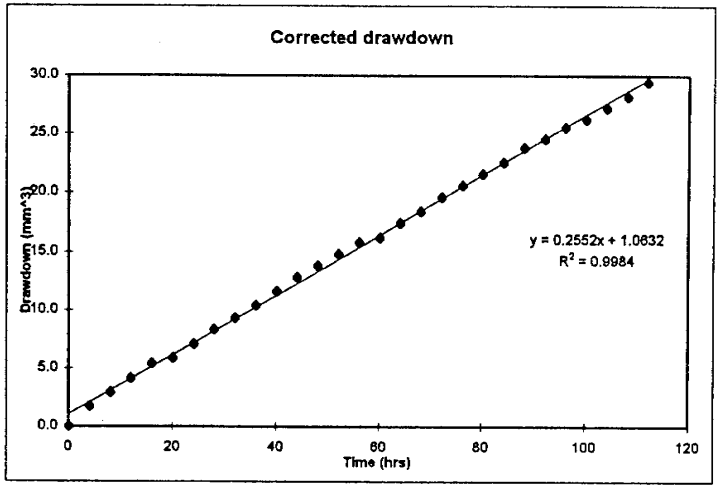

The corrected drawdown graph accounts for the volume removed during sampling

Deuterium – Liquid Island Experiment

Begin Date 8/18/98
Begin Time 0:20
Interval 4 hr

	Temperature (C)		
	8/18/98	8/19/98	8/20/98
Min	27.41	27.28	27.52
Max	29.03	28.99	28.99
Ave	28.98	28.92	28.93

	Actual OD (mm)	Actual ID (mm)	Projected OD
left column	5.22	3.5	19.8

Initial Island Molality
2.6

Photo	Date	Time	Hour	Projected pure drawdown	Actual pure drawdown (mm)	Pure volume decrease (mm^3)	Corrected pure volume decrease (mm^3)	Length of Island (mm)
1	8/18/98	0:20	0	0.0	0.00	0.00	0.00	6.67
2		4:20	4	1.2	0.32	3.04	3.04	6.67
3		8:20	8	2.1	0.55	5.33	5.33	6.67
4		12:20	12	2.9	0.76	7.36	7.36	6.67
5		16:20	16	3.8	1.00	9.64	9.64	6.67
6		20:20	20	4.5	1.19	11.41	11.41	6.67
7	8/19/98	0:20	24	5.5	1.45	13.95	13.95	6.67
8		4:20	28	6.0	1.58	15.22	15.22	6.67
9		8:20	32	6.9	1.82	17.50	17.50	6.67
10		12:20	36	11.6	3.06	29.42	20.42	6.67
11		16:20	40	12.4	3.27	31.45	22.45	6.67
12		20:20	44	13.1	3.45	33.23	24.23	6.67
13	8/20/98	0:20	48	13.9	3.66	35.26	26.26	6.67
14		4:20	52	14.7	3.88	37.29	28.29	6.67
15		8:20	56	15.5	4.09	39.32	30.32	6.67
16		12:20	60	18.6	4.90	47.18	32.18	6.67
17		16:20	64	19.5	5.14	49.46	34.46	6.67
18		20:20	66	20.3	5.35	51.49	36.49	6.670

Note: Island location varried – unreliable calculated lengths. Instead, get length from rate versus island length regression.

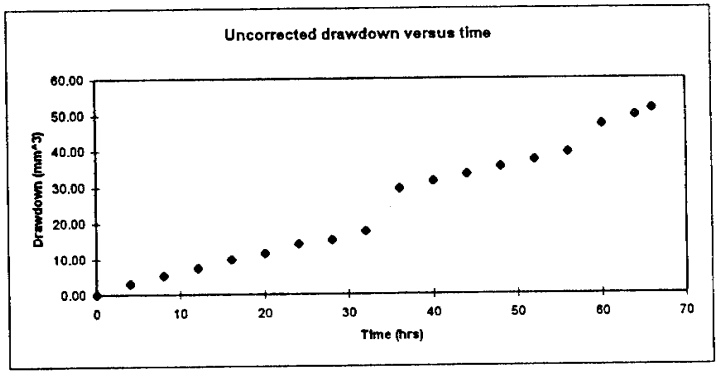

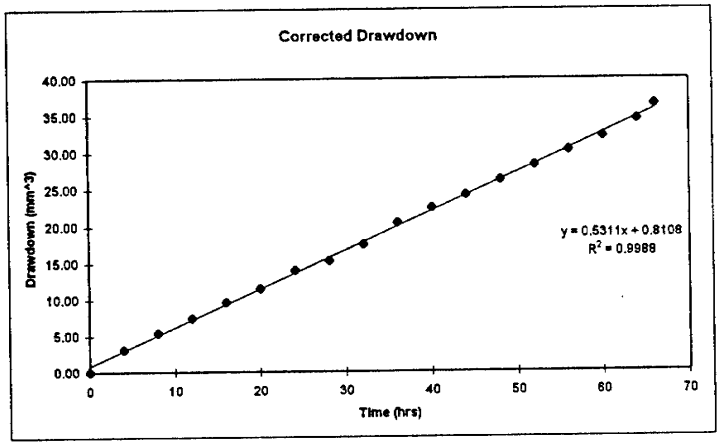

The corrected drawdown graph accounts for the volume removed during sampling

Gas Deuterium Experiment

Sample ID	Hour	Measured del			Corrected del		
		Upgradient	Downgradient	Island	Upgradient	Downgradient	Island
L1A	0	17.3			-8.0		
L1B	0	14.9			-10.3		
L2A	0		-218.9			-232.6	
L3A	0			-233.4			-246.3
L3B	0			-238.6			-251.3
L4A	12		-199.9			-214.5	
L5A	24		-178.9			-194.5	
L6A	36		-163.5			-179.9	
L7A	36	19.3			-6.1		
L8A	48		-161			-177.5	
L8B	48		-164.5			-180.8	
L9A	60		-149.1			-166.2	
L10A	60	28.2			2.4		
L10B	60	28.2			2.4		
L11A	72		-130.5			-148.5	
L11B	72		-130.1			-148.1	
L12A	72	36.4			10.2		
L12B	72	34.5			8.4		
L13A	72			-63.4			-84.7
L13B	72			-75.5			-96.2

Liquid Island Deuterium Experiment

Sample ID	Hour	Measured del		Corrected del	
		Upgradient	Downgradient	Upgradient	Gas experiment
D1A	0	7.9		-16.9	
D1B	0	14.4		-10.8	
D2A	0		-216.3		-230.1
D3A	12		-213.5		-227.4
D3B	12		-204.6		-219.0
D4A	24		-199.3		-213.9
D5A	36	17.9		-7.4	
D6A	36		-156.2		-172.9
D6B	36		-196.1		-210.9
D6C	36		-170.8		-186.8
D7A	48		-166		-182.3
D7B	48		-171.7		-187.7
D8A	60		-179.2		-194.8
D9A	60	27.2		1.4	
D10A	72		-162.4		-178.8
D11A	84		-150.8		-167.8
D12A	96		-139		-156.6
D13A	108		-131.3		-149.3
D14A	120		-120		-138.5
D14B	120		-123		-141.4
D15A	120	45.8		19.1	
D15B	120	39.7		13.3	

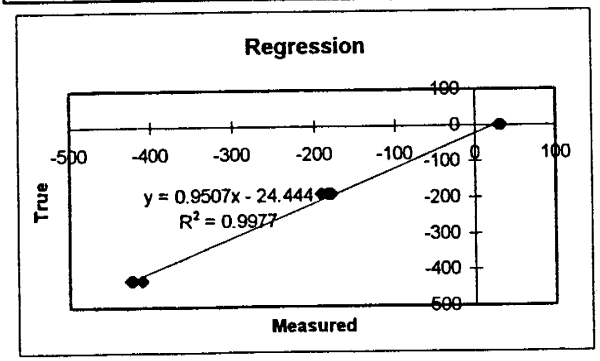

Appendix L --Models

Appendix L contains three models. The first model by Dr. J. L. Wilson describes enhancement as a function of two pore-throat geometries. The second model explains the results seen in the deuterium experiments. The third model presents a discussion on resistance in the dual-pore-throat apparatus.

A model of enhanced vapor phase diffusion through a single pore-throat

John L. Wilson

July 20, 1998

Consider quasi-steady flow through the diffusion cell experimental apparatus at some instant in time. Ignore the changing reservoir levels, and assume they are fixed. Then define a curvilinear coordinate, s, along the mean path, from the upgradient reservoir to the downgradient reservoir. Let the cross-sectional area normal to this coordinate be designated as $A(s)$, which varies along the path. Assume uniform vapor pressures across area A in the vapor-filled portions of the apparatus, and uniform liquid pressure and salt concentration in the liquid-filled portions. Ignore the effects of gravity as insignificant in both liquid and vapor.

Vapor Phase

The basic model for steady state vapor flux transport is given by

$$J_v^M = x_v\left(J_v^M + J_a^M\right) - cD\frac{dx_v}{ds} \tag{L1}$$

where the superscript M refers to molar flux (moles/m^2 s), the subscript v refers to water vapor and a refers to air, x refers to mole fraction, D is the molecular diffusion coefficient of the water vapor in air, and c is the molar density (moles/m^3) of the air (Bird et al, 1960). In this case we can assume no net flux of the air, that is J_a^M, is zero, and the vapor flux becomes:

$$J_v^M = \frac{-cD}{1-x_v}\frac{dx_v}{ds} \tag{L2}$$

The total vapor flux, Q^M(moles/s), is proportional to the cross-sectional area, and for steady flow along a continuous vapor phase it must be constant along path s:

$$Q_v^M = \frac{-cD}{\int \frac{ds}{A(s)}} \int \frac{dx_v}{1-x_v} = \frac{cD}{\int \frac{ds}{A(s)}} \ln(1-x_v) \qquad \text{(L3)}$$

We have ignored the constant of integration.

Suppose there is no liquid-island. Then this equation applies along all s, between the upgradient and downgradient reservoirs. If x_{v1} represents the mole fraction above the upgradient reservoir, and x_{v4} represents the same above the downgradient reservoir, then we can find an expression for total vapor flux:

$$Q_v^M = \frac{cD}{\int_{s1}^{s4} \frac{ds}{A(s)}} \ln\left(\frac{1-x_{v4}}{1-x_{v1}}\right) \equiv Q_{vo}^M \qquad \text{(L4)}$$

We assign the notation Q_{vo}^M to represent this reference situation. Vapor transport increases with the diffusion coefficient, the cross-sectional area, and the vapor pressure gradient as represented by the mole fraction ratio. It decreases with a longer flow path. The denominator is a length weighted harmonic average of the cross-sectional area. Figure L1 shows a schematic diagram of the diffusion cell with numbered reservoirs.

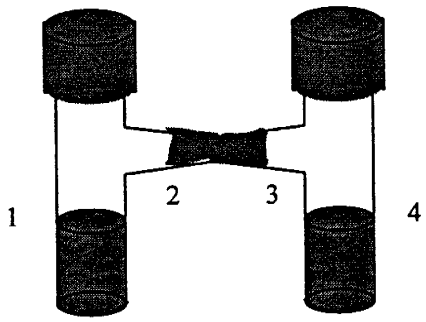

Figure L1. Schematic diagram of diffusion cell numbering scheme for the enhancement model.

To explore this relationship let's assume that the path consists of three sections: an upgradient zone of larger area A_1 and length L_1, a similar downgradient area, A_4, and length, L_4, and an intermediate pore-throat of length L_{23} but with a much smaller area, A_{23}. Then the denominator in (L4) is

$$\int_{s1}^{s4} \frac{ds}{A(s)} = \frac{L_1}{A_1} + \frac{L_{23}}{A_{23}} + \frac{L_4}{A_4} \tag{L5}$$

If the pore-throat area is sufficiently small, and the throat long enough, then the pore-throat will dominate the flow, and

$$\int_{s1}^{s4} \frac{ds}{A(s)} \cong \frac{L_{23}}{A_{23}} \tag{L6}$$

The diffusion cell was designed with this as a goal.

In the presence of a liquid-island in the pore-throat we can perform similar calculations for the vapor phase. Let the upgradient end of the liquid-island be located at s_2 and the downgradient end at $s_3 > s_2$. Then let x_2 and x_3 be the vapor phase mole fractions at these two gas-liquid interfaces, giving for steady flow

$$Q_v^M = \frac{cD}{\int_{s1}^{s2} \frac{ds}{A(s)}} \ln\left(\frac{1-x_{v2}}{1-x_{v1}}\right) = \frac{cD}{\int_{s3}^{s4} \frac{ds}{A(s)}} \ln\left(\frac{1-x_{v4}}{1-x_{v3}}\right) \tag{L7}$$

The enhancement factor, $E = Q_v^M / Q_{vo}^M$, is given by the flow rate in this liquid-island system divided by the vapor only flow rate in (L4). We can get to it by manipulating (L7) and relating it to (L4):

$$\int_{s1}^{s2} \frac{ds}{A(s)} + \int_{s2}^{s3} \frac{ds}{A(s)} + \int_{s3}^{s4} \frac{ds}{A(s)} = \frac{cD}{Q_v^M} \ln\left(\frac{1-x_{v2}}{1-x_{v1}}\right) + \int_{s2}^{s3} \frac{ds}{A(s)} + \frac{cD}{Q_v^M} \ln\left(\frac{1-x_{v4}}{1-x_{v3}}\right)$$

$$= \int_{s1}^{s4} \frac{ds}{A(s)} = \frac{cD}{Q_{vo}^M} \ln\left(\frac{1-x_{v4}}{1-x_{v1}}\right) \tag{L8}$$

In other words,

$$\frac{Q_v^M}{Q_{vo}^M} = \frac{\ln\left(\frac{1-x_{v2}}{1-x_{v1}}\right)+\ln\left(\frac{1-x_{v4}}{1-x_{v3}}\right)}{\ln\left(\frac{1-x_{v4}}{1-x_{v1}}\right)} + \frac{Q_v^M}{cD}\frac{\int_{s2}^{s3}\frac{ds}{A(s)}}{\ln\left(\frac{1-x_{v4}}{1-x_{v1}}\right)} \qquad \text{(L9)}$$

We divide the last term in (L9) by (L4) and manipulate to get

$$E = \frac{Q_v^M}{Q_{vo}^M} = \frac{\ln\left(\frac{1-x_{v2}}{1-x_{v1}}\right)+\ln\left(\frac{1-x_{v4}}{1-x_{v3}}\right)}{\ln\left(\frac{1-x_{v4}}{1-x_{v1}}\right)} \quad \frac{\int_{s1}^{s4}\frac{ds}{A(s)}}{\int_{s1}^{s4}\frac{ds}{A(s)}-\int_{s2}^{s3}\frac{ds}{A(s)}} \qquad \text{(L10)}$$

If the liquid-island length $L_{23} = s_3 - s_2 = 0$, then $x_{v2}=x_{v3}$, and $E=1$, as it should. This equation involves the product of two terms. The first term represents the vapor pressure gradients. If diffusion dominates in the liquid-island, no concentration gradient exists within the island, and $x_{v2}=x_{v3}$, and therefore the first term can be neglected.

The second term reprepresents the geometry, involving both the area and length of each vapor section and the liquid-island. We can explore the effect of the second term in (L10),

$$E \propto \frac{\int_{s1}^{s4}\frac{ds}{A(s)}}{\int_{s1}^{s4}\frac{ds}{A(s)}-\int_{s2}^{s3}\frac{ds}{A(s)}} = 1+\frac{\int_{s2}^{s3}\frac{ds}{A(s)}}{\int_{s1}^{s4}\frac{ds}{A(s)}-\int_{s2}^{s3}\frac{ds}{A(s)}}, \qquad \text{(L11)}$$

by considering two special cases. In the first case let's assume that locations s_i, and liquid-island length L_{23}, are fixed, and examine the effect of spatially varying area $A(s)$. Take the area between 1 and 2, and between 3 and 4, as constant. Then let the area in the liquid-island contract. In the second case fix the A as a constant over the entire model, and examine the effect of varying liquid-island length, L_{23}.

Suppose that the variable area in the liquid-island is described by $A(s') = a - b\cos(\pi s'/L_{23})$, where a and b refer to the vertical shift and amplitude

of the function describing the area respectively. If s' is measured from the center of a symmetrical pore-throat, $b<a$, and $L_{23}=s_3 - s_2$, then

$$E \propto 1+\frac{\int_{-L_{23}/2}^{+L_{23}/2} \frac{ds'}{a-b\cos(\pi s'/L_{23})}}{\frac{s_2-s_1}{A_1}+\frac{s_4-s_3}{A_4}} = 1+\frac{a}{2(s_2-s_1)}\frac{2L_{23}}{\pi\sqrt{a^2-b^2}}\tan^{-1}\left[\frac{\sqrt{a^2-b^2}\tan\left(\pi s'/2L_{23}\right)}{a-b}\right]_{-L_{23}/2}^{+L_{23}/2}$$

or,

$$E \propto 1+\frac{2(s_3-s_2)}{(s_2-s_1)\pi\sqrt{1-(b/a)^2}}\tan^{-1}\sqrt{\frac{a+b}{a-b}} \qquad \text{(L12)}$$

We have assumed complete symmetry, if $A_1=A_2=a$. When $b=0$ there is no contraction (uniform area) and the enhancement is proportional to the length of the liquid-island divided by the gas filled length. Additional enhancement due to the contraction increases with b, accelerating as b approaches a. For example, when $b=0.5a$ the enhancement increases by a factor of 2 over the no contraction condition; when $b=0.9a$ it is 4.5 times higher. Figure L2 examines enhancement over a range of b values for 2 different a values (with fixed s_2-s_1 and s_3-s_2 values).

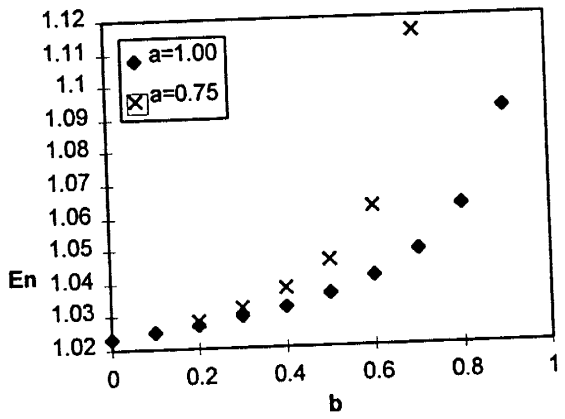

Figure L2. Enhancement over a range of *b* values for 2 values of *a*.

In the second case, area is constant and enhancement E becomes

$$E \propto \frac{s_4 - s_1}{s_4 - s_1 - L_{23}} = \frac{L}{L - L_{23}} = 1 + \frac{L_{23}}{L} + \left[\frac{L_{23}}{L}\right]^2 + \left[\frac{L_{23}}{L}\right]^3 + \ldots \cong 1 + \frac{L_{23}}{L} + \left[\frac{L_{23}}{L}\right]^2 \quad \text{(L13)}$$

where L is the total distance between reservoirs, and we have approximated this term by a binomial series. The last expression on the right is the quadratic that results from truncating the series. Figure L3 shows the shape of the enhancement function over dimensionless island length (L_{23} / L).

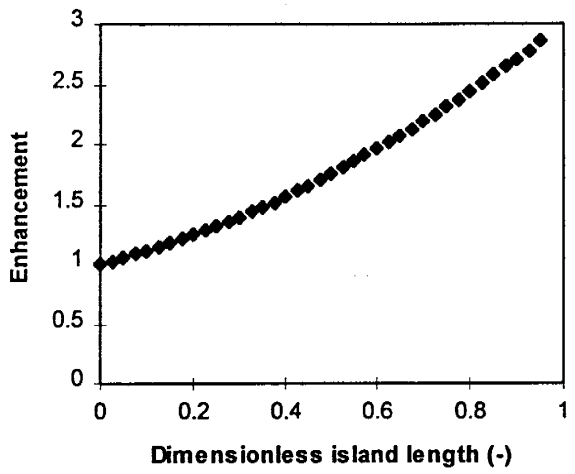

Figure L3. Enhancement versus dimensionless island length.

Isotope Transport Model

This section describes a simple lumped parameter model of deuterium transport through the single-pore diffusion cell. The model examines transport through both a gas-filled and liquid-filled pore-throat. In each case, the upgradient reservoir is initially deuterium enriched with respect to the downgradient reservoir and island, if present. Deuterium is assumed to move in the vapor phase only as water vapor and is transported according to a prescribed molar flux based on the values in the results section of this report. Deuterium fractionation between liquid and vapor is accounted for at each liquid-vapor interface according to the equilibrium fractionation factor. This model attempts to explain the trends seen in the results of the gas and liquid-filled pore-throat experiments. The model uses mole fraction (x) of deuterium / hydrogen to perform the calculations and to demonstrate mass balance. Results in the paper are given in δ notation relative to SMOW (Standard Mean Oceanic Water). The notation can be related to mole fraction by

$$\delta = \frac{x_{sample} - x_{SMOW}}{x_{SMOW}} * 1000 \qquad (L14)$$

Figure L4 shows a schematic diagram of the apparatus with liquid and vapor reservoirs labeled for identification. The integers correspond with the liquid or vapor reservoirs while the fractions denote the interface between reservoirs.

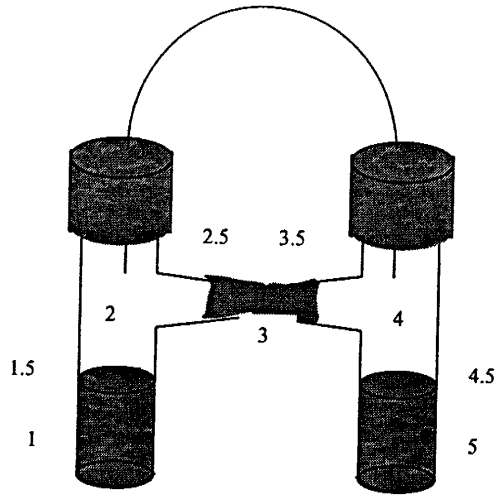

Figure L4. Schematic diagram of model liquid, vapor and interface notation.

We describe the molar flux through each liquid and gas reservoir using five coupled ordinary differential equations (ODEs) which calculate net mass flux based on the evaporation and condensation at each interface. The generic equations for the upgradient and downgradient reservoirs are

$$\frac{d}{dt}\left(\frac{\rho_i}{M}V_i x_i\right) = A_{i+\frac{1}{2}} J^M x_{i+1} k_i^C \left(\frac{h_{i+1}}{|a_i - h_{i+1}|}\right) - A_{i+\frac{1}{2}} J^M x_1 k^E \left(\frac{a_i}{|a_i - h_{i+1}|}\right) \qquad (L15)$$

$$\frac{d}{dt}\left(\frac{\rho_i}{M}V_i x_i\right) = A_{i-\frac{1}{2}} J^M x_{i-1} k^C \left(\frac{h_{i-1}}{|a_i - h_{i-1}|}\right) - A_{i-\frac{1}{2}} J^M x_1 k^E \left(\frac{a_i}{|a_i - h_{i-1}|}\right) \qquad (L16)$$

Where:

a = activity of water (-)
A = area at interface (mm^2)
ρ = density of water (g/mm^3)
h = relative humidity (-)
J^M = molar flux of water (mol/mm^2 hr)
k = fractionation factor for deuterium
subscripts C and E refer to condensation and evaporation respectively

M = molar mass of water (g/mol)
V = volume of reservoir (mm^3)
x = mol fraction of deuterium $\cong$ moles of deuterium / moles of hydrogen

The first term on the right hand side of (L15) and (L16) accounts for the condensation on the reservoir which is described by the ratio of relative humidity to the absolute value of the difference between the activity of the solution and the relative humidity (Wexler, 1965). The second term in these equations accounts for evaporation from the liquid surface. Evaporation is described by a similar quotient with the same denominator, but with the activity of the solution in the numerator, instead of relative humidity. Inherent in (L15) and (L16) is the assumption that $k^C = k^E$; the fractionation difference between condensation and evaporation is accounted for in and that the In both (L15) and (L16) the volume term is within the derivative since it changes with time for both reservoirs.

Table L1 lists the parameter values used for the gas-filled and liquid-filled pore-throat models.

Table L1. Values used for a) general model parameters; b) each vapor or liquid reservoir; and c) each vapor-liquid interface.

a)

Parameter	Value
J^M gas-filled pore-throat (mm^3/hr)	0.24
J^M liquid-filled pore-throat (mm^3/hr)	0.53
M (g/mol)	18
k^C (at 29 °C)	1.076
k^E (at 29 °C)	0.939
ρ liquid (g/mm^3)	1.0×10^{-3}
ρ vapor density (g/mm^3)	$*1.73 \times 10^{-5}$

* denotes ρ value used, actual value = 1.73×10^{-8}

b)

Reservoir	Activity	Relative humidity	Volume (mm^3)	Initial δ
1	0.99	--	94	-10
2	--	0.77	60	-230
3	0.55	--	7	-230
4	--	0.33	60	-230
5	0.11	--	57	-230

c)

Interface	Area when pore is:	
	Gas-filled (mm^2)	Liquid-filled (mm^2)
1.5	9.6	9.6
2.5	9.0	7.5
3.5	9.0	7.5
4.5	9.6	9.6

The values of J^M for both the gas and liquid-filled pore-throat model were determined experimentally. The fractionation factors, k^C and k^E, are defined by the quotient x_{liquid} / x_{vapor} and x_{vapor} / x_{liquid} respectively (Friedman and O'Neil, 1977). Due to its higher mass and stronger hydrogen bonding, deuterium has a higher tendency to remain in liquid form relative to hydrogen. Thus, we should

see each liquid reservoir become more deuterium enriched with time. The value for area A at interfaces 1.5 and 4.5 was estimated from the calibration described in Appendix B. The area at interfaces 2.5 and 3.5 was more difficult to estimate since the pore-throat has a non-uniform taper. Imprecision in estimating this area, as well as the simplicity of the model limit the model to studying trends.

This simple model assumes that the density of each liquid is unity and the density of the vapor phase on either side of the liquid-island is equal to the product of the vapor saturation at 29°C and the assigned relative humidity of the vapor phase. The relative humidity values were assigned approximately midway between the activities of the two adjacent liquid reservoirs. The activity values of the upgradient and downgradient reservoirs were assigned according to tabulated values of pure water and saturated LiCl solution (1 and 0.11 respectively). The activity of the liquid-island was assigned as 0.51 based on the approximate activity of the solution at saturation. Varying this value over a range of 25% had a negligible effect on the deuterium enrichment in the downgradient reservoir. Implicit in these assigned parameter values is that activity and relative humidity are constant over the length of each respective liquid or vapor reservoir.

For the gas-filled pore-throat experiment, the value of J^M was reduced to reflect the lower flux through the gas-filled pore. Also, the area at interfaces 2.5 and 3.5 was reduced to account for the smaller flux area through the gas-filled pore-throat (really there is no interface at this point since the pore-throat is gas-filled, but the A value was changed in reservoir 3 to reflect a lower average cross sectional area caused by a lack of liquid-island). The fractionation factor was also

neglected between reservoirs 2 and 3, as well as between 3 and 4 since each reservoir was vapor filled.

Since the liquid-island has an upgradient and downgradient interface, the molar flux can be described by the sum (L15) and (L16),

$$\frac{\rho_i}{M} V_i \frac{dx_i}{dt} = A_{i-\frac{1}{2}} J^M x_{i-1} k^C \left(\frac{h_{i-1}}{|a_i - h_{i-1}|} \right) - A_{i-\frac{1}{2}} J^M x_1 k^E \left(\frac{a_i}{|a_i - h_{i-1}|} \right)$$
$$+ A_{i+\frac{1}{2}} J^M x_{i+1} k^C \left(\frac{h_{i+1}}{|a_i - h_{i+1}|} \right) - A_{i+\frac{1}{2}} J^M x_i k^E \left(\frac{a_i}{|a_i - h_{i+1}|} \right) \qquad (L17)$$

The terms from (L15) account for the evaporation and condensation at the downstream end of the liquid-island and the terms from (L16) account for the condensation and evaporation at the upstream end of the liquid-island. In (L17) the volume term is taken outside of the derivative since liquid-island volume is assumed constant.

The equation describing isotope flux through the vapor phase is similar to the equation for the liquid-island since each vapor phase has two interfaces where exchange occurs. The generic equation is identical for both upgradient and downgradient vapor reservoirs,

$$\frac{d}{dt}\left(\frac{\rho_i}{M} V_i x_i \right) = A_{i-\frac{1}{2}} J^M x_{i-1} k^E \left(\frac{a_{i-1}}{|a_{i-1} - h_i|} \right) - A_{i-\frac{1}{2}} J^M x_1 k^C \left(\frac{h_i}{|a_{i-1} - h_i|} \right)$$
$$+ A_{i+\frac{1}{2}} J^M x_{i+1} k^E \left(\frac{a_{i+1}}{|a_{i+1} - h_i|} \right) - A_{i+\frac{1}{2}} J^M x_i k^C \left(\frac{h_i}{|a_{i+1} - h_i|} \right); \; i = 2, 4 \qquad (L18)$$

Now, we have five first order, linear ODEs and five unknowns (x_1 through x_5). The system of ordinary differential equations is solved by the Matlab routine

ODE23. The solution of this problem, however, is difficult since the density values between liquid and vapor are 5 orders of magnitude different. This makes the problem too "stiff" to be solved by this conventional approach. The stiffness problem, however, can be avoided by neglecting storage in the two vapor reservoirs. By assuming instantaneous vapor transport through the vapor phase (i.e. dx/dt=0 in both vapor equations), we can transform the two vapor reservoir ODEs to algebraic equations which can be substituted into the remaining ODEs as appropriate. This new approach solves the three ODEs in terms of mole fraction (x) in each of the three liquid reservoirs. Neglecting gas phase storage in this model is a reasonable assumption due to the very small volume of water vapor compared to liquid water. Estimates of the total mass of deuterium in the vapor phase, taken from the mass balance calculations, are negligible compared to the mass in the liquid reservoirs. To demonstrate model mass balance, Figure L5 shows the amount of moles of deuterium in each liquid phase and the cumulative amount over time for the liquid-island model.

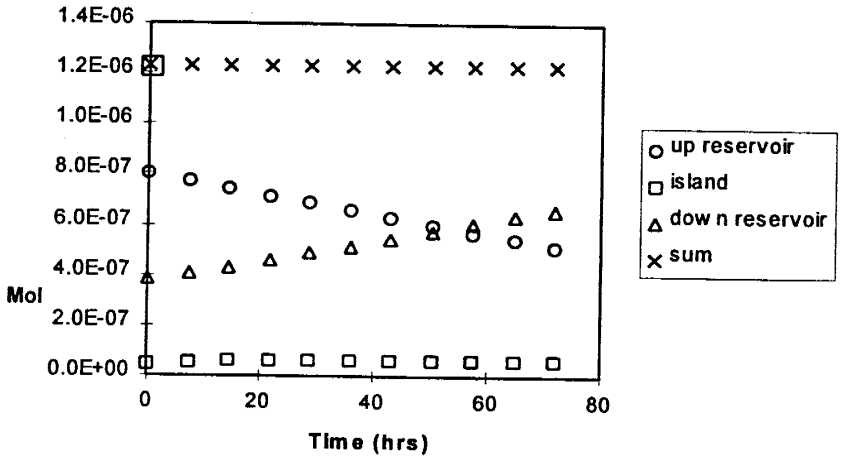

Figure L5. Moles of deuterium in each reservoir for the liquid-island experiment

A plot of deuterium mole fraction versus time for the liquid-island experiment is shown in Figure L6a. This plot shows that the mole fraction in each of the three liquid reservoirs increases over time. The rate of increase of x in the liquid-island is dramatic for the first 12 hours. This feature can be explained through a simple calculation of residence time; with a flux rate of 0.5 mm^3/hr and a liquid-island volume of approximately 7 mm^3 the volume of liquid in the pore-throat is replaced after about 12.5 hours. After the initial steep increase, the mole fraction in the liquid-island reaches steady state where the rate of increase in mole fraction is approximately equal to the rate of increase in the upgradient solution. The mole fraction in the downgradient reservoir increases slowly at first, then accelerates at approximately the same time as the liquid-island reaches steady state. The degree of mole fraction increase in the downgradient reservoir is most sensitive to the area at the pore-throat interface (interface 2.5 and 3.5). Figure 6 a,b shows a comparison of deuterium mole fractions in each reservoir for two different effective pore-throat areas.

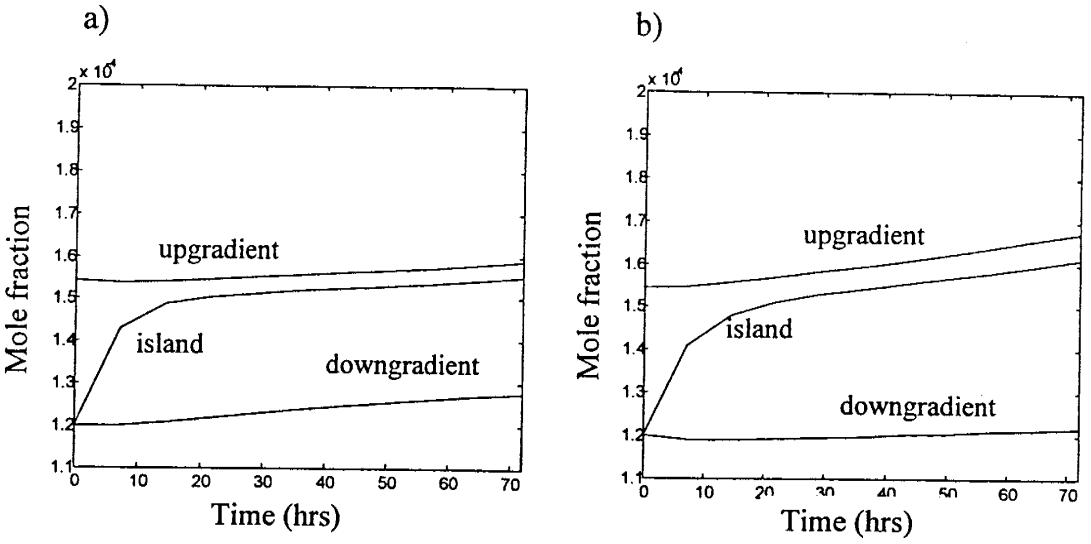

Figure L6. Mole fraction of deuterium for each liquid reservoir over time for the liquid-filled pore-throat model with a pore-throat interface area of a) 9 mm^2; and b) 7 mm^2.

As mentioned earlier, differences in relative humidities and the activity values in reservoirs 2, 3, and 4 had a negligible effect on the deuterium enrichment in the downgradient reservoir, provided the activity values of reservoir 1 and 5 remained constant. Similarly, the model was insensitive to density difference between liquid and vapor reservoirs. Using a vapor density value approximately mid-way between liquid density and actual water vapor density (1.73×10^{-5}) reduced the stiffness sufficiently to allow all five ODEs to be solved simultaneously. The results were comparable to the solution with no storage in the vapor phase, as shown in Figure L7. Since the model was not sensitive to vapor density, this approximation was used to solve all five ODEs to show deuterium enrichment in the downgradient reservoir for the gas-filled pore-throat experiment. Figure L8a shows the deuterium mole fraction over time in the upgradient and downgradient reservoirs for the gas-filled pore-throat and liquid-

filled pore-throat models, while Figure L8b shows the same thing with δ notation. Notice that the thick lines represent the gas-filled pore-throat scenario, which had a duration of approximately 120 hours versus 70 hours for the liquid-filled pore-throat experiments

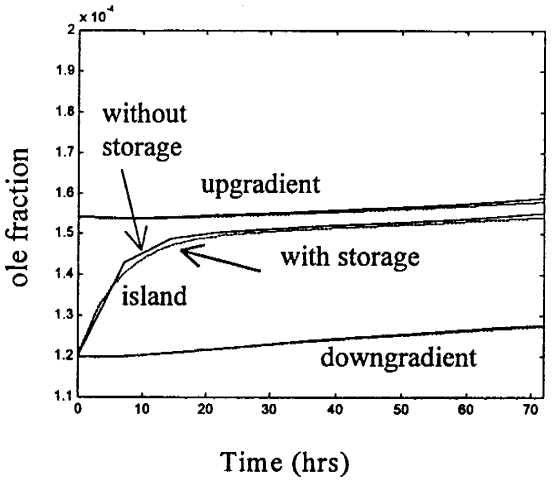

Figure L7. Comparison of mole fraction for each liquid reservoir over time neglecting storage in the vapor reservoir and including storage (assuming ρ_v=1.73x10^{-5} g mm^{-3}).

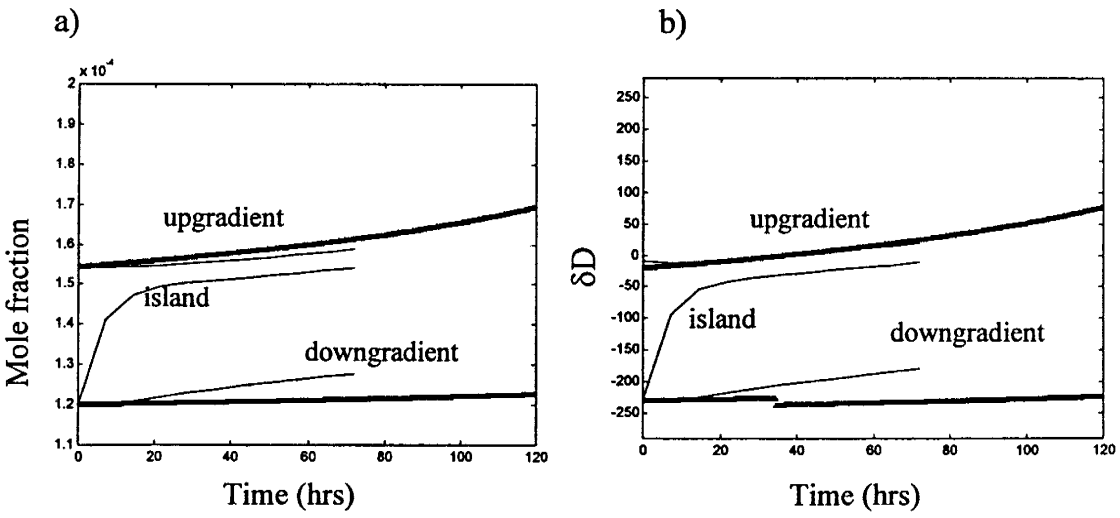

Figure L8. A comparison of deuterium in the upgradient, liquid-island, and downgradient reservoir in a) mole fraction notation; and b) del notation with the liquid-filled and gas-filled pore-throat. The thick lines indicate the gas-filled pore-throat values; the thin lines indicate the liquid-filled pore-throat values.

Figure L8 shows that the isotope transfer rate through the liquid-island model is faster than through the gas-filled pore-throat model. Figures L9 a,b compares the experimental results to the model results for both the gas-filled and liquid-filled pore-throat experiments. This comparison shows that in the actual experiment, the rate of deuterium enrichment in the downgradient reservoir is significantly faster than is predicted by the model. The underestimate of the model results may be attributed to the fact that the model does not account for diffusion under a deuterium gradient.

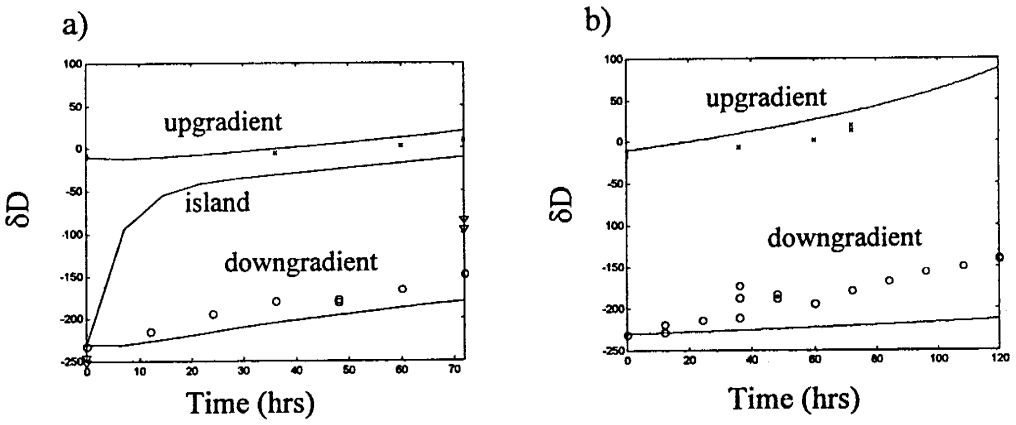

Figure L9. A comparison of experimental to model predicted values of del deuterium in each liquid reservoir for a) the liquid-island experiment; and b) the gas-filled pore-throat experiment. The solid lines indicate model predicted results while the o's indicate experimental values for the downgradient reservoir, the ∇'s indicate the liquid-island experimental results, and the x's represent the upgradient reservoir experimental results.

Dual-pore-throat Resistance Model

A simple parallel circuit analogy is used to describe the resistance in each section of the dual-pore-throat diffusion cell. Figure L10 shows a schematic diagram of the electrical analogy where R corresponds to the resistance at each section of the apparatus.

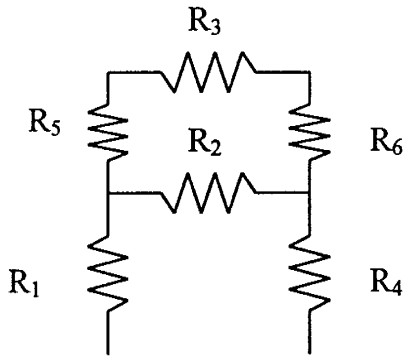

Figure L10. Parallel circuit schematic diagram

R_1, R_4, R_5, and R_6, represent resistances to vapor phase diffusion in the vertical column of the experimental apparatus. R_2 and R_3 represent resistances to vapor phase diffusion when a pore-throat is gas-filled or a combination of gas and liquid-filled when the pore-throat contains a liquid-island. We first examine this model for the condition when both pore-throats are gas-filled, then revisit it for the liquid-filled pore-throat conditions.

We assume that the R is a function of the length of the section (L) and effective area (A) and that $R \propto L/A$. We know $A_1 \cong A_4 \cong A_5 \cong A_6$ and $L_1 \cong L_4$, $L_5 \cong L_6$, and $L_2 \cong L_3$. We relate R_1, R_4, R_5, and R_6 by the relative L values measured from the projected image and find $R_1 \cong R_4$ and $R_5 \cong R_6 \cong 0.75R_1$. This

reduces the number of unknowns to three (R_1, R_2, and R_3), equal to the number of equations representing the three gas diffusion experiments (G/G, G/M, and M/G).

$$R_{G/M} = R_1 + R_5 + R_3 + R_6 + R_4 = 3.5R_1 + R_3 \qquad (L19a)$$

$$R_{M/G} = R_1 + R_2 + R_4 = 2R_1 + R_2 \qquad (L19b)$$

$$R_{G/G} = R_1 + R_4 + \frac{1}{\frac{1}{R_2} + \frac{1}{R_5 + R_3 + R_6}} = 2R_1 + \frac{R_2(1.5R_1 + R_3)}{1.5R_1 + R_2 + R_3} \qquad (L19c)$$

$R_{i/j}$ (the subscripts i/j refer to the top and bottom pore respectively) values are determined for G/G, G/M and M/G by the expressions,

$$R_{G/G} = \frac{\Delta h}{Q_{G/G}}; \quad R_{G/M} = \frac{\Delta h}{Q_{G/L}}; \quad R_{M/G} = \frac{\Delta h}{Q_{L/G}}, \qquad (L20)$$

where $Q_{i/j}$ is the volumetric flux (mm^3/hr) given by the experimental results and Δh is the vapor pressure difference between reservoirs (mm of H_2O). (Δh = 3567 mm of H_2O between pure water and LiCl solution based on vapor pressure above both solutions at 29 degrees Celsius.) Solving (L19) with the experimental values of $R_{i/j}$ calculated from (L20) yields estimates of the R's: R_{1G}=R_{4G}= 1,440 hr/mm^2, R_{2G}= 9,430 hr/mm^2, R_{3G}= 6,120 hr/mm^2, and R_{5G}=R_{6G}= 1,080 hr/mm^2 (a subscript G or L is added to denote when the pore-throat is gas or liquid-filled). The resistance in the top pore-throat is nearly 35% lower than in the bottom pore. By association, we know that the effective area is nearly 35% greater in the top pore-throat than in the bottom pore-throat, since $L_2 \cong L_3$ and $R \propto L/A$.

A similar calculation is performed to determine the pore-throat resistance when liquid-filled. In the liquid-island experiments, R_2 and R_3 account for both

gas and liquid resistances in the pore-throats. $R_{i/j}$ in (L20) is recalculated with the vapor fluxes for the L/M and M/L experiments and (L19a) and (L19b) are used to determine the values of R_{2L}, and R_{3L} (using the values of R_{1G}, R_{4G}, R_{5G}, and R_{6G} found from the all gas condition described earlier). The values of R_{2L}, and R_{3L} are calculated to be 2,570 hr/mm^2 and 1,230 hr/mm^2 respectively. Again, the resistance in the top pore is substantially lower than the bottom by nearly 52%. The increased difference in resistance is likely caused by a longer liquid-island length in the upper pore-throat as seen in Table 3 of the results section.

We can use the value for R_1 and the corresponding $R_{2(L\text{ or }G)}$ and $R_{3(L\text{ or }G)}$ values to predict the vapor flux through the L/G, G/L and L/L experiments using (L20), provided the liquid-island lengths between experiments are approximately equal. The value for $Q_{L/G}$ and $Q_{G/L}$ calculated by this method yields the values 0.67 mm^3/hr (experimental value = 0.67 mm^3/hr) and 0.74 mm^3/hr (experimental value = 0.73 mm^3/hr) respectively. The calculated $Q_{L/L}$ value was approximately 0.83 mm^3/hr compared with the experimentally measured value of 0.92 mm^3/hr. The calculated $Q_{L/G}$ and $Q_{G/L}$ values show excellent correlation to the experimentally measured values while the calculated $Q_{G/L}$ value is 10% smaller than the experimentally derived value. This difference may be attributed to different liquid-island lengths from one experiment to the next, and the model simplicity.

We relate the resistances of the top pore and bottom pore to the resistance of the gas-filled pore-throat (R_{2S}) in the single pore-throat apparatus using R_1 calculated earlier and equations (L19b) and (L20). We find R_{2S} = 11,990

hr/mm^2, 48% and 21% larger than the top and bottom pore respectively. The lower resistance of each pore-throat in the dual cell suggests the maximum enhancement is significantly less in the dual cell than in the single cell.

Comparing the diffusion flux in the L/M versus the L/G experiment we notice that the flux is higher when both pores (L/G) are available to vapor transfer. Although we cannot show the relative degree through which water vapor passes through each pore, we know that vapor does flow through both a gas and liquid-filled pore simultaneously.

This thesis is accepted on behalf of the faculty

of the institute by the following committee:

John L. Wilson

Advisor

Jeff Phillips

Steve W. Wolf

Clifford K. Ho

February 3, 1999

Date